Increasing the NADPH supply for whole-cell biotransformation and development of a novel biosensor

Inaugural-Dissertation

zur Erlangung des Doktorgrades
der Mathematisch-Naturwissenschaftlichen Fakultät
der Heinrich-Heine-Universität Düsseldorf

vorgelegt von

Solvej Siedler

aus Bad Segeberg

Jülich, September 2012

Aus dem Institut für Bio-und Geowissenschaften, IBG-1: Biotechnologie der

Forschungszentrum Jülich GmbH angeschlossen an die Heinrich-Heine Universität

Düsseldorf

Gedruckt mit der Genehmigung der

Mathematisch-Naturwissenschaftlichen Fakultät der

Heinrich-Heine-Universität Düsseldorf

Referent: Prof. Dr. Michael Bott

                 Institut für Bio- und Geowissenschaften, IBG-1:Biotechnoogie

                 Forschungszentrum Jülich

Korreferent: Prof. Dr. Georg Groth

                 Institut für Biochemische Pflanzenphysiologie

                 Heinrich-Heine-Universität Düsseldorf

Tag der mündlichen Prüfung: 18.12.2012

Results described in this dissertation have been published in the following original publications:

Siedler S, Bringer S, Bott M (2011) Increased NADPH availability in *Escherichia coli*: improvement of the product per glucose ratio in reductive whole-cell biotransformation. Appl Microbiol and Biotechnol 92(5):929-37.

Siedler S, Bringer S, Blank LM, Bott M (2012) Engineering yield and rate of reductive biotransformation in *Escherichia coli* by partial cyclization of the pentose phosphate pathway and PTS-independent glucose transport. Appl Microbiol Biotechnol 93 (4):1459-1467.

*Siedler S, *Lindner SN, Bringer S, Wendisch VF, Bott M. (2012) Reductive whole-cell biotransformation with *Corynebacterium glutamicum:* improvement of NADPH generation from glucose by a cyclized pentose phosphate pathway using *pfkA* and *gapA* deletion mutants. Appl Microbiol Biotechnol. DOI 10.1007/s00253-012-4314-7

Siedler S, Polen T, Bringer S, Bott M. NADPH-dependent reductive biotransformation with *Escherichia coli* and its *pfkA* deletion mutant: Influence on global gene expression and role of oxygen supply. To be submitted

Siedler S, Schendzielorz G, Binder S, Eggeling L, Bringer S, Bott M. SoxR as Single-Cell Biosensor for NADPH-Consuming Enzymes in *Escherichia coli*. Submitted to ACS Synth Biol

Parts of this thesis were published in the following patent application:
Siedler S, Schendzielorz G, Binder S, Eggeling L, Bringer S, Bott M. (2012) Sensoren für NADP(H) und Entwicklung von Alkoholdehydrogenasen. Invention disclosure was received by the German Patent and Trademark Office on August 27, 2012, and was assigned with serial number 10 2012 017 026.2

*These authors contributed equally to this work

Content

1. Summary

In the first part of this work, the pentose phosphate pathway (PPP) was investigated as a source of NADPH in reductive whole-cell biotransformation using *Escherichia coli* and *Corynebacterium glutamicum* as hosts and glucose as reductant. The reduction of methyl acetoacetate to the chiral (*R*)-methyl hydroxybutyrate (MHB) served as a model reaction for NADPH-dependent reactions and was catalyzed by an alcohol dehydrogenase (ADH) from *Lactobacillus brevis*. Partial cyclization of the PPP in *E. coli* and *C. glutamicum* was achieved by deletion of the phosphofructokinase gene *pfkA*, which prevents fructose 6-phosphate catabolism in the glycolytic pathway. The *pfkA*-deficient mutants carrying the *L. brevis* ADH showed a doubled MHB-per-glucose ratio compared to the parent strains. In *E. coli* the partial PPP cyclization in the $\Delta pfkA$ mutant was proven by ^{13}C-flux analysis, which showed a negative net flux through the phosphoglucose isomerase reaction. Furthermore, the flux through pyruvate kinase was found to be absent in the $\Delta pfkA$ mutant, indicating that a low phosphoenolpyruvate (PEP) concentration limited glucose uptake via the phosphotransferase system (PTS). PTS-independent glucose uptake and phosphorylation via the glucose facilitator and glucose kinase from *Zymomonas mobilis* enhanced the specific MHB productivity by 21% in the *E. coli* $\Delta pfkA$ mutant. Deletion of glyceraldehyde 3-phosphate dehydrogenase (*gapA*) theoretically results in a completely cyclized PPP and a ratio of 12 mol NADPH per mol glucose 6-phosphate. A *C. glutamicum* $\Delta gapA$ mutant showed a ratio of 7.9 mol MHB per mol glucose, which is the highest one reported so far. Formation of the by-product glycerol presumably was responsible for not achieving a higher ratio.

In the second part of this work, a biosensor was developed which is capable of detecting a lowered intracellular NADPH/NADP$^+$ ratio and trigger the synthesis of an autofluorescent protein. DNA microarray analysis of *E. coli* during biotransformation showed an upregulation of *soxS* transcription after MAA addition, suggesting that the SoxR regulator known to upregulate *soxS* expression is activated by a lowered NADPH/NADP$^+$ ratio. Subsequently, the *soxS* promoter was fused on a plasmid with the gene encoding yellow fluorescent protein (eYFP). *E. coli* transformed with this plasmid showed fluorescence when MAA was added to the culture. The final fluorescence

intensity and thus the final eYFP titer correlated with the period of a lowered NADPH/NADP$^+$ ratio, which was varied by adding different amounts of MAA. Furthermore, the kinetics of the fluorescence increase was dependent on the ADH activity, which determines the kinetics of MAA reduction and thus the kinetics of the decline of the NADPH/NADP$^+$ ratio. The biosensor was used to screen a library of ADH mutants with the non-natural substrate 4-methyl-2-pentanone (MP). Single cells of the library showing increased fluorescence in the presence of MP were isolated using fluorescence-activated cell sorting (FACS). One of the isolated ADH mutants was shown to have a 35% higher specific MP reduction activity than the wild-type ADH, which demonstrates the applicability of this sensor in the development of NADPH-dependent enzymes.

1.1 Zusammenfassung

Im ersten Teil dieser Arbeit wurde der Pentosephosphat Weg (PPP) als NADPH Quelle für reduktive Ganzzell-Biotransformationen mit *Escherichia coli* und *Corynebacterium glutamicum* untersucht. Die Reduktion von Methylacetoacetat (MAA) zu dem chiralen (*R*)-Methyl-hydroxybutyrat (MHB) diente als Modellreaktion und wurde von der Alkohol Dehydrogenase (ADH) aus *Lactobacillus brevis* katalysiert. Die partielle Zyklisierung des PPP in *E. coli* und *C. glutamicum* konnte durch die Deletion der Phosphofructokinase Gens (*pfkA*) erreicht werden; diese Deletion verhindert den Abbau von Fructose-6-Phosphat über die Glykolyse. Expression des Gens der ADH aus *L. brevis* in der Δ*pfkA* Mutante führte in der Biotransformation zu einer zweifachen Steigerung des Verhältnisses von MHB-pro-Glucose. Eine ^{13}C-Flussanalyse validierte die partielle Zyklisierung des PPP in *E. coli*, da der Nettofluss durch die Phosphoglucose Isomerase in gluconeogenetischer Richtung erfolgte. Außerdem zeigte sich, dass kein Fluss durch die Pyruvatkinase in der Δ*pfkA* Mutanten vorhanden war. Dieses lässt darauf schließen, dass die Verfügbarkeit von Phosphoenolpyruvat (PEP) in der Δ*pfkA* Mutante limitiert ist, was zu einer geringeren Glucose Aufnahme mittels des Phosphotransferase Systems (PTS) führt. Eine PTS-unabhängige Glucose Aufnahme und Phosphorylierung wurde durch die heterologe Expression eines Glucose Facilitators und einer Glucosekinase aus *Zymomonas moblis* erreicht und führte in der *E. coli* Δ*pfkA* Mutante zu einer

Erhöhung der spezifischen Biotransformationsgeschwindigkeit um 21%. Die Deletion des Glycerinaldehyd-3-Phosphat Dehydrogenase Gens (*gapA*) kann theoretisch zu einer vollständigen Zyklisierung des PPP und einer Ausbeute von 12 mol NADPH pro mol Glucose-6-Phosphat führen. Mit einer *C. glutamicum gapA* Deletionsmutante wurde die höchste bisher beschriebene Ausbeute von 7,9 mol MHB pro mol Glucose erreicht.

In dem zweiten Teil dieser Doktorarbeit wurde ein Redox Sensor entwickelt, der niedrige intrazelluläre NADPH/NAD$^+$ Verhältnisse detektiert und die Synthese eines Autofluoreszenzproteins induziert. DNA-Microarray Analysen von *E. coli* während der Biotransformation zeigten eine Erhöhung der Transkription des Gens von SoxS nach Zugabe von MAA. Dies wies darauf hin, dass der Regulator des *soxS* Gens SoxR durch die Absenkung des NADPH/NADP$^+$ Verhältnisses aktiviert wird. Der *soxS* Promotor wurde mit dem Gen des gelb fluoreszierenden Proteins (eYFP) auf einem Plasmid fusioniert. Dieses Plasmid wurde in *E. coli* eingebracht wonach die Bakterienzellen fluoreszierten, wenn MAA zu der Kultur gegeben wurde. Die maximale Fluoreszenzintensität und somit die maximale eYFP Konzentration korrelierte mit der Dauer der Absenkung des NADPH/NADP$^+$ Redox-Verhältnisses, die durch die Zugabe von verschiedene MAA Konzentrationen variiert wurde. Weiterhin hing die Kinetik des Fluoreszenzanstiegs von der ADH-Aktivität ab, die die Kinetik der MAA Reduktion und der Absenkung des NADPH/NADP$^+$ Verhältnisses bestimmt. Mittels dieses Biosensors konnten mutagenisierte ADH-Bibliotheken mit dem unnatürlichen Substrat 4-Methyl-2-Pentanon (MP) untersucht werden. Einzelne Zellen dieser Bibliothek, die eine erhöhte Fluoreszenz in Anwesenheit von MP zeigten, wurden über Fluoreszenz-aktivierte Zellsortierung (FACS) ausgewählt. Dabei wurde eine Mutante mit einer um 35% gesteigerten spezifischen MP-Reduktionsrate im Vergleich zur Wildtyp-ADH isoliert. Dieser Sensor eröffnet somit die Möglichkeit, NADPH abhängige Enzyme mittels Hoch-Durchsatz Screenings zu evolvieren.

2. Introduction

2.1 Whole-cell biotransformation

Reductive whole-cell biotransformation is an important method for industrial synthesis of chemical compounds. The advantages of the implementation of biocatalysts compared to chemical processes are that milder conditions can be applied like lower pressure and temperature. The main advantage is the ability for stereoselective reduction of prochiral substrates, an often challenging task with chemical processes (Faber 2000; Straathof et al. 2002). Examples of industrial synthetic processes with whole cells were reviewed by Ishige and coworkers in 2005, including syntheses of amino acids, vitamins and pharmaceuticals or their intermediates (Ishige et al. 2005). Especially chiral alcohols are of great interest because they can serve as building blocks of pharmaceuticals (Panke and Wubbolts 2005). A variety of oxidoreductases catalyzes the enantio- and regioselective reduction of ketones and depends on nicotinamide adenine dinucleotide cofactors (NADH or NADPH) for hydride transfer. Alcohol dehydrogenases (ADH) are most interesting for the production of chiral alcohols because these enzymes show notable chemo-, regio-, and enantioselectivity (Goldberg et al. 2007).

2.1.1   Cofactor regeneration with single enzymes

The reduction of ketones by ADHs depends on nicotinamide adenine dinucleotide coenzymes, either NADH or NADPH. For commercially relevant processes cofactor regeneration is important. The following requirements have to be kept in mind for the selection of an appropriate regeneration system: The reaction should be thermodynamically favored and the co-product and co-substrate should not interfere with main reactants and enzymes and by-product formation should be negligible (Hummel and Kula 1989). With *Escherichia coli*, different approaches for cofactor regeneration have been applied using one-enzyme coupled systems. For the regeneration of NADH the use of formate dehydrogenase (FDH) was established (Shaked and Whitesides 1980). This enzyme links the oxidation of formate to CO_2 to the reduction of NAD^+

(Egorov et al. 1979; Lamzin et al. 1992). The volatile product CO_2 has many advantages because it disappears from the reaction solution and does not accumulate during the process. Additionally, this causes an irreversible reaction with the equilibrium towards NADH (Kula and Wandrey 1987; Weckbecker et al. 2010). The FDH of *Mycobacterium vaccae* was successfully adopted for cofactor regeneration, e.g. for the production of L-amino acids (Galkin et al. 1997), mannitol (Kaup et al. 2004, 2005; Bäumchen and Bringer-Meyer 2007; Bäumchen et al. 2007), methyl-hydroxybutyrate (Ernst et al. 2005) or succinate (Litsanov et al. 2012).
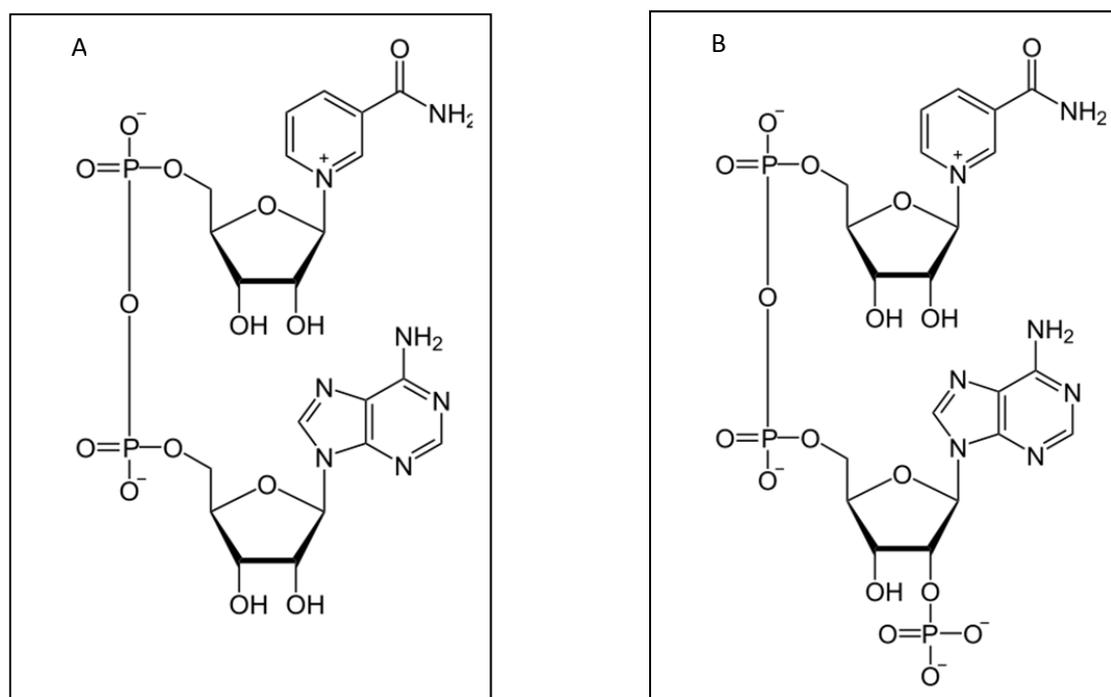
Fig. 1: Nicotinamide adenine dinucleotide cofactors. A) NAD^+ and B) $NADP^+$

For the reduction of $NADP^+$ to NADPH glucose dehydrogenase (GDH) is applicable. The reaction is nearly irreversible due to the hydrolysis of the primary oxidation product gluconolactone. *In vitro* cofactor regeneration was implemented in the production of (6*S*)-tetrahydrofolate from dihydrofolate using purified GDH from *Gluconobacter scleroides* KY3613 (Eguchi et al. 1992). In whole cells a GDH from *Bacillus megaterium* was used in combination with the glucose facilitator (Glf) from *Zymomonas mobilis* for the catalysis of α-pinene to α-pinene oxide, verbenol, and myrtenol (Schewe et al. 2008)

and for the conversion of methyl acetoacetate to (*R*)-methyl-hydroxybutyrate (Heuser et al. 2007).

2.1.2   Cofactor regeneration via sugar metabolism

When using either FDH or GDH, one mol NAD^+ or of one mol $NADP^+$ can be reduced by one mol formate or one mol glucose. When using the endogeneous sugar metabolism of cells for biotransformation, it is possible to reach much higher NADH per glucose or NADPH per glucose ratios (Chin and Cirino 2011), thus offering an advantage to the single enzyme regeneration systems.

In *E. coli* glucose is taken up and simultaneously phosphorylated by the phosphoenolpyruvate phosphotransferase system (PTS) (Kundig et al. 1964; Gabor et al. 2011). Glucose 6-phosphate can be catabolized either via glycolysis or via the pentose phosphate pathway (PPP) (Fig. 2). The distribution depends on different parameters such as the growth rate and varies during growth on glucose between 55-70% flux through glycolysis and 30-45% flux through the PPP (Zhao and Shimizu 2003). Redox cycling agents like paraquat induce superoxide stress conditions and enhance the flux through the PPP (Rui et al. 2010), which is probably due to a higher NADPH demand of the cell (Krapp et al. 2011). In *E. coli* and many other organisms, NADPH is predominantly produced in the PPP by glucose 6-phosphate dehydrogenase (EC 1.1.1.49), which catalyzes the oxidation of glucose 6-phosphate to 6-phosphoglucono-δ-lactone, and by 6-phosphogluconate dehydrogenase (EC 1.1.1.44), which catalyzes the oxidative decarboxylation of 6-phosphogluconate to ribulose 5-phosphate (Stephanopoulos et al. 1998). The two enzymes are encoded by the genes *zwf* and *gnd*, respectively.

The non-oxidative part of the PPP consists of transketolase, transaldolase, ribulose-phosphate 3-epimerase, and ribose phosphate isomerase. Transketolase and transaldolase catalyze the reversible transfer of a ketol group or of an activated dihydroxyacetone moiety, respectively, between several donor and acceptor substrates, thus creating a reversible link between glycolysis and the PPP (Sprenger 1995). Ribose 5-phosphate isomerase catalyzes the conversion between ribose 5-phosphate and

ribulose 5-phosphate, ribulose phosphate 3-epimerase catalyzes the conversion of ribulose 5-phosphate to xylulose 5-phosphate.
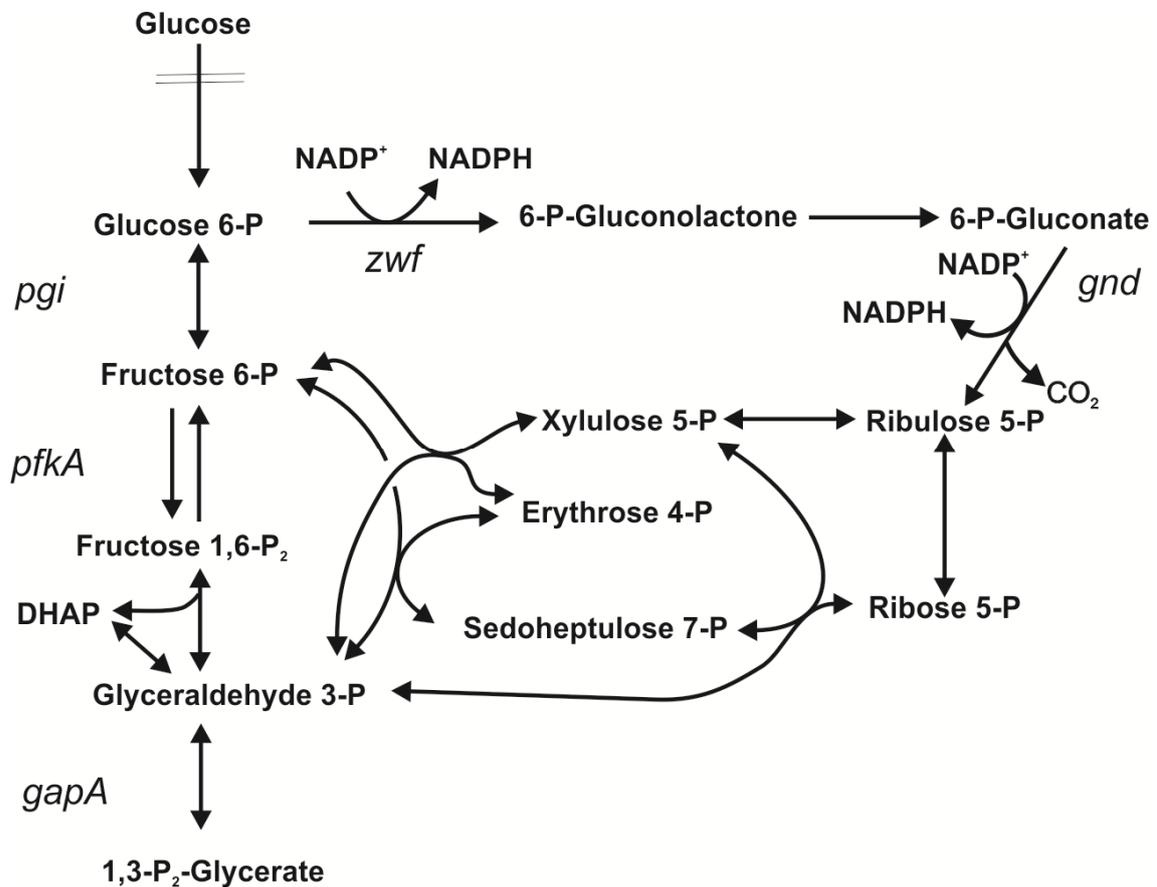
Fig. 2: Overview of the upper part of glycolysis and the PPP

2.1.3   Metabolic engineering of the pentose phosphate pathway

Different approaches to increase the flux through the PPP and thus the NADPH per glucose yield by metabolic engineering have been reported. Overexpression of genes involved in the PPP resulted in *E. coli* and *Ralstonia eutropha* in a higher poly-hydroxybutyrate (PHB) production (Lim et al. 2002; Lee et al. 2003). Due to the higher flux through the PPP a 6-fold higher NADPH to $NADP^+$ ratio (1.1 compared to 6.6) was measured in *E. coli* overexpressing *zwf* (Lim et al. 2002). In an independent study a 37% higher $NADPH/NADP^+$ ratio was achieved in *E. coli* overexpressing *zwf*. This resulted in

a 21% enhancement in GDP-L-fucose production (Lee et al. 2011). In *Aspergillus niger* it was shown that overexpression of genes of the PPP increase the NADPH concentration in the cells by the factor of ~2.3 in the exponential growth phase (Poulsen et al. 2005). In summary, overexpression of genes of the PPP resulted in a higher flux through the PPP and a higher NADPH/NADP$^+$ ratio and this is true not only for *E. coli*.

Redirection of glucose 6-phosphate flux to the PPP can also be brought about by deletion of *pgi* gene with a theoretical yield of 2 mol NADPH per mol glucose from the PPP (Kruger and von Schaewen 2003). Cononaco and coworkers could show via ^{13}C flux analysis that glucose catabolism proceeds predominantly (almost 100%) via the PPP in the Δ*pgi* mutant of *E. coli* (Canonaco et al. 2001). The complete flux through the PPP in the Δ*pgi* mutant was also independent on growth phase in batch cultivation (Toya et al. 2010).

Similar to *zwf* overexpression deletion of *pgi* resulted in a 39% higher NADPH/NADP$^+$ ratio (0.71 in the parental strain compared to 0.98 in the Δ*pgi* deletion mutant), which led to a higher thymidine production (Lee et al. 2010). The deletion of *pgi* was also beneficial for a higher xylitol per glucose yield (4 mol mol^{-1}) compared to the parent strain (3.4 mol mol^{-1}) (Chin et al. 2009). Using a theoretical approach, the NADPH production rate was proposed to be increased by 300% by deletion of *pgi* in comparison to wild type *E. coli* (Chemler et al. 2010).

2.2 The (*R*)-specific alcohol dehydrogenase from *Lactobacillus brevis*

The alcohol dehydrogenase from *L. brevis* (*Lb*ADH) belongs to the short-chain ADHs and is NADPH-dependent (Riebel 1996). The crystal structure of this protein composed of 251 amino acids was reported in 2005 (Fig. 3) (Schlieben et al. 2005). The structure showed a tetramer which is supposed to be the active form of the protein (Riebel 1996) and revealed insights into the amino acids involved in substrate and cofactor binding. The substrate phenylethanol retained in the binding pocket by interactions with Ala93, Leu152, Val195, Leu198 and Met205. Whereas an amino acid exchange from glycine to aspartate at position 37 (G37D) changed cofactor specificity from NADPH toward NADH

(Schlieben et al. 2005), a change of substrate specificity may be possible by exchange of the amino acids involved in substrate binding.
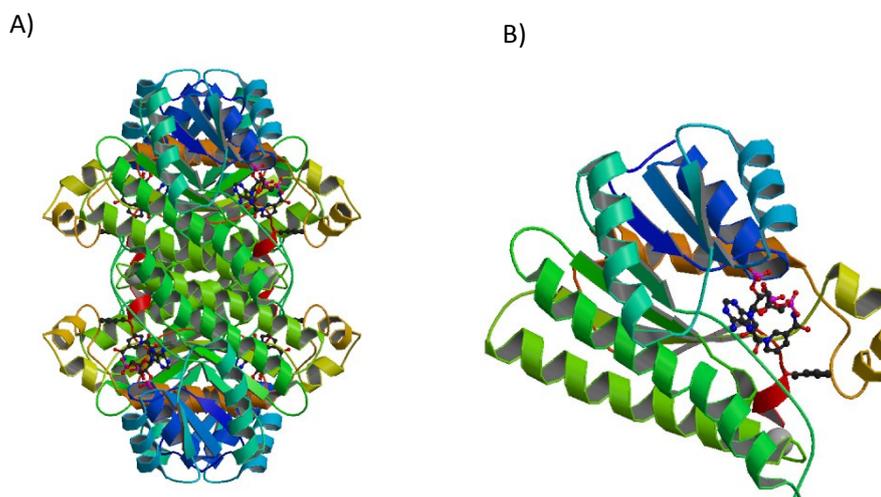
Fig. 3: Crystal structures of the wild type *Lb*ADH tetramer (A) and monomer (B) in complex with acetophenone and NADP (PDB 1ZK4) (Schlieben et al. 2005).

The *Lb*ADH is applicable for biotechnological processes for asymmetric organic synthesis (Hummel 1999). It catalyzes the reduction of a variety of prochiral ketones to secondary alcohols. The preferred *Lb*ADH substrate for *in vitro* studies is acetophenone, which is not accepted as a substrate by any of the commercially available ADHs and which is reduced by *Lb*ADH to *R*-phenyl ethanol with 100% enantiomeric excess (Hummel 1997).

2.3 **Biosensors**

The establishment of new biocatalytic processes of requires the identification of enzymes with the desired substrate specificity. High-throughput screening (HTS) is a challenging method because for each substrate a new system needs to be applied (Reetz 2003). In vitro screening systems often depend on an optical readout of surrogate substrates, such as ω-oxycarboxylic acids coupled to p-nitrophenolate, which shows a strong absorption at 405 nm (Schwaneberg et al. 2001). For NAD(P)H-

dependent processes mutant libraries were screened by monitoring the cofactor consumption during substrate oxidation (Boddupalli et al. 1990; Appel et al. 2001). This method was modified and adapted to microtiter plate scale by Tsotsou and coworkers enabling a HTS method (Tsotsou et al. 2002). Mutated derivatives of cytochrome P450 monooxygenase from *Bacillus megaterium* were tested with different substrates and their activities were measured by detection of the alkaline products of NAD(P)H-oxidation. The assay is not substrate-specific and can thus be applied to testing substrate mixtures. However, this method needs the addition of NAD(P)H which is cost-intensive. Utilization of whole cells is advantageous because they contain this cofactor naturally. Application of transcriptional regulators to correlate gene expression to a read out of fluorescent protein is an upcoming method for the detection of small molecules (Gredell et al. 2012). Such biosensors are applied in whole cells for the detection of metabolites by the use of the natural transcriptional regulator repertoire of the cells, e.g. for amino acids (Binder et al. 2012; Mustafi et al. 2012), or by evolution of the AraC–P_{BAD} regulatory system as a screening tool for the improvement of mevalonate production (Tang and Cirino 2011). These systems have in common a direct readout of the fluorescence correlated to the specific effector concentration. One major advantage of using fluorescent marker proteins is the ability to use fluorescence activated cell sorting (FACS) for HTS, which shortens the time of analyzing millions of mutants drastically (Binder et al. 2012).

2.3.1 The SoxRS system

The bacterial response to oxidative stress is well studied in *E. coli* (Green and Paget 2004). Especially the SoxRS regulatory system was supposed to respond to superoxide anions, as it was activated by redox-cycling agents like paraquat (PQ), menadione and plumbagin (Nunoshiba et al. 1992; Wu and Weiss 1991). These reagents produce superoxide at the expense of the oxidation of NADPH, decreasing the reducing capacity of the cell. The reduction of these chemicals and thereby formation of a radical is often catalyzed by flavoproteins such as NADPH-dependent cytochrome P-450 reductases. The free radical then reacts rapidly with O_2 generating O_2^- and other reactive oxygen species (Cohen and d'Arcy Doherty 1987).

SoxR belongs to the MerR family of metal-binding transcription factors and is a homodimer in solution. Each subunit contains a [2Fe-2S] cluster that can be reversibly oxidized. In the reduced state the SoxR regulator is inactive. It was supposed that exposure to superoxide oxidizes the [2Fe-2S] clusters and thereby activates SoxR, which then activates the transcription of the *soxS* gene (Hidalgo and Demple 1994; Gaudu and Weiss 1996). In recent studies it was shown that SoxRS can also be activated by a decrease of the NADPH content in the absence of superoxide stress (Krapp et al. 2011; Gu and Imlay 2011). SoxR is kept in its inactive state by a NADPH dependent reduction, e.g. catalyzed by the proteins RseC and RsxBC (Koo et al. 2003). The SoxS protein belongs to the AraC family and increases the transcription of many genes through binding to their promoter regions and interaction with RNA polymerase (Li and Demple 1994, 1996; Jair et al. 1996; Martin et al. 2002). SoxS activates the transcription of ~100 genes (Blanchard et al. 2007), which include *sodA* (Mn-containing SOD), *nfo* (endonuclease IV, a DNA repair enzyme of oxidative damage), *frp* (ferredoxin reductase), *acrAB* (cellular efflux pumps), and *fumC* (redox-resistant fumarase). Another target of the SoxRS-regulatory system is the *zwf* gene encoding glucose 6-phosphate dehydrogenase. This enzyme catalyzes the first step of PPP, the NADP-dependent oxidation of glucose 6-phosphate to 6-phosphogluconolactone. The PPP is the main source of NADPH beside the isocitrate dehydrogenase-, transhydrogenase (PntAB)- and malic enzyme-catalyzed reactions in *E. coli*.

2.4   Aim of this work

The first aim of this work was to optimize endogenous sugar metabolism in order to increase the NADPH yield per glucose in whole-cell biotransformation processes. To this end, the PPP should be partially cyclized or completely cyclized. Partial cyclization of the PPP by elimination of phosphofructokinase activity should increase the NADPH per glucose yield to a theoretically maximal value of 6 mol mol^{-1}. In this situation, fructose 6-phosphate cannot be metabolized in glycolysis, but has to be isomerized to glucose 6-phosphate again and degraded in the oxidative PPP. Complete oxidation of glucose via a cyclic PPP requires complete recycling of both fructose 6-phosphate and glyceraldehyde 3-phosphate formed in the PPP and can be achieved by elimination of

glyceraldehyde 3-phosphate dehydrogenase activity. In this situation, up to 12 mol NADPH should be formed per mol glucose 6-phosphate (Kruger and von Schaewen 2003). The NADPH-dependent reduction of the prochiral β-ketoester methyl acetoacetate (MAA) to the chiral hydroxy ester (*R*)-methyl 3-hydroxybutyrate (MHB) catalyzed by the *R*-specific alcohol dehydrogenase from *L. brevis* served as a model reaction to test the above metabolic engineering approaches in *E. coli* and *Corynebacterium glutamicum* (Fig. 4). The second topic of this work was the establishment of a redox sensor that is able to detect a lowered intracellular NADPH/NADP$^+$ ratio and convert this signal into a fluorescence signal. Such a biosensor is expected to have broad applicability for the high-throughput screening of NADPH-dependent enzymes which need to be altered or optimized with respect to the substrate spectrum or to activity under certain conditions of pH, temperature, etc.
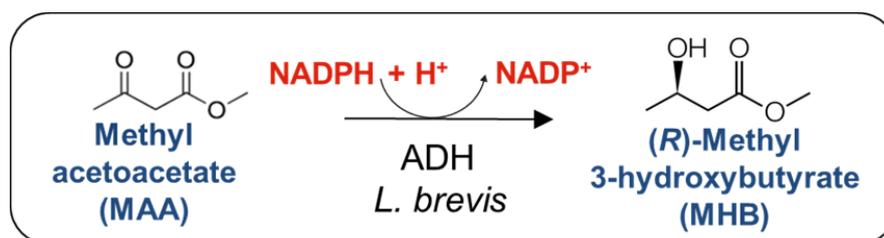
Fig. 4: Scheme of the model reaction catalyzed by the *R*-specific alcohol dehydrogenase from *L. brevis*.

3. Results

The first topic of this thesis was the characterization of recombinant strains of *Escherichia coli* and *Corynebacterium glutamicum* in which the carbon flux from glucose was rerouted from glycolysis to the pentose phosphate pathway (PPP) in order to increase the NADPH yield per glucose in reductive whole-cell biotransformation processes. The results allocated to this research field have been summarized in three publications in "Applied Microbiology and Biotechnology".

The first publication (vol. 92, pp. 929-937, 2011) entitled "Increased NADPH availability in *Escherichia coli*: improvement of the product per glucose ratio in reductive whole-cell biotransformation" describes that the product per glucose yield of the reduction of methylacetoacetate (MAA) to methyl-3-hydroxybutyrate (MHB) catalyzed by the *R*-specific alcohol dehydrogenase (ADH) from *Lactobacillus brevis* was increased from 2.44 to 3.78 mol_{MHB} $\text{mol}_{glucose}^{-1}$ in mutant (Δpgi) lacking the phosphoglucose isomerase gene. Even higher yields of 4.79 and 5.46 mol_{MHB} $\text{mol}_{glucose}^{-1}$, were obtained with mutants lacking either phosphofructokinase A ($\Delta pfkA$) or phosphofructokinases A and B ($\Delta pfkA\Delta pfkB$), respectively.

In the second publication (volume 93, pp. 1459-1467, 2012) entitled "Engineering yield and rate of reductive biotransformation in *Escherichia coli* by partial cyclization of the pentose phosphate pathway and PTS-independent glucose transport" the partial cyclization of the PPP in strains with reduced or absent phosphofructokinase activity was experimentally shown via ^{13}C flux analysis, as a net flux from fructose 6-phosphate to glucose 6-phosphate was measured in the $\Delta pfkA$ mutant. Furthermore, almost no carbon flux through pyruvate kinase was detectable in this mutant, indicating that a low intracellular PEP concentration is limiting glucose uptake via the phosphotransferase system. This was confirmed by overexpression of the glucose facilitator and glucokinase from *Zymomonas mobilis*, which allowed for PTS-independent glucose uptake and phosphorylation and resulted in a higher glucose uptake rate and a 20% higher specific MHB production rate.

The third publication entitled "Reductive whole-cell biotransformation with *Corynebacterium glutamicum*: improvement of NADPH generation from glucose by a

cyclized pentose phosphate pathway using *pfkA* and *gapA* deletion mutants" (DOI 10.1007/s00253-012-4314-7, 2012) showed that the results from *E. coli* were transferable to *C. glutamicum*. With a *pfkA* deletion mutant of *C. glutamicum*, the same yield of 4.8 mol_{MHB} $mol_{glucose}^{-1}$ was reached as with the *E. coli* $\Delta pfkA$ strain. Furthermore, cyclization of the PPP was accomplished by deletion of *gapA* resulting in a yield of 7.9 mol_{MHB} $mol_{glucose}^{-1}$.

The second topic of this thesis describes the development of a biosensor capable of detecting a decrease in the intracellular $NADPH/NADP^+$ ratio. The basis for this development was a study in which the influence of the *pfkA* deletion in *E. coli* on global gene expression during reductive whole-cell biotransformation was studied and also the influence of oxygen on reductive biotransformation. In these studies, evidence was obtained that expression of the *soxS* gene is activated by a lowered $NADPH/NADP^+$ ratio. The corresponding results are summarized in a manuscript entitled "NADPH-dependent reductive biotransformation with *Escherichia coli* and its *pfkA* deletion mutant: Influence on global gene expression and role of oxygen supply".

Based on the increased *soxS* expression during increased NADPH consumption via reduction of MAA to MHB, a plasmid-based sensor was constructed in which the *soxS* promoter controls expression of the gene encoding the autofluorescent protein EYFP. Studies with this sensor supported the view that *soxS* expression is activated by a decreased $NADPH/NADP^+$ ratio. Furthermore, it was shown that this sensor can be used for HT-screening of NADPH-dependent enzymes, which is of high interest in the field of biocatalysis and metabolic engineering. The results on the biosensor are summarized in a manuscript entitled "SoxR as Single-Cell Biosensor for NADPH-Consuming Enzymes in *Escherichia coli*". These results are also the basis of patent application (Submitted to the German Patent and Trademark Office at the 27.08.2012).

Increased NADPH availability in *Escherichia coli*: Improvement of the product per glucose ratio in reductive whole-cell biotransformation

Solvej Siedler · Stephanie Bringer · Michael Bott

Abstract A basic requirement for the efficiency of reductive whole-cell biotransformations is the reducing capacity of the host. Here, the pentose phosphate pathway (PPP) was applied for NADPH regeneration with glucose as the electron-donating co-substrate using *Escherichia coli* as host. Reduction of the prochiral β-keto ester methyl acetoacetate (MAA) to the chiral hydroxy ester (*R*)-methyl 3-hydroxybutyrate (MHB) served as a model reaction, catalyzed by an *R*-specific alcohol dehydrogenase. The main focus was maximization of the reduced product per glucose yield of this pathway-coupled cofactor regeneration with resting cells. With a strain lacking the phosphoglucose isomerase, the yield of the reference strain was increased from 2.44 to 3.78 mol MHB/mol glucose. Even higher yields were obtained with strains lacking either phosphofructokinase I (4.79 mol MHB/mol glucose) or phosphofructokinase I and II (5.46 mol MHB/mol glucose). These results persuasively demonstrate the potential of NADPH generation by the PPP in whole-cell biotransformations.

S. Siedler · S. Bringer · M. Bott
Institut für Bio- und Geowissenschaften, IBG-1: Biotechnologie,
Forschungszentrum Jülich,
52425 Jülich, Germany

S. Bringer (*) · M. Bott (*)
Institut für Biotechnologie 1, Forschungszentrum Jülich GmbH,
52425 Jülich, Germany
e-mail: st.bringer-meyer@fz-juelich.de

M. Bott
e-mail: m.bott@fz-juelich.de

Introduction

Utilization of microorganisms for reductive whole-cell biotransformation under resting cell conditions has become an important method in chemoenzymatic synthesis, e. g. for the production of chiral intermediates required in the synthesis of pharmaceuticals. A variety of dehydrogenases catalyzes the enantio- and regioselective reduction of ketones and depends on nicotinamide adenine dinucleotide coenzymes (NADH or NADPH) for hydride transfer. Efficient coenzyme recycling by recombinant enzymes transforming the oxidized coenzyme back to its reduced form is essential for the productivity of reductive whole-cell biotransformations. Prominent products whose synthesis by biotransformation requires NAD(P)H are chiral alcohols that serve as building blocks in the synthesis of statins, compounds that dominate the world market for cholesterol-lowering drugs (Panke and Wubbolts 2005; Liljeblad et al. 2009).

The advantages of using whole cells for biotransformations compared to isolated enzymes are (i) the possibility to regenerate cofactors *in vivo* via cheap electron-donating co-substrates, (ii) the use of enzymes without cost-intensive purification and (iii) an extended life period of the catalysts. With *Escherichia coli* different approaches for cofactor regeneration have been applied, e.g. using one-enzyme-coupled systems, like formate dehydrogenase (Kaup et al. 2004; Ernst et al. 2005; Kaup et al. 2005) or glucose dehydrogenase (Eguchi et al. 1992; Heuser et al. 2007; Zhang et al. 2009), which oxidize one 1 formate to CO_2 or 1 mol glucose to gluconate, respectively, for regeneration of 1 mol NAD(P)H.

Another possibility is to take advantage of the metabolism of the cell for cofactor regeneration (Walton and Stewart 2004; Blank et al. 2008; Bühler et al. 2008; Chin et al. 2009; Fasan et al. 2010; Akinterinwa and Cirino 2011).

Directing the metabolism in an efficient way to the reduction of NAD(P)H is complex, since these cofactors play important roles in a large number of cellular reactions (Blank et al. 2008; Holm et al. 2010). Nevertheless, increasing the yield of reduced product per glucose, Y_{RPG}, as defined by Akinterinwa and Cirino (Akinterinwa and Cirino 2011), is essential for an enhancement of the efficiency of whole-cell biotransformation. This has exemplarily been shown for different NADPH-dependent processes. With a mutant of *E. coli* incapable of fermentation, a Y_{RPG} of 4 mol xylitol per mol glucose was achieved under anaerobic conditions (Akinterinwa and Cirino 2011). With an engineered P_{450} monooxygenase, a Y_{RPG} of 1.71 was reached with an *E. coli* mutant lacking *ndh, adh, ldh* (Fasan et al. 2010).

In *E. coli* and many other organisms, NADPH is mostly produced in the pentose phosphate pathway (PPP) by glucose-6-phosphate dehydrogenase (EC 1.1.1.49), which catalyzes the oxidation of glucose 6-phosphate to 6-phosphoglucono-δ-lactone, and by 6-phosphogluconate dehydrogenase (EC 1.1.1.44), which catalyzes the oxidative decarboxylation of 6-phosphogluconate to ribulose 5-phosphate (Stephanopoulos et al. 1998). The two enzymes are encoded by the genes *zwf* and *gnd*, respectively. Different approaches to increase the NADPH per glucose yield of the PPP by metabolic engineering have been reported, either by overexpression of genes involved in the PPP (Lim et al. 2002; Lee et al. 2003; Poulsen et al. 2005) or by deletion of the phosphoglucose isomerase (*pgi*) gene (Canonaco et al. 2001; Lee et al. 2010).

The deletion of *pgi* prohibits glucose catabolism via the glycolytic pathway and enforces glucose 6-phosphate catabolism via the PPP, with two mol NADPH being formed per mol glucose. Complete oxidation of glucose via a cyclic PPP, which requires complete recycling of both fructose 6-phosphate and triose phosphate, theoretically affords the generation of 12 mol reduction equivalents per mol glucose 6-phosphate (Kruger and von Schaewen 2003). While deletion of *pgi* renders cyclization impossible, diversion of glucose catabolism from glycolysis to the PPP can be brought about by reduction of phosphofructokinase (EC 2.7.1.11) activity. *E. coli* possesses two non-homologues phosphofructokinases, Pfk I and Pfk II (Fraenkel et al. 1973), which are encoded by the gene *pfkA* and *pfkB*, respectively. About 90-95% of the total phosphofructokinase activity in *E. coli* is contributed by Pfk I (Vinopal et al. 1975; Vinopal and Fraenkel 1975). Phosphofructokinase I (ΔpfkA) deficient and phosphofructokinase I and II (ΔpfkAΔpfkB) double deletion mutants theoretically should afford 6 mol NADPH per mol glucose by completely converting fructose 6-phosphate to glucose 6-phosphate and

recycling through the PPP (Kruger and von Schaewen 2003). This partial cycling allows catabolism of glyceraldehyde 3-phosphate produced in the PPP via the lower part of glycoysis (Embden-Meyerhof pathway, EMP) and the tricarboxylic acid cycle (TCC). Under resting cell conditions this carbon flux through EMP and TCC is necessary and beneficial for energy generation and sustainment of glucose uptake by the phosphoenolpyruvate- dependent phosphotransferase system.

In the present work the NADPH-dependent reduction of the β-keto ester methyl acetoacetate (MAA) to the chiral hydroxy ester (*R*)-methyl 3-hydroxybutyrate (MHB) catalyzed by *Lactobacillus brevis* alcohol dehydrogenase served as a model reaction for a reductive whole-cell biotransformation. A PPP which was partially disconnected from the EMP was applied for cofactor regeneration with glucose as the electron-donating co-substrate. While the present paper was submitted, an online publication with a similar objective was issued (Chin and Cirino 2011).

Materials and Methods

Chemicals and enzymes

Chemicals were obtained from Sigma-Aldrich (Taufkirchen, Germany), Operon (Munich, Germany), Qiagen (Hilden, Germany), Merck (Darmstadt, Germany), and Roche Diagnostics (Mannheim, Germany).

Bacterial strains, plasmids media and growth conditions

Strains and plasmids used in this work are listed in Table 1. *E. coli* strains were transformed by the method described by Hanahan (1983) and cultivated in LB medium (Miller 1972) or in 2xYT medium (16 g l^{-1} tryptone, 10 g l^{-1} yeast extract, 5 g l^{-1} sodium chloride). *E. coli* DH5α (Hanahan 1983) was used for cloning purposes and *E. coli* BL21 Star (DE3) (Invitrogen, Karlsruhe, Germany) and derivatives for gene expression and whole-cell biotransformation. Plasmids were selected by adding antibiotics to the medium at a final concentration of 100 μg ampicillin ml^{-1} (pBtac*Lbadh*), and 25 μg chloramphenicol ml^{-1} (pKO3).

Recombinant DNA work

Standard methods like PCR, restriction or ligation were carried out according to established protocols (Sambrook and Russell 2001). *E. coli* cells were transformed by the CaCl$_2$ method (Hanahan et al. 1991). DNA sequencing was performed by Agowa (Berlin, Germany). Oligonucleotides were synthesized by Biolegio bv (Nijmegen, The Netherlands) and are listed in Table 1.

Table 1 Strains, plasmids and oligonucleotides used in this work

Strains, plasmids and oligonucleotides	Relevant characteristics/ 5´-3´sequence	Reference
Strains		
DH5α	F⁻ ø80Δ*lacZ*ΔM15 Δ(*lacZYA-argF*) U169 *deoR recA*1 *endA*1 *hsdR*17 (rk⁻, mk⁺) *phoA supE*44 λ⁻ *thi*-1 *gyrA*96 *relA*1	Hanahan 1983, Invitrogen
BL21 Star (DE3)	F⁻ *omp*T *hsdS*$_B$(r$_B$⁻, m$_B$⁻) *gal dcm rne*131 (DE3)	Invitrogen
Reference strain for biotransformation	BL21 Star (DE3) with pBtac*Lbadh*	This study
Δ*pfkA*	BL21 Star (DE3) Δ*pfkA* with pBtac*Lbadh*	This study
Δ*pfkA*Δ*pfkB*	BL21 Star (DE3) Δ*pfkA*Δ*pfkB* with pBtac*Lbadh*	This study
Δ*pfkB*	BL21 Star (DE3) Δ*pfkB* with pBtac*Lbadh*	This study
Δ*pgi*	BL21 Star (DE3) Δ*pgi* with pBtac*Lbadh*	This study
Plasmids		
pBTac1	Amp^R, P$_{tac}$, *lacI*; expression vector for *E. coli*	Boehringer Mannheim
pBTac-*Lbadh*	pBtac1 derivative with *adh* gene from *Lactobacillus brevis*	X-Zyme, Ernst *et al.* 2005
pKO3	Cam^R, allelic replacement vector	Link *et al.* 1997
pKO3 Δ*pfkA*	pKO3 derivative; deletion plasmid of *pfkA*	This study
pKO3 Δ*pfkB*	pKO3 derivative; deletion plasmid of *pfkB*	This study
pKO3 Δ*pgi*	pKO3 derivative; deletion plasmid of *pgi*	This study
Oligonucleotides		
pfkA1	GCTACCCGGGCCGATGCTCTGTTTGCATTG	
pfkA2	CAGTTTTTTCGCGCACATCGAAGTGATCCAACGAATGTGCAAATAGTATA	
pfkA3	TGGATCACTTCGATGTGCGCGAAAAAACTGTATTAATGATTTCGGAAAAA	
pfkA4	CAGTGGATCCTGAACCACCGTGGGACTG	
pfkB1	GCTACCCGGGGGTGGTGTCAGCCGTAAG	
pfkB2	GGAAAGGTAAGCGTACATTTCCTCCTATAGGCTGATTTCAGTCTGGCACC	
pfkB3	CTATAGGAGGAAATGTACGCTTACCTTTCCCGCTAACAAAAACATTCCCC	
pfkB4	CTGAGGATCCGATCATAAGGTTAGCGCAAGAATG	
pgi1	GCTACCCGGGACATAACTACCTCGTGTCAG	
pgi2	GCGCCACGCTTTATACATTAGCAATACTCTTCTGATTTTGAGAATTGTGA	
pgi3	AGAGTATTGCTAATGTATAAAGCGTGGCGCGGTTAATCATCGTCGATATG	
pgi4	GCTACCCGGGCGGGATCGAGTATACACAAC	
pfkAproof_for	ATAGCGCGTTACGCATGGG	
pfkAproof_rev	TCCACGTCATAGGCCAGAG	
pfkBproof_for	GAAGTATTACTGGCGTTCCC	
pfkBproof_rev	CGATTTCGCCTTCACCTAAC	
pgiproof_for	CACGTTGGCATCAGAAAGC	
pgiproof_rev	TCGCCGCAAGCGCAGATATG	

In-frame deletion mutants of the genes *pfkA* (ECBD_4108), *pfkB* (ECBD_1922) and *pgi* (ECBD_4012) were constructed with slight modifications *via* the two-step homologous recombination procedure as described previously (Link et al. 1997). The procedure will be exemplified for *pfkA*. Deletion of *pfkB* and the *pgi* gene was performed comparably; the same oligonucleotide nomenclature was used. The up- and downstream regions of *pfkA* were amplified using the oligonucleotide pairs pfkA1/pfkA2 and pfkA3/pfkA4. The resulting PCR products served as template for an overlap extension PCR with the oligonucleotides

pfkA1/pfkA4. The approximately 1 kb product was digested with XmaI and BamHI and cloned into the vector pKO3. The resulting derivatives pKO3Δ*pkfA*, pKO3Δ*pkfB* and pKO3Δ*pgi* were suitable for performing an allelic exchange by homologous recombination into the chromosome of *E. coli* BL21(DE3) resulting in mutant strains *E. coli* BL21(DE3) Δ*pkfA*, *E. coli* BL21(DE3) Δ*pkfB*, *E. coli* BL21(DE3) Δ*pkfA*Δ*pkfB* and *E. coli* BL21(DE3) Δ*pgi*, respectively. The mutants were verified by a PCR reaction using oligonucleotide pair pfkAproof_for/pfkAproof_rev (etc.), flanking the deleted region.

Whole-cell biotransformation

For cultivation of the different recombinant *E. coli* BL21(DE3) strains carrying the pBtac*Lbadh* plasmid, a single colony of each strain was inoculated into 5 ml 2xYT medium containing the appropriate selection marker as described above and grown overnight at 37°C and 130 rpm. These pre-cultures were used for inoculation of the main cultures to an optical density at 600 nm (OD_{600}) of 0.05. Main cultures were grown in 100 ml 2xYT medium in the presence of the appropriate selection marker at 37°C and 130 rpm to an OD_{600} of 0.3, induced with 1 mM IPTG, incubated at 37°C and 130 rpm for another 3 h and harvested at an OD_{600} between 2 and 4.5, which had been determined as the optimal cell density for subsequent whole-cell biotransformation.

The cells were harvested by centrifugation (4,000 g, 7 min) and resuspended in reaction buffer containing 2% (w/v) glucose, 2 mM $MgSO_4$ and 250 mM potassium phosphate buffer, pH 6.5 to a cell density of 3 g cell dry weight (cdw) l^{-1}. The reaction was started by adding 60 mM MAA. Biotransformation was conducted at 37°C and 130 rpm to prevent cell sedimentation. Specific productivities (mmol MHB h^{-1} (g cdw)$^{-1}$) were determined by taking samples at 15 min time intervals over a period of 2 h. MHB and glucose concentrations of the samples were determined (see below). Specific productivities were calculated by dividing the slope of graphs showing MHB concentration vs. time by the cell dry weight.

Enzyme activity assays

Cell harvesting was carried out by centrifugation (10,000 g, 4°C, 5 min). The cells were resuspended in 100 mM potassium phosphate buffer, pH 6.5, with 1 mM dithiothreitol and 1 mM $MgCl_2$. Cells were disrupted at 4°C by 3 x 15 sec bead-beating with 0.1 mm diameter glass beads using a Silamat S5 (Ivoclar Vivadent GmbH, Germany) and crude extracts were centrifuged at 16,000 g (4°C, 20 min) to remove intact cells and cell debris. The supernatants were used as cell-free extracts. Enzyme activities were measured photometrically at 340 nm using different dilutions of the cell-free extract. Alcohol dehydrogenase activity was determined using a mixture of 10 mM methyl acetoacetate, 250 μM NADPH, and 1 mM $MgCl_2$ in 100 mM potassium phosphate buffer, pH 6.5, and cell-free extract. Phosphofructokinase activity was determined using a coupled enzymatic assay with pyruvate kinase and lactate dehydrogenase modified from (Santamaría et al. 2002). The assay mixture contained 100 mM Tris-HCl pH 7,5, 50 mM KCl, 5 mM NH_4Cl, 5 mM $MgCl_2$, 0.5 mM ATP, 0.25 mM NADH, 2.5 mM fructose 6-phosphate, 0.5 U pyruvate kinase, 0.5 U lactate dehydrogenase, 2 mM phosphoenolpyruvate, and cell-free extract. The reaction was started by addition of phosphoenolpyruvate. Unspecific activity was monitored with test mixtures where fructose 6-phosphate was omitted. The assay mixture for phosphoglucose

isomerase (Fraenkel and Levisohn 1967) consisted of 100 mM Tris-HCl, pH 7.5, 10 mM $MgCl_2$, 1 U glucose 6-phosphate dehydrogenase, 1 mM $NADP^+$, 2.5 mM fructose 6-phosphate, and cell-free extract. One unit of enzyme activity was defined as the amount of enzyme catalyzing the conversion of 1 μmol min^{-1} pyridine nucleotide at 30°C under the specified conditions. Protein concentrations were determined by the method of Bradford (Bradford 1976) using bovine serum albumin as a standard.

Analyses of substrates and products

Methyl acetoacetate (MAA) and (*R*)-methyl 3-hydroxybutyrate (MHB) were analyzed by HPLC using a Synergi 4u Polar-RP 80A column (Phenomenex, Aschaffenburg, Germany) at ambient temperature. Separation was achieved using 10% (v/v) methanol at a flow rate of 1 ml min^{-1}. The components were quantified by the refraction index. Calibration curves were prepared using five defined concentrations of MAA and MHB.

Extracellular metabolites were analyzed by HPLC using an Aminex HPX-87H column (Bio-Rad). The operating temperature was 40°C. Separation was achieved using 0.06 mM H_2SO_4 at a flow rate of 0.4 ml/min. The metabolites were quantified by UV absorbance at 210 nm. A calibration curve was made using six different metabolite concentrations.

The glucose concentration was determined via HPLC as described for MAA and MHB determination, or enzymatically by using the glucose Gluc-DH FS* Kit according to the instructions of the manufacturer (DiaSys, Holzheim, Germany).

Analysis of NAD(P)H and NAD(P)$^+$

Intracellular pyridine nucleotides NAD(P)H and NAD(P)$^+$ were extracted using EnzyChrom^{TM} NAD(P)$^+$/NAD(P)H assay kit (BioAssay Systems, Hayward, CA) following the manufacturer's instructions and as previously described by Lee et al. (Lee et al. 2010). For rapid inactivation of the cellular metabolism, the cell pellets obtained after centrifugation were frozen in liquid nitrogen and stored at -20°C. Pellets were resuspended with Acid extraction buffer (BioAssay Systems) or Base extraction buffer (BioAssay Systems) to extract oxidized pyridine nucleotides or reduced pyridine nucleotides, respectively (Matsumura and Miyachi 1980). This extraction method prevented oxidation, reduction, or breakdown of nucleotides during the process of cell lysis and extract preparation (Lundquist and Olivera 1971; Grose et al. 2006). The relative amounts of NAD^+, NADH, $NADP^+$, and NADPH in each extract were then quantified by the enzymatic methods of Zerez et al. (Zerez et al. 1987) by using an $NADP^+$-specific glucose 6-phosphate dehydrogenase and an NAD^+-specific yeast alcohol dehydrogenase (BioAssay Systems).

Results

Activity of phosphofructokinase and phosphoglucose isomerase in *E. coli* reference strain and mutant strains

In order to increase NADPH production from glucose in *E. coli*, mutants of strain BL21(DE3) were constructed in which the genes *pfkA* (phosphofructokinase I), *pfkB* (phosphofructokinase II), *pfkA* and *pfkB*, or *pgi* (glucose 6-phosphate isomerase) were deleted. To determine the consequences of these deletions at the enzymatic level, the activities of phosphofructokinase and glucose 6-phosphate isomerase were measured in cell-free extracts of the reference strain and the deletion mutants (Table 2).

The phosphofructokinase (Pfk) activity of the reference strain was 0.64 U (mg protein)$^{-1}$ and was set as 100%. As already observed in earlier work (Vinopal et al. 1975), most of the Pfk activity is provided by Pfk I, as the Δ*pfkA* mutant showed a residual activity of only 22%. The Δ*pfkB* mutant had a residual activity of 78%, indicating that Pfk II contributed 22% of the total Pfk activity. Surprisingly, the absence of both *pfkA* and *pfkB* did not result in a complete loss of phosphofructokinase activity, as the Δ*pfkA*Δ*pfkB* mutant showed a residual phosphofructokinase activity of 27% of the reference strain activity (Table 2). Similar results during *in vitro* assays of Δ*pfkA*Δ*pfkB* mutants were already reported most recently (Chin and Cirino 2011). The residual phosphofructokinase *in vitro* activity in Δ*pfkA*Δ*pfkB* mutants could possibly be due to a side activity of an enzyme belonging to the PfkB family of phosphosugar kinases, which form a subset of the ribokinase superfamily (Park and Gupta 2008). Possibly, ribokinase or another member of this family phosphorylates fructose 6-phosphate to fructose-1,6-diphosphate *in vitro* which may be due to the dilution of an allosteric inhibitor in the *in vitro* assay. The differences of growth in Δ*pfkA*Δ*pfkB* and Δ*pfkA* mutants (not shown) and in biotransformation yield (in the following) indicate that the residual phosphofructokinase activity may be attenuated *in vivo*.

The activity of phosphoglucose isomerase was similar in the reference strain, the Δ*pfkA* and Δ*pfkB* strains, and slightly elevated in the Δ*pfkA*Δ*pfkB* double mutant. No residual phosphoglucose isomerase was measurable in the Δ*pgi* strain (Table 2).

Biotransformation of MAA to MHB with the reference and the mutant strains

For the biotransformation of methyl acetoacetate (MAA) to (*R*)-methyl-3-hydroxybutanoate (MHB), the gene encoding the (*R*)-specific alcohol dehydrogenase of *Lactobacillus brevis* (*Lbadh*) was overexpressed in *E. coli* BL21(DE3) as well as in the mutant strains Δ*pgi*, Δ*pfkA*, Δ*pfkB* and Δ*pfkA*Δ*pfkB*. The activity of the alcohol dehydrogenase was high and not limiting in all strains, ranging from 17–28 U mg^{-1} in independent biotransformations. The kinetics of MHB production and glucose consumption were completely or almost completely linear over the assay period of 120 min (Fig. 1).

The MHB production rates of the reference strain and mutants ranged between 8.51 and 9.11 mmol MHB h^{-1} (g cdw)$^{-1}$ (Fig. 2). Those of the reference strain and the Δ*pfkB* mutant were similar with 8.57 ± 0.15 and 8.51 ± 0.03 mmol MHB h^{-1} (g cdw)$^{-1}$, respectively. The Δ*pfkA* mutant showed the highest productivity (9.11 ± 0.29 mmol MHB h^{-1} (g cdw)$^{-1}$) followed by the Δ*pgi* mutant (8.86 ± 0.32 mmol MHB h^{-1} (g cdw)$^{-1}$) and the Δ*pfkA*Δ*pfkB* double mutant (8.84 ± 0.63 mmol MHB h^{-1} (g cdw)$^{-1}$). Even though the MHB production rates were similar, the glucose consumption rates differed greatly between reference strain and Δ*pfkB* mutant on the one hand and the Δ*pgi*, Δ*pfkA* and Δ*pfkA*Δ*pfkB* mutants on the other hand. The reference strain and the Δ*pfkB* mutant consumed 3.38 ± 0.26 and 3.58 ± 0.17 mmol glucose h^{-1} (g cdw)$^{-1}$, respectively, which was in the range of published values for glucose consumption rates of growing cells at 37°C (Hua et al. 2003; Nor'Aini et al. 2006). The molar ratio of produced MHB to consumed glucose (Y$_{RPG}$) was 2.44 ± 0.15 for the reference strain and 2.53 ± 0.03 for the Δ*pfkB* strain.

Generally, disruption of the *pgi* gene encoding phosphoglucose isomerase is known to prevent or delay the glucose utilization in cells and retards cell growth due to a limited capacity for reoxidation of excess NADPH produced in the PPP (Canonaco et al. 2001; Sauer et al. 2004). Likewise, also in our study the deletion of the *pgi* gene resulted in a lowered glucose consumption rate of 2.30 ± 0.10 mmol glucose h^{-1} (g cdw)$^{-1}$, which was also reported for growing cells (Hua et al. 2003; Nor'Aini et al. 2006; Blank et al. 2008; Lee et al. 2010).

Table 2 Specific activities of phosphofructokinase and phosphoglucose isomerase in *Escherichia coli* reference strain and deletion mutants.

Strain	Phosphofructokinase μmol min^{-1} (mg protein)$^{-1}$	Phosphoglucose isomerase μmol min^{-1} (mg protein)$^{-1}$
Reference strain	0.64 ± 0.07 (100%)	0.33 ± 0.08
Δ*pfkA*	0.15 ± 0.05 (23%)	0.30 ± 0.03
Δ*pfkB*	0.50 ± 0.16 (78%)	0.27 ± 0.05
Δ*pfkA*Δ*pfkB*	0.17 ± 0.05 (27%)	0.45 ± 0.01
Δ*pgi*	0.53 ± 0.09 (83%)	0

Standard deviations are from two biological experiments with two technical replicates, each.

Fig. 1 Representative kinetics of MHB production (□) and glucose consumption (■) during biotransformation with *E. coli* BL21(DE3) reference strain and deletion mutants lacking either one or both of the phosphofructokinase genes *pfkA* and *pfkB* and the phosphoglucose isomerase gene *pgi*. All strains carried the plasmid pBtac*Lbadh*.

The Δ*pgi* mutants invariably metabolise glucose via the PPP and therefore produce 2 mol NADPH per mol glucose via this pathway. However, during biotransformation the Y_{RPG} was 3.78 ± 0.23 mol MHB/mol glucose, indicating that additional reactions coupled with NADPH formation such as isocitrate dehydrogenase or transhydrogenase were going on.

For the Δ*pfkA*Δ*pfkB* strain a specific glucose consumption rate of 1.49 ± 0.10 mmol glucose h⁻¹ (g cdw)⁻¹ and an Y_{RPG} of 5.46 ± 0.15 mol MHB/mol glucose were measured. The single deletion mutant Δ*pfkA* showed a glucose consumption rate of 1.76 ± 0.13 mmol glucose h⁻¹ (g cdw)⁻¹ and an Y_{RPG} of 4.79 ± 0.08 mol MHB/mol glucose.
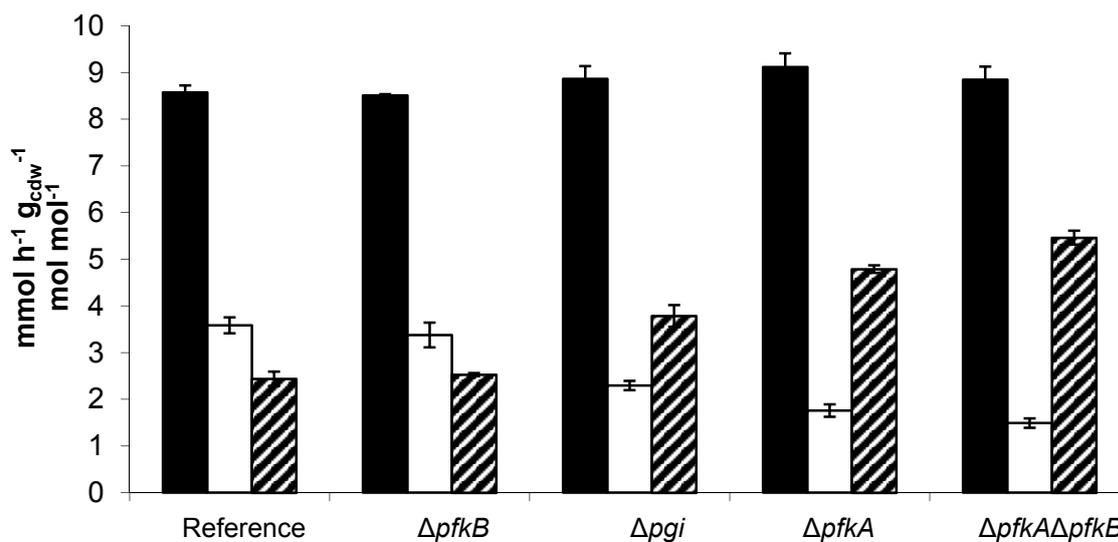
Fig. 2 Specific MHB production rates (black bars, mmol h⁻¹ (g cdw)⁻¹), specific glucose consumption rates (white bars, mmol h⁻¹ (g cdw)⁻¹) and ratio of MHB per consumed glucose (striped bars, mol mol⁻¹) of biotransformations with *E. coli* BL21(DE3) reference strain and deletion mutants. All strains carried the plasmid pBtac*Lbadh*. Mean values and standard deviations from at least three independent experiments are shown.

Fig. 3 Formation of by-products by *Escherichia coli* BL21(DE3) pBtac*Lbadh* (black bars), *E. coli* BL21(DE3) Δ*pfkA* pBtac*Lbadh* (white bars) and *Escherichia coli* BL21(DE3) Δ*pfkA*Δ*pfkB* pBtac*Lbadh* (grey bars) after 120 min biotransformation. Mean values from two independent experiments are shown.
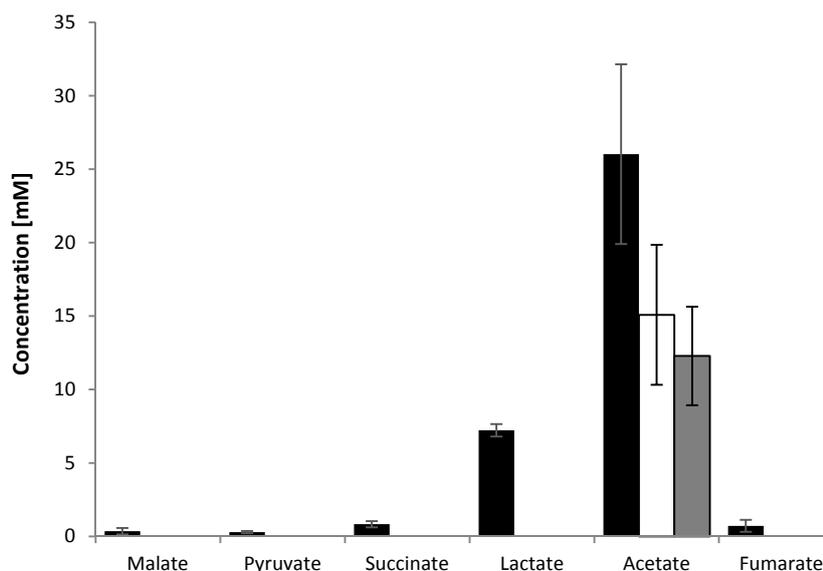
Formation of extracellular by-products during biotransformation

Samples for extracellular metabolite analysis were taken after 2 h of biotransformation (Fig. 3). The reference strain produced significant concentrations of lactate (7.2 ± 0.4 mM) and acetate (26.0 ± 6.1 mM). In the mutant strains Δ*pfkA* and Δ*pfkA*Δ*pfkB* no lactate and significantly lower concentrations of acetate (15.1 ± 3.9 mM and 12.3 ± 3.4 mM) were formed, caused by the redirection and reduction of the glucose flux. The decreased by-product formation also contributes to the increased Y_{RPG} of the mutant strains.

Intracellular redox ratios of pyridine nucleotides

The ratios of the redox pairs NADH/NAD$^+$ and NADPH/NADP$^+$ in the reference strain and the different deletion mutants were determined at three time points of the biotransformation (Table 3). The concentrations of

the pyridine nucleotides are listed in Table S1A, S1B. The ratios at time point zero were measured before the addition of the substrate MAA to the cells, but in the presence of glucose. The initial NADPH/NADP$^+$ ratios of the reference strain and the Δ*pfkB* mutant were similar corresponding to their similar Y_{RPG} values. Likewise, mutants Δ*pgi*, Δ*pfkA* and Δ*pfkA*Δ*pfkB* showed initial ratios of this redox pair which correlated with their biotransformation yields (Figure S2). The samples taken 30 and 120 min after the addition of MAA showed the expected drop of the NADPH/NADP$^+$ ratio, due to the rapid consumption of NADPH by the highly active, recombinant alcohol dehydrogenase. The ratios of NADH/NAD$^+$ before and after addition of the substrate MAA were similar in the reference strain and in the deletion mutants.

Table 3 Ratios of [NADPH]/[NADP$^+$] and [NADH]/[NAD$^+$] in *E. coli* reference strain and deletion mutants at three time points during biotransformation.

Strain	[NADPH]/[NADP$^+$]			[NADH]/[NAD$^+$]		
	Time (min)			Time (min)		
	0	30	120	0	30	120
Reference strain	0.21 ± 0.03	0.17 ± 0.04	0.17 ± 0.05	0.39 ± 0.10	0.48 ± 0.08	0.65 ± 0.03
Δ*pfkB*	0.22 ± 0.01	0.10 ± 0.02	0.15 ± 0.07	0.39 ± 0.07	0.42 ± 0.30	0.73 ± 0.35
Δ*pfkA*	0.50 ± 0.04	0.28 ± 0.02	0.21 ± 0.05	0.35 ± 0.19	0.44 ± 0.10	0.46 ± 0.05
Δ*pfkA*Δ*pfkB*	0.61 ± 0.09	0.10 ± 0.01	0.11 ± 0.07	0.30 ± 0.08	0.45 ± 0.24	0.40 ± 0.11
Δ*pgi*	0.46 ± 0.05	0.26 ± 0.09	0.16 ± 0.09	0.30 ± 0.18	0.42 ± 0.29	0.61 ± 0.30

All strains expressed the plasmid-encoded alcohol dehydrogenase gene from *Lactobacillus brevis*. Samples taken at the time point zero did not yet contain the biotransformation substrate MAA. Results were derived from at least two independent experiments.

Discussion

For reductive whole-cell biotransformations requiring NADPH, attempts were made in this work to increase the yield of mol NADPH per mol glucose in *E. coli*. In growing cells of *E. coli*, 12% of the glucose is catabolized via the PPP (Fuhrer et al. 2005). It may be assumed that this value is also true for glucose-metabolizing resting cells of *E. coli*. In order to increase the carbon flux from glucose through the PPP, glycolysis was interrupted either at the level of phosphoglucose isomerase (encoded by *pgi*) or at the level of phosphofructokinase I and II (encoded by *pfkA* and *pfkB*). The deletion of *pgi* likely results in a situation where 100% of glucose has to be metabolized via the PPP in a linear, non-cyclic fashion, yielding two mol NADPH per mol glucose. As a Y_{RPG} value of 3.8 mol MHB/mol glucose was obtained with the Δpgi mutant, additional NADPH must be generated by isocitrate dehydrogenase and/or transhydrogenase activities (Fuhrer and Sauer 2009). A slower glucose uptake rate of a Δpgi mutant was already reported previously and a connection between the re-oxidation rate of NADPH and the glucose uptake rate was shown (Sauer et al. 2004). A Δpgi mutant showed a growth defect, while a $\Delta pgi\Delta udhA$ double deletion mutant lacking in addition to phosphoglucose isomerase the soluble transhydrogenase UdhA did not grow on glucose at all. However, under our biotransformation conditions the NADPH level was kept low by the recombinant alcohol dehydrogenase, as shown by the decrease of the NADPH/NADP$^+$ ratio after addition of the substrate MAA (Table 3). Therefore, there must be a different reason for the lowered glucose uptake rate of the Δpgi mutant in our biotransformations, such as a limited flux capacity of the PPP or some kind of regulatory effect on enzymes involved in glucose uptake (Morita et al. 2003) or the PPP.

The deletion of *pfkA* and *pfkB* should result in a situation where fructose 6-phosphate formed either by glucose 6-phosphate isomerase or by transketolase or transaldolase cannot be channelled into glycolysis but has to be metabolized in the PPP. However, as the $\Delta pfkA\Delta pfkB$ still possessed residual phosphofructokinase activity, a minor fraction of fructose 6-phosphate might still be metabolized via the glycolytic pathway. With the $\Delta pfkA$ and the $\Delta pfkA\Delta pfkB$ mutants, Y_{RPG} values of 4.8 and 5.4 mol MHB/mol glucose were reached, respectively, indicating a partial cyclization of the PPP. The glucose consumption rates of these two mutants were even lower than that of the Δpgi mutant, possibly for the similar reasons described above for the Δpgi mutant and a limited availability of phosphoenolpyruvate (PEP) for glucose uptake via the PEP-dependent phosphotransferase system (PTS) (Roehl and Vinopal 1976). A consequence of the decreased carbon flux through the lower part of glycolysis and the tricarboxylic acid cycle was the significantly reduced formation of

acetate and the absence of lactate as a by-product in the $\Delta pfkA$ and $\Delta pfkA\Delta pfkB$ deletion mutants.

Work by Chin and Cirino (2011) published when the present paper was submitted presents results on the reduction of xylose to xylitol by engineered strains of *E. coli* using glucose as reductant. In these studies, the highest Y_{RPG} of 5.4 mol xylitol/mol glucose was obtained with a mutant lacking *pfkA* and *sthA* (alternative gene designation for *udhA*), which matches the highest Y_{RPG} of 5.46 mol MHB/mol glucose obtained in our work with a $\Delta pfkA\Delta pfkB$ mutant.

In the present work we show that the PPP can be implemented for an efficient regeneration of NADPH with glucose as the electron donor. Interruption of glycolysis by deletion of the genes encoding phosphofructokinases I and II resulted in a 44% higher ratio of reduced product per glucose (mol/mol) than by deletion of the *pgi* gene encoding phosphoglucose isomerase. Further studies aim at the elucidation and elimination of productivity-limiting bottlenecks of this reductive whole-cell biotransformation system.

References

Akinterinwa O, Cirino PC (2011) Anaerobic obligatory xylitol production in *Escherichia coli* strains devoid of native fermentation pathways. Appl Environ Microbiol 77:706-709

Blank LM, Ebert BE, Bühler B, Schmid A (2008) Metabolic capacity estimation of *Escherichia coli* as a platform for redox biocatalysis: constraint-based modeling and experimental verification. Biotechnol Bioeng 100:1050-1065

Bradford MM (1976) A rapid and sensitive method for the quantitation of microgram quantities of protein utilizing the principle of protein-dye binding. Anal Biochem 72:248-254

Bühler B, Park JB, Blank LM, Schmid A (2008) NADH availability limits asymmetric biocatalytic epoxidation in a growing recombinant *Escherichia coli* strain. Appl Environ Microbiol 74:1436-1446

Canonaco F, Hess TA, Heri S, Wang T, Szyperski T, Sauer U (2001) Metabolic flux response to phosphoglucose isomerase knock-out in *Escherichia coli* and impact of overexpression of the soluble transhydrogenase UdhA. FEMS Microbiol Lett 204:247-252

Chin JW, Cirino PC (2011) Improved NADPH supply for xylitol production by engineered *Escherichia coli* with glycolytic mutations. Biotechnol Prog 27:333-341

Chin JW, Khankal R, Monroe CA, Maranas CD, Cirino PC (2009) Analysis of NADPH supply during xylitol production by engineered *Escherichia coli*. Biotechnol Bioeng 102:209-220

Eguchi T, Kuge Y, Inoue K, Yoshikawa N, Mochida K, Uwajima T (1992) NADPH regeneration by glucose dehydrogenase from *Gluconobacter scleroides* for l-leucovorin synthesis. Biosci Biotechnol Biochem 56:701-703

Ernst M, Kaup B, Müller M, Bringer-Meyer S, Sahm H (2005) Enantioselective reduction of carbonyl compounds by whole-cell biotransformation, combining a formate dehydrogenase and a (*R*)-

specific alcohol dehydrogenase. Appl Microbiol Biotechnol 66:629-634

Fasan R, Crook NC, Peters MW, Meinhold P, Buelter T, Landwehr M, Cirino PC, Arnold FH (2010) Improved product-per-glucose yields in P450-dependent propane biotransformations using engineered *Escherichia coli*. Biotechnol Bioeng 108:500-510

Fraenkel DG, Kotlarz D, Buc H (1973) Two fructose 6-phosphate kinase activities in *Escherichia coli*. J Biol Chem 248:4865-4866

Fraenkel DG, Levisohn SR (1967) Glucose and gluconate metabolism in an *Escherichia coli* mutant lacking phosphoglucose isomerase. J Bacteriol 93:1571-1578

Fuhrer T, Fischer E, Sauer U (2005) Experimental identification and quantification of glucose metabolism in seven bacterial species. J Bacteriol 187:1581-1590

Fuhrer T, Sauer U (2009) Different biochemical mechanisms ensure network-wide balancing of reducing equivalents in microbial metabolism. J Bacteriol 191:2112-2121

Grose JH, Joss L, Velick SF, Roth JR (2006) Evidence that feedback inhibition of NAD kinase controls responses to oxidative stress. Proc Natl Acad Sci U S A 103:7601-7606

Hanahan D (1983) Studies on transformation of *Escherichia coli* with plasmids. J Mol Biol 166:557-580

Hanahan D, Jessee J, Bloom FR (1991) Plasmid transformation of *Escherichia coli* and other bacteria. Methods Enzymol 204:63-113

Heuser F, Schroer K, Lütz S, Bringer-Meyer S, Sahm H (2007) Enhancement of the NAD(P)(H) pool in *Escherichia coli* for biotransformation. Eng Life Sci 7:343-353.

Holm AK, Blank LM, Oldiges M, Schmid A, Solem C, Jensen PR, Vemuri GN (2010) Metabolic and transcriptional response to cofactor perturbations in *Escherichia coli*. J Biol Chem 285:17498-17506

Hua Q, Yang C, Baba T, Mori H, Shimizu K (2003) Responses of the central metabolism in *Escherichia coli* to phosphoglucose isomerase and glucose-6-phosphate dehydrogenase knockouts. J Bacteriol 185:7053-7067

Kaup B, Bringer-Meyer S, Sahm H (2004) Metabolic engineering of *Escherichia coli*: construction of an efficient biocatalyst for D-mannitol formation in a whole-cell biotransformation. Appl Microbiol Biotechnol 64:333-339

Kaup B, Bringer-Meyer S, Sahm H (2005) D-Mannitol formation from D-glucose in a whole-cell biotransformation with recombinant *Escherichia coli*. Appl Microbiol Biotechnol 99:397-403

Kruger NJ, von Schaewen A (2003) The oxidative pentose phosphate pathway: structure and organisation. Curr Opin Plant Biol 6:236-246

Lee HC, Kim JS, Jang W, Kim SY (2010) High NADPH/NADP$^+$ ratio improves thymidine production by a metabolically engineered *Escherichia coli* strain. J Biotechnol 149:24-32

Lee JN, Shin HD, Lee YH (2003) Metabolic engineering of pentose phosphate pathway in *Ralstonia eutropha* for enhanced biosynthesis of poly-beta-hydroxybutyrate. Biotechnol Prog 19:1444-1449

Liljeblad A, Kallinen A, Kanerva LT (2009) Biocatalysis in the preparation of the statin side chain. Curr Org Synth 6:362-379

Lim SJ, Jung YM, Shin HD, Lee YH (2002) Amplification of the NADPH-related genes *zwf* and *gnd* for the oddball biosynthesis of PHB in an *E. coli* transformant harboring a cloned *phbCAB* operon. J Biosci Bioeng 93:543-549

Link AJ, Phillips D, Church GM (1997) Methods for generating precise deletions and insertions in the genome of wild-type *Escherichia coli*: application to open reading frame characterization. J Bacteriol 179:6228-6237

Lundquist R, Olivera BM (1971) Pyridine nucleotide metabolism in *Escherichia coli*. I. Exponential growth. J Biol Chem 246:1107-1116

Matsumura H, Miyachi S (1980) Cycling assay for nicotinamide adenine dinucleotides. Meth Enzymol 69:465

Morita T, El-Kazzaz W, Tanaka Y, Inada T, Aiba H (2003) Accumulation of glucose 6-phosphate or fructose 6-phosphate is responsible for destabilization of glucose transporter mRNA in *Escherichia coli*. J Biol Chem 278:15608-15614

Nor'Aini AR, Shirai Y, Hassan MA, Shimizu K (2006) Investigation on the metabolic regulation of *pgi* gene knockout *Escherichia coli* by enzyme activities and intracellular metabolite concentrations. Malaysian Journal of Microbiology 2:24-31

Panke S, Wubbolts M (2005) Advances in biocatalytic synthesis of pharmaceutical intermediates. Curr Opin Chem Biol 9:188-194

Park J, Gupta RS (2008) Adenosine kinase and ribokinase--the RK family of proteins. Cell Mol Life Sci 65:2875-2896

Poulsen RB, Nøhr J, Douthwaite S, Hansen LV, Iversen JJL, Visser J, Ruijter GJG (2005) Increased NADPH concentration obtained by metabolic engineering of the pentose phosphate pathway in *Aspergillus niger*. FEBS J 272:1313-1325

Roehl RA, Vinopal RT (1976) Lack of glucose phosphotransferase function in phosphofructokinase mutants of *Escherichia coli*. J Bacteriol 126:852-860

Sambrook J, Russell DW (2001) Molecular cloning: a laboratory manual, 3rd ed. Cold Spring Harbor Laboratory Press, Cold Spring Harbor, N.Y.

Santamaría B, Estevez AM, Martinez-Costa OH, Aragon JJ (2002) Creation of an allosteric phosphofructokinase starting with a nonallosteric enzyme. The case of *Dictyostelium discoideum* phosphofructokinase. J Biol Chem 277:1210-1216

Sauer U, Canonaco F, Heri S, Perrenoud A, Fischer E (2004) The soluble and membrane-bound transhydrogenases UdhA and PntAB have divergent functions in NADPH metabolism of *Escherichia coli*. J Biol Chem 279:6613-6619

Stephanopoulos GN, Aristidou AA, Nielsen J (1998) Review of cellular metabolism. In: Stephanopoulos, GN, Aristidou, AA, Nielsen, J (eds), Metabolic engineering: principles and methodologies. Academic Press, San Diego:21-79

Vinopal RT, Clifton D, Fraenkel DG (1975) *PfkA* locus of *Escherichia coli*. J Bacteriol 122:1162-1171

Vinopal RT, Fraenkel DG (1975) *PfkB* and *pfkC* loci of *Escherichia coli*. J Bacteriol 122:1153-1161

Walton AZ, Stewart JD (2004) Understanding and improving NADPH-dependent reactions by nongrowing *Escherichia coli* cells. Biotechnol Prog 20:403-411

Zerez CR, Moul DE, Gomez EG, Lopez VM, Andreoli AJ (1987) Negative modulation of *Escherichia coli* NAD kinase by NADPH and NADH. J Bacteriol 169:184-188

Zhang W, O'Connor K, Wang DI, Li Z (2009) Bioreduction with efficient recycling of NADPH by coupled permeabilized microorganisms. Appl Environ Microbiol 75:687-694

Own proportion to this work: 70%

I performed the experimental work and wrote a draft of the manuscript.

Published in: Applied Microbiology and Biotechnology

Impact factor: 3.4

BIOTECHNOLOGICAL PRODUCTS AND PROCESS ENGINEERING

Engineering yield and rate of reductive biotransformation in *Escherichia coli* by partial cyclization of the pentose phosphate pathway and PTS-independent glucose transport

Solvej Siedler · Stephanie Bringer · Lars M. Blank · Michael Bott

Abstract Optimization of yields and productivities in reductive whole-cell biotransformations is an important issue for the industrial application of such processes. In a recent study with *Escherichia coli*, we analyzed the reduction of the prochiral β-ketoester methyl acetoacetate by an *R*-specific alcohol dehydrogenase (ADH) to the chiral hydroxy ester (*R*)-methyl 3-hydroxybutyrate (MHB) using glucose as substrate for the generation of NADPH. Deletion of the phosphofructokinase gene *pfkA* almost doubled the yield to 4.8 mol MHB per mole of glucose, and it was assumed that this effect was due to a partial cyclization of the pentose phosphate pathway (PPP). Here, this partial cyclization was confirmed by ^{13}C metabolic flux analysis, which revealed a negative net flux from glucose 6-phosphate to fructose 6-phosphate catalyzed by phospho-glucose isomerase. For further process optimization, the genes encoding the glucose facilitator (*glf*) and glucokinase (*glk*) of *Zymomonas mobilis* were overexpressed in recombinant *E. coli* strains carrying ADH and deletions of either *pgi* (phosphoglucose isomerase), or *pfkA*, or *pfkA* plus *pfkB*. In all cases, the glucose uptake rate was increased (30–47%), and for strains Δ*pgi* and Δ*pfkA* also, the specific MHB production rate was increased by 15% and 20%, respectively. The yield of the latter two strains slightly dropped by 11% and 6%, but was still 73% and 132% higher compared to the reference strain with intact *pgi* and *pfkA* genes and expressing *glf* and *glk*. Thus, metabolic engineering strategies are presented for improving yield and rate of reductive redox biocatalysis by partial cyclization of the PPP and by increasing glucose uptake, respectively.

Keywords *Escherichia coli* · NADPH yield · ^{13}C flux analysis · *pfkA* · *pfkB* · *pgi* · Reductive whole-cell biotransformation · *glf*

S. Siedler · S. Bringer (✉) · M. Bott (✉)
Institut für Bio- und Geowissenschaften, IBG-1: Biotechnologie,
Forschungszentrum Jülich,
52425 Jülich, Germany
e-mail: st.bringer-meyer@fz-juelich.de
e-mail: m.bott@fz-juelich.de

L. M. Blank
Department of Biochemical and Chemical Engineering,
TU Dortmund University,
Emil-Figge-Str. 66,
44227 Dortmund, Germany

L. M. Blank
Institute of Applied Microbiology, RWTH Aachen,
Worringerweg 1,
52074 Aachen, Germany

Introduction

Reductive whole-cell biotransformation is an important method for stereoselective industrial synthesis of chemical compounds. A variety of dehydrogenases catalyzes the enantio- and regioselective reduction of ketones and depends on nicotinamide adenine dinucleotide coen-zymes (NADH or NADPH) for hydride transfer. Especially alcohol dehydrogenases are most interesting for the production of chiral alcohols because these enzymes show notable chemo-, regio-, and enantiose-lectivity (Goldberg et al. 2007). Efficient coenzyme recycling by recombinant enzymes converting the oxidized coenzyme back to its reduced form is essential for the productivity of reductive whole-cell biotransfor-mations. In *Escherichia coli*, diverse strategies for cofactor regeneration have been applied: one-enzyme-

coupled systems (Eguchi et al. 1992; Ernst et al. 2005; Seelbach et al. 1996; Wichmann and Vasic-Racki 2005) and approaches taking advantage of the metabolism of the cell (Walton and Stewart 2004; Chin et al. 2009; Fasan et al. 2011; Blank et al. 2008, 2010).

In a recent study with *E. coli*, we analyzed the NADPH-dependent reduction of the prochiral β-ketoester methyl acetoacetate (MAA) to the chiral hydroxy ester (*R*)-methyl 3-hydroxybutyrate (MHB) using glucose as substrate for the generation of NADPH (Siedler et al. 2011). The reduction is catalyzed by an *R*-specific alcohol dehydrogenase (ADH) from *Lactobacillus brevis*, and MHB serves as a building block of statins (Panke and Wubbolts 2005). Redirection of glucose catabolism from glycolysis to the pentose phosphate pathway (PPP) was accomplished by deletion of phosphoglucose isomerase (*pgi*) or the phosphofructokinase isoenzyme (*pfkA, pfkB*) genes resulting in a higher MHB to glucose yield (Siedler et al. 2011). Similar results were obtained in a parallel study analyzing the reduction of xylose to xylitol in *E. coli* with an NADPH-dependent xylose reductase from *Candida boidinii* (Chin and Cirino 2011). Based on the product/glucose yields obtained with the $\Delta pfkA\Delta pfkB$ mutant, a partial cyclization of the PPP was assumed because these yields were near the theoretical maximum yield of 6 mol reduced product per mole of glucose consumed (Kruger and von Schaewen 2003).

To further elucidate and verify this assumption, we performed ^{13}C-based metabolic flux analyses with the $\Delta pfkA$ mutant in comparison to the Δpgi mutant, where a linear flux through the PPP is anticipated, as well as with the reference strain *E. coli* BL21(DE3). ^{13}C-based metabolic flux analysis is a key technology for attaining an overview on the carbon fluxes within the cell. It also represents the only technique to date that allows the determination of the cofactor regeneration rate, which is a valuable parameter for estimating for the capacity of metabolism for redox biocatalysis (Blank et al. 2008).

Furthermore, we tested the influence of an alternative glucose uptake system on the performance of the reductive biotransformation. For this purpose, we introduced into the *E. coli* strains the *glf* and *glk* genes of *Zymomonas mobilis* ATCC29191, which encode the glucose facilitator (Glf) and glucokinase (Glk). *Z. mobilis* has a three to ten times higher glucose uptake rate than *E. coli*, which is due to the high velocity of the glucose facilitator Glf (Parker et al. 1995; Weisser et al. 1995). Overexpression of *glf* is feasible for increasing the glucose uptake rate of *E. coli* and was successfully used in combination with the cofactor regenerating system glucose dehydrogenase for production of α-pinene oxide (Schewe et al. 2008) and mannitol (Kaup et al. 2004, 2005).

Materials and methods

Bacterial strains and plasmids

Strains and plasmids used in this work are listed in Table 1. The mutant strains were constructed as described previously (Siedler et al. 2011). *E. coli* strains were transformed by the method described by Hanahan (1983). Plasmids were selected by adding antibiotics to the medium at final concentrations of 100 μg ampicillin per milliliter (pBtac-*Lbadh*) and 50 μg kanamycin (pVWEx1, pVWEx1-*glf-glk*).

Media and growth conditions

Cells were cultivated in LB medium, 2xYT medium (16 g L^{-1} tryptone, 10 g L^{-1} yeast extract, 5 g L^{-1} sodium chloride) or M9 minimal medium (Sambrook and Russell 2001) containing 4 g L^{-1} glucose and supplemented with 1 mg mL^{-1} thiamine, 4 mg L^{-1} FeSO$_4\times$7 H$_2$O, 1 mg L^{-1} MnSO$_4$, 0.2 mg L^{-1} ZnSO$_4\times$7 H$_2$O, 0.4 mg L^{-1} CoCl$_2$, 0.1 mg L^{-1} CuCl$_2$, 0.2 mg L^{-1} Na$_2$MoO$_4\times$2 H$_2$O, and 0.005 mg L^{-1} H$_3$BO$_3$. Solid media contained 1.5% (*w/v*) agar. Liquid cultures were routinely incubated in test tubes or 500-mL-baffled Erlenmeyer flasks overnight at 37 °C and 130 rpm. For stock cultures, 1 mL of overnight LB culture was gently mixed with 1 mL 30% (*v/v*) glycerol and stored at −80 °C.

[13]C-Labeling experiments

The first preculture of *E. coli* was performed in 5 mL of LB medium for 9 h at 37 °C and 130 rpm. The cells were then transferred to the second preculture containing 10 mL of M9 minimal medium and grown overnight at 37 °C and 130 rpm, followed by inoculation of 50 mL of M9 medium after a washing step with M9 medium without glucose to an OD$_{600}$ of 0.05. In the main culture (50 mL M9 medium in a 500-mL Erlenmeyer flask) a mixture of 80% naturally labeled glucose and 20% [U-^{13}C] glucose was used. Samples were taken to determine the growth rate and the glucose uptake rate. For ^{13}C, metabolic flux analysis cells from 2-mL cultures were harvested during the exponential growth phase at an OD$_{600}$ of ~0.7.

The cells were washed with cold 2.7% (*w/v*) NaCl solution; the pellets were resuspended in 6 M HCl and incubated for 24 h at 105 °C for hydrolysis of proteins. The samples were dried in a Speedvac (Eppendorf concentrator 5301) under a hood. The dried hydrolysates were derivatized for Gas chromatography and mass spectrometry (GC–MS) analysis using 50 μL *N,N*-dimethylformamide and 50 μL *N*-(tert-butyldimethyl-silyl)-*N*-methyltrifluoroacetamide. GC–MS analysis was

Table 1 Strains and plasmids used in this work

Strains and plasmids	Relevant characteristics	Reference
Strains		
BL21 Star (DE3) (reference)	F⁻ *ompT hsdS*$_B$(r$_B$⁻, m$_B$⁻) *gal dcm rne*131 (DE3)	Invitrogen
Δpgi	BL21 Star (DE3) Δpgi	(Siedler et al. 2011)
$\Delta pfkA$	BL21 Star (DE3) $\Delta pfkA$	(Siedler et al. 2011)
$\Delta pfkA\Delta pfkB$	BL21 Star (DE3) Δpgi	(Siedler et al. 2011)
SS01	BL21 Star (DE3) with pBtac-*Lbadh*	(Siedler et al. 2011)
SS02	BL21 Star (DE3) Δpgi with pBtac-*Lbadh*	(Siedler et al. 2011)
SS03	BL21 Star (DE3) $\Delta pfkA$ with pBtac-*Lbadh*	(Siedler et al. 2011)
SS04	BL21 Star (DE3) $\Delta pfkA\Delta pfkB$ with pBtac-*Lbadh*	(Siedler et al. 2011)
Plasmids		
pBTac1	Amp^R, P$_{tac}$, *lacI*; expression vector for *E. coli*	Boehringer Mannheim GmbH
pBTac-*Lbadh*	pBtac1 derivative with *adh* gene from *Lactobacillus brevis*	X-Zyme, (Ernst et al. 2005)
pVWEx1	Kan^R; *C. glutamicum*/*E. coli* shuttle vector (P$_{tac}$, *lacI*^{q}; pHM1519, oriV$_{C.\ glutamicum}$, oriV$_{E.\ coli}$)	(Peters-Wendisch et al. 2001)
pVWEx1-*glf-glk*	pVWEx1 derivative with *glf* and *glk* genes from *Zymomonas mobils*	Eggeling et al. unpublished

carried out using a GC 3800, combined with an MS/MS 1200 unit (Varian Deutschland GmbH, Darmstadt, Germany). Fifteen detectable amino acids were separated on a FactorFour VF-5ms column (Varian Deutschland GmbH) at a constant flow rate of 1 mL helium per minute. The split ratio was 1:20, the injection volume was 1 μL, and the injector temperature was 250 °C. The temperature of the GC oven was kept constant for 2 min at 150 °C and was afterwards increased to 250 °C with a slope of 3 °C min⁻¹. The temperature of the transfer line and the source was 280 and 250 °C, respectively. Ionization was performed by electron impact ionization at −70 eV. For enhanced detection, a selected ion monitoring frame was defined for every amino acid (Wittmann 2007) GC–MS raw data were analyzed using the Workstation MS Data Review (Varian Deutschland GmbH) to check for detector overload (Heyland et al. 2009).

¹³C-constrained metabolic flux analysis

The stoichiometric model, implemented in FiatFlux (Zamboni et al. 2005b) for ¹³C-constrained metabolic flux analysis comprises the major pathways of *E. coli* central carbon metabolism (Fischer et al. 2004). To calculate intracellular fluxes, the stoichiometric model was constrained with three extracellular fluxes (growth rate, glucose uptake rate, and acetate formation rate) and five intracellular flux ratios (fraction of oxaloacetate originating from phosphoenolpyruvate, fraction of oxaloacetate derived through anaplerosis, fraction of phosphoenolpyruvate originating from oxaloacetate, and upper and lower bounds of pyruvate derived through malic enzyme). Error minimization during flux calculation

using the determined equation system was carried out as described previously (Fischer et al. 2004). The method for the determination of flux ratios is described in detail by Nanchen and coworkers (Nanchen et al. 2007), while the ¹³C-constrained flux analysis is described by Zamboni and coworkers (Zamboni et al. 2009).

Whole-cell biotransformation

For cultivation of the different recombinant *E. coli*, BL21 (DE3) strains carrying the plasmids pBtac-*Lbadh* and pVWEx1 or pVWEx1-*glf-glk*, a single colony of each strain, was inoculated into 5 mL of 2xYT medium containing the appropriate antibiotics and grown overnight at 37 °C and 170 rpm. These pre-cultures were used for inoculation of the main cultures to an OD$_{600}$ of 0.05. Main cultures were grown in 100 mL of 2xYT medium in the presence of the appropriate antibiotics at 37 °C and 130 rpm to an OD$_{600}$ of 0.3, induced with 1 mM of IPTG, incubated at 37 °C and 130 rpm for another 3 h and harvested at an OD$_{600}$ between 2 and 4.5, which had been determined as the optimal cell density for subsequent whole-cell biotransformation.

The cells were harvested by centrifugation (4,000×g, 7 min) and resuspended in reaction buffer containing 278 mM glucose, 2 mM MgSO$_4$, and 250 mM potassium phosphate buffer, pH 6.5, to a cell density of 3 g cell dry weight (cdw) per liter. The reaction started by adding 60 mM of MAA. Biotransformations were performed at 37 °C and 130 rpm to prevent cell sedimentation. Specific productivities (millimole MHB per hour per gram cdw) were determined by taking samples at 15-min time intervals over a period of 2 h. MHB and glucose concentrations of

the samples were determined (see below). Specific productivities were calculated by dividing the slope of graphs showing MHB concentration vs. time by the cell dry weight.

Analysis of substrates and products

Methyl acetoacetate (MAA), (R)-methyl 3-hydroxybutyrate (MHB), glucose and extracellular metabolites were analyzed by HPLC as described previously (Siedler et al. 2011). Glucose concentrations were also determined enzymatically by using the glucose Gluc-DH FS* Kit according to the instructions of the manufacturer (DiaSys, Holzheim, Germany).

Results

Growth behavior of reference and mutant strains

The growth kinetics of the reference and deletion strains were determined in M9 minimal medium (Fig. 1). The reference strain E. coli BL21(DE3) had the highest growth rate of 0.60 h^{-1} followed by the $\Delta pfkA$ mutant and the
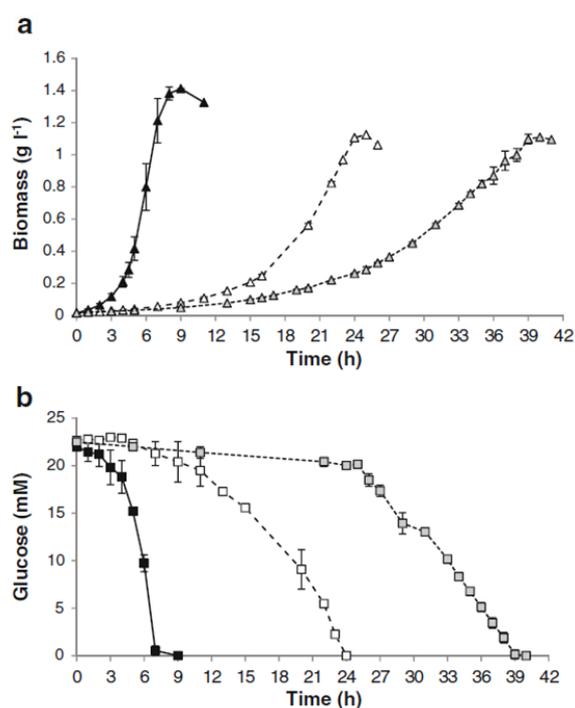
Δpgi mutant with 0.18 and 0.11 h^{-1}, respectively (Table 2). The specific glucose uptake rate was very high for the reference strain (11.3 mmol h^{-1} g$_{cdw}$$^{-1}$) but in the range of previously reported values (Toya et al. 2010) and significantly lower for the $\Delta pfkA$ mutant (4.0 mmol h^{-1} g$_{cdw}$$^{-1}$) and the Δpgi mutant (2.7 mmol h^{-1} g$_{cdw}$$^{-1}$). We chose the $\Delta pfkA$ mutant instead of the $\Delta pfkA \Delta pfkB$ mutant for flux analysis because of the very slow growth of the latter strain in glucose minimal media (Table 2).

In order to show cyclization of the PPP and to gain more insight into the metabolic network upon genetic perturbation of glycolysis, we measured the carbon fluxes of the reference strain and of the deletion strains Δpgi and $\Delta pfkA$ during growth in minimal medium with glucose as the sole carbon source (Fig. 2). Samples were taken in the early exponential growth phase at an OD$_{600}$ of ~0.7 where pseudo steady state conditions can be assumed. The reference strain showed similar flux distributions as reported previously for a batch culture with exception of a higher flux through the tricarboxylic acid (TCA) cycle and a much lower acetate formation (Toya et al. 2010). These differences might be due to the different origins of the E. coli B strain BL21(DE3) and the E. coli K12 strain BW25113 used by Toya and coworkers. The Δpgi mutant of BL21(DE3) showed a linear flux through the PPP, similar to the BW25113-derived Δpgi mutant, but again a twofold higher flux through the TCA cycle. The $\Delta pfkA$ mutant of BL21(DE3) showed a partial cyclization of the PPP with a negative net flux through the reaction from glucose 6-phosphate to fructose 6-phosphate catalyzed by phosphoglucose isomerase. This was consistent with the estimated carbon flux-based on the molar product per glucose yield achieved in the biotransformations reported previously (Chin and Cirino 2011). According to our flux analysis, the $\Delta pfkA$ mutant possessed about 30% residual phosphofructokinase activity. This value is close to the one obtained by in vitro enzyme activity measurements with cell extracts, which revealed 20% residual phosphofructo-

Fig. 1 a Growth of E. coli BL21(DE3) (black triangle) and the mutants $\Delta pfkA$ (white triangle) and Δpgi (gray triangle). **b** Glucose uptake of E. coli BL21(DE3) (black square) and the mutants $\Delta pfkA$ (white square) and Δpgi (gray square)

Table 2 Growth rates, glucose uptake rates, and cell yields (gram cdw per gram glucose) of the reference strain E. coli BL21(DE3) and three deletion mutants used in this study

Strain	Growth rate μ(h^{-1})	Glucose uptake rate (mmol h^{-1} g$_{cdw}$$^{-1}$)	Cell yield $Y_{X/S}$ (g g^{-1})
Reference	0.60±0.01	11.33±0.02	0.36±0.01
Δpgi	0.11±0.01	2.76±0.09	0.28±0.01
$\Delta pfkA$	0.18±0.01	4.00±0.08	0.28±0.01
$\Delta pfkA \Delta pfkB$	0.01±0.01	nd	nd

Mean values and standard deviations from at least three independent experiments are shown

nd not determined
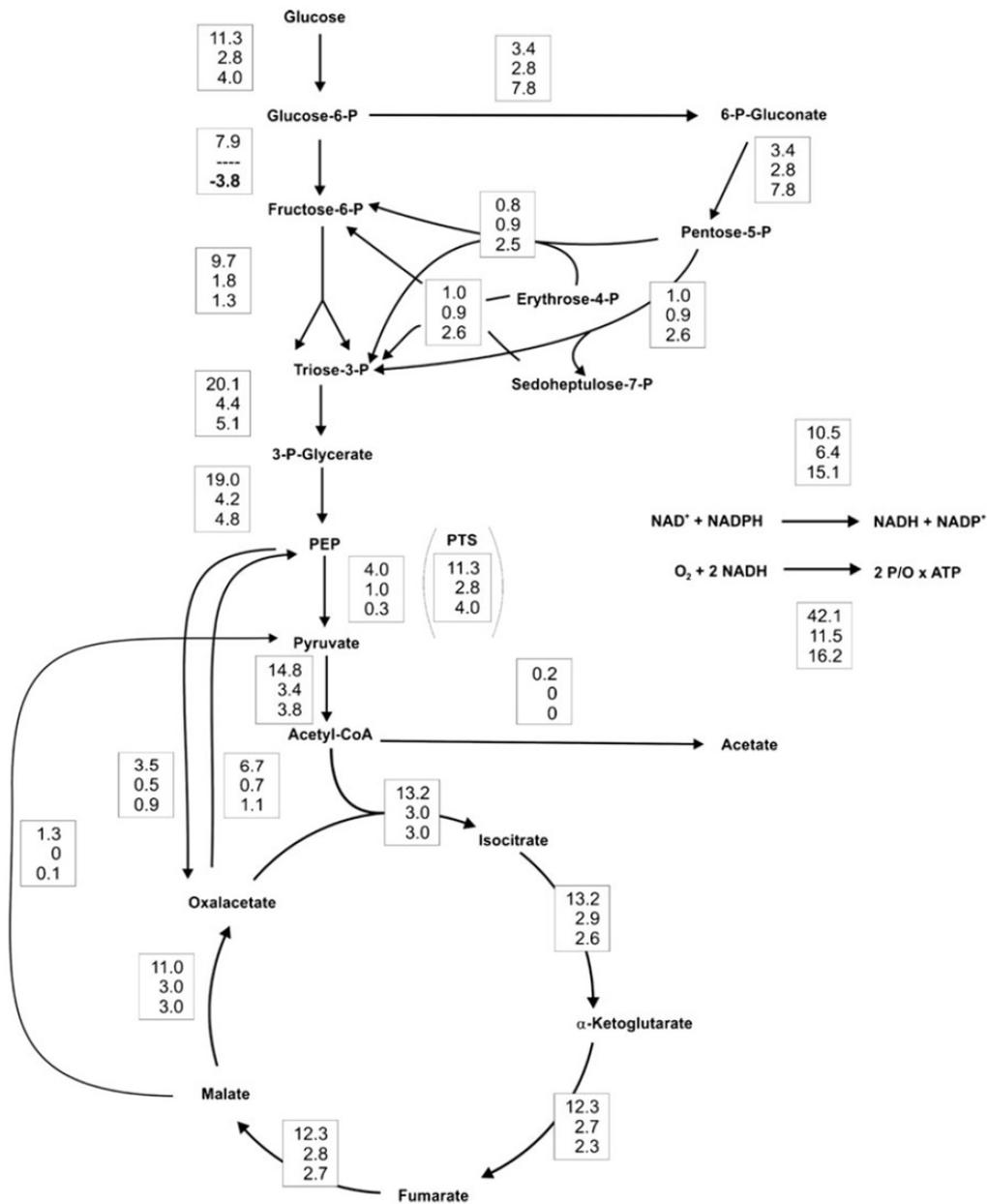
Fig. 2 Results of ^{13}C-based metabolic flux analysis of *E. coli* BL21 (DE3) (*upper number*) and mutant strains Δ*pgi* (*middle number*) and Δ*pfkA* (*lower number*) during exponential growth on glucose. In vivo carbon fluxes in central metabolism are shown as millimole per hour per gram cdw. Relative to the glucose uptake rate, the confidence intervals were 20% for the NADPH balance, below 15% for TCA cycle and malic enzyme, and less than 5% for all other fluxes. *Arrowheads* indicate the direction of a given flux

kinase activity in this mutant (Siedler et al. 2011). The residual activity is due to the PfkII isoenzyme.

Additionally, we calculated the NADH regeneration rates and the fluxes through the soluble transhydrogenase for an estimation of the reduced cofactor availability in the cells (Table 3). The NADH regeneration rates relative to the glucose uptake rates of all strains were similar, in contrast to a significantly higher flux through the soluble transhydrogenase UdhA in the Δ*pfkA* mutant (Table 3).

Table 3 NADH regeneration rates and fluxes through transhydrogenase UdhA calculated from the ^{13}C metabolic flux analysis

	Glucose uptake rate		NADH regeneration rate		NADPH+NAD$^+$→NADP$^+$+NADH	
	(mmol $g_{cdw}^{-1}h^{-1}$)	Percent	(mmol $g_{cdw}^{-1}h^{-1}$)	Percent	(mmol $g_{cdw}^{-1}h^{-1}$)	Percent
Reference strain	11.3	100	21.1	186	10.5	93
Δ*pgi*	2.8	100	5.8	205	6.4	229
Δ*pfkA*	4	100	8.1	203	15.1	378

The glucose uptake rates were set to 100%

Improvement of glucose uptake in whole-cell biotransformations

The ^{13}C metabolic flux analysis had indicated a very low flux through the reaction catalyzed by pyruvate kinase in the Δ*pgi* and especially the Δ*pfkA* mutant (Fig. 2), indicating that glucose uptake could be limited by PEP availability. This was also supported by the much lower specific glucose uptake rates of these two mutants (Table 2). Therefore, we tried to increase the glucose uptake rate and possibly also the biotransformation rate by introduction of an additional glucose uptake system. The glucose facilitator Glf from *Z. mobilis*, a transporter with a high velocity but a low affinity (Parker et al. 1995; Weisser et al. 1995), and the glucose kinase Glk of the same organism was chosen as an alternative pathway for increasing the rate of glucose uptake. As in our previous studies, the NADPH-dependent reduction of MAA to MHB by the (*R*)-specific alcohol dehydrogenase of *Lactobacillus brevis* was used as a model reaction for biotransformation, and the corresponding *adh* gene was overexpressed in all strains.

Overexpression of *glf* and *glk* using plasmid pVWEx1-*glf-glk* in the reference strain SS01 (*E. coli* BL21(DE3) containing pBTac-*Lbadh*) led to a 46% increased specific glucose uptake rate (Table 4), confirming the functional expression of the heterologous genes. However, the higher glucose uptake rate did not result in a higher biotransformation rate compared to the control strain SSO1 with plasmid pVWEx1. The molar yield of MHB per glucose

was even decreased by 34% in strain SS01/pVWEx1-*glf-glk* (Table 4). Expression of *glf* and *glk* in strains SS02 (containing the *pgi* deletion) and SS03 (containing the *pfkA* deletion) led to 30% and 41% increased glucose uptake rates, respectively, and also to 15% and 20% improved MHB production rates, compared to the corresponding strains with the empty vector pVWEx1. The ratio of MHB produced per glucose consumed decreased also in these strains by 11% (Δ*pgi* mutant) and 6% (Δ*pfkA* mutant) compared to the corresponding reference strains. This decrease could be due to the overexpression of *glf* and *glk*, leading to a high metabolic burden of heterologous protein production (Schweder et al. 2002; Dong et al. 1995; Bhattacharya and Dubey 1995). In the case of strain SS04 (deletion of *pfkA* and *pfkB*), overexpression of *glf* and *glk* led to a 40% increased glucose uptake rate, whereas MHB production rate was slightly decreased by 4% and the molar yield by 31% compared to the reference strain. The presence of the vector pVWEx1 showed no significant influence in strains SS01, SS02, and SS03 compared to the strains without this plasmid, but caused a much lower specific MHB production rate by strain SS04 compared to SS04 without pVWEx1.

Discussion

To improve reductive biotransformation we engineered the metabolic network of *E. coli*. Optimization of the

Table 4 Parameters for the whole-cell biotransformation of MAA to MHB with glucose as donor of reducing equivalents using the indicated *E. coli* strains

The detailed conditions are described in "Materials and methods." Mean values and standard deviations from at least three independent experiments are shown

Strain/Plasmid	MHB production rate (mmol h^{-1} g_{cdw}^{-1})	Glucose uptake rate (mmol h^{-1} g_{cdw}^{-1})	Yield (mol$_{MHB}$ mol$_{Glucose}^{-1}$)
SS01/pVWEx1	8.5±0.1	3.0±0.1	2.9±0.2
SS01/pVWEx1-*glf-glk*	8.6±0.3	4.4±0.2	1.9±0.1
SS02/pVWEx1	8.6±0.3	2.3±0.1	3.7±0.2
SS02/pVWEx1-*glf-glk*	9.9±0.4	3.0±0.3	3.3±0.3
SS03/pVWEx1	8.6±0.2	1.7±0.2	4.7±0.3
SS03/pVWEx1-*glf-glk*	10.3±0.1	2.4±0.3	4.4±0.2
SS04/pVWEx1	5.6±0.3	1.0±0.2	5.5±0.3
SS04/pVWEx1-*glf-glk*	5.4±0.4	1.4±0.1	3.8±0.4

yield was achieved by deleting phosphofructokinase genes resulting in a partial cyclization of the PPP. An increase of the glucose uptake rate by overexpression of the glucose facilitator gene *glf*, and the glucokinase gene *glk* from *Zymomonas mobilis* resulted in a higher specific biotransformation rate in the strains SS02 (*pgi* deletion) and SS03 (*pfkA* deletion).

Partial cyclization of the PPP in strain SS03 was confirmed by ^{13}C metabolic flux analysis of cells grown in glucose minimal medium, which revealed a negative net flux from glucose 6-phosphate to fructose 6-phosphate catalyzed by phosphoglucose isomerase. Under resting cell conditions, this partial cyclization resulted in a significant increase of the whole-cell biotransformation yield. A yield of 4.7 $mol_{MHB} mol_{Glucose}^{-1}$ was attained with strain SS03, which contained residual phosphofructokinase activity originating from *pfkB*. Although not shown by ^{13}C flux analysis, cyclic flux through the PPP should be even more intense in strain SS04 (*pfkApfkB* deletion) because the yield of strain SS04 with 5.5 $mol_{MHB} mol_{Glucose}^{-1}$ almost reached the theoretical maximum yield of 6 $mol_{NADPH} mol_{Glucose}^{-1}$ (Kruger and von Schaewen 2003). Strain SS02 displayed a somewhat higher yield (3.7 $mol_{MHB} mol_{Glucose}^{-1}$) than theoretically expected for reasons discussed recently (Siedler et al. 2011).

The Δpgi and $\Delta pfkA$ mutant strains showed strongly reduced glucose uptake rates, in agreement with previous studies (Sauer et al. 2004; Nanchen et al. 2007). Several reasons for the lower glucose uptake rate have already been discussed in literature. The Δpgi mutant has a high glucose 6-phosphate pool, which was reported to destabilize the *ptsG* mRNA and therefore decreases the glucose uptake capacity of the cell (Morita et al. 2003). For the $\Delta pfkA$ mutant, a second assumption was reported by Roehl and Vinopal (1976) according to which the reduced PEP concentration in this mutant decreases the glucose uptake rate because PEP is essential for glucose uptake by the phosphotransferase system. This assumption is consistent with the carbon fluxes through the pyruvate kinase reaction determined here, which were lower in the Δpgi mutant and nearly absent in the $\Delta pfkA$ mutant (Fig. 2).

In the SS01 strain, an increased glucose uptake rate did not result in higher rate of MAA reduction to MHB, indicating that another factor was limiting the rate of biotransformation, presumably NADPH availability (see below). In strains SS02 and SS03, glucose uptake limited the specific biotransformation rate, as shown by the increased MHB production rate upon overexpression of *glf* and *glk*.

For whole-cell biotransformation several limitations are possible, such as, enzyme activity, substrate import and product export, product toxicity, and cofactor regeneration rate, but most of them can be excluded in the model system used here. The alcohol dehydrogenase showed in vitro activities of 17 to 28 $U mg^{-1}$ in cell extracts (Siedler et al. 2011), which is comparable to a rate of at least 418 $mmol\ h^{-1}\ g_{cdw}^{-1}$ in vivo assuming that 41% of the cell dry weight is made up of soluble proteins (Zamboni et al. 2005a; Wittmann et al. 2007). This value is 40 times higher than the observed specific biotransformation rate and consequently, ADH activity is not limiting. Substrate and product transport can also be ruled out as limiting factors, because biotransformation rates of 33 $mmol_{MHB} h^{-1}\ g_{cdw}^{-1}$ were previously achieved using a substrate coupled biotransformation strategy with ADH catalyzing both, the reduction of MAA and the regeneration of NADPH by oxidation of 2-propanol (Schroer et al. 2009). With a formate dehydrogenase-coupled NADPH regeneration system, a value of 12 $mmol_{MHB} h^{-1}\ g_{cdw}^{-1}$ has been reported (Ernst et al. 2005). For the conversion of MAA to MHB, it was shown that there is no substrate and product inhibition, and neither substrate nor product are toxic to the cells under the chosen conditions (Tan 2006). Taken together, the biotransformation system used in this work is applicable for the detection of cofactor regeneration capabilities because this seems to be the limiting step.

Calculation of the NADH regeneration rate and transhydrogenase activity from ^{13}C flux analysis in growing cells revealed differences in the analyzed strains (Fig. 2). The relative fluxes through the soluble transhydrogenase UdhA converting NADPH to NADH were 2.5 and 4.1 times higher in the Δpgi mutant and the $\Delta pfkA$ mutant compared to the reference strain, respectively (Table 3). The yield of the biotransformation increased 1.3-fold in the SS02 strain and 1.6-fold in the SS03 strain compared to the SS01 strain, which indicated that under resting cell conditions ADH was competitive to UdhA with respect to NADPH utilization. Hence, deletion of UdhA would probably result in an increased yield, as was already demonstrated with another biotransformation system (Chin and Cirino 2011).

Having increased product yield and production rate by different strategies, future studies aim to combine these and additional strategies for further optimization of reductive whole-cell redox biocatalysis.

References

Bhattacharya SK, Dubey AK (1995) Metabolic burden as reflected by maintenance coefficient of recombinant *Escherichia coli* overexpressing target gene. Biotechnol Lett 17:1155–1160

Blank LM, Ebert BE, Bühler B, Schmid A (2008) Metabolic capacity estimation of *Escherichia coli* as a platform for redox biocatalysis: constraint-based modeling and experimental verification. Biotechnol Bioeng 100(6):1050–1065

Blank LM, Ebert BE, Bühler K, Bühler B (2010) Redox biocatalysis and metabolism: molecular mechanisms and metabolic network analysis. Antioxid Redox Signal 13(3):349–394

Chin JW, Cirino PC (2011) Improved NADPH supply for xylitol production by engineered *Escherichia coli* with glycolytic mutations. Biotechnol Prog 27(2):333–341

Chin JW, Khankal R, Monroe CA, Maranas CD, Cirino PC (2009) Analysis of NADPH supply during xylitol production by engineered *Escherichia coli*. Biotechnol Bioeng 102(1):209–220

Dong H, Nilsson L, Kurland CG (1995) Gratuitous overexpression of genes in *Escherichia coli* leads to growth inhibition and ribosome destruction. J Bacteriol 177(6):1497–1504

Eguchi T, Kuge Y, Inoue K, Yoshikawa N, Mochida K, Uwajima T (1992) NADPH regeneration by glucose dehydrogenase from *Gluconobacter scleroides* for l-leucovorin synthesis. Biosci Biotechnol Biochem 56(5):701–703

Ernst M, Kaup B, Müller M, Bringer-Meyer S, Sahm H (2005) Enantioselective reduction of carbonyl compounds by whole-cell biotransformation, combining a formate dehydrogenase and a (R)-specific alcohol dehydrogenase. Appl Microbiol Biotechnol 66(6):629–634

Fasan R, Crook NC, Peters MW, Meinhold P, Buelter T, Landwehr M, Cirino PC, Arnold FH (2011) Improved product-per-glucose yields in P_{450}-dependent propane biotransformations using engineered *Escherichia coli*. Biotechnol Bioeng 108(3):500–510

Fischer E, Zamboni N, Sauer U (2004) High-throughput metabolic flux analysis based on gas chromatography-mass spectrometry derived ^{13}C constraints. Anal Biochem 325(2):308–316

Goldberg K, Schroer K, Lütz S, Liese A (2007) Biocatalytic ketone reduction-a powerful tool for the production of chiral alcohols-part II: whole-cell reductions. Appl Microbiol Biotechnol 76(2):249–255

Hanahan D (1983) Studies on transformation of *Escherichia coli* with plasmids. J Mol Biol 166(4):557–580

Heyland J, Fu J, Blank LM (2009) Correlation between TCA cycle flux and glucose uptake rate during respiro-fermentative growth of *Saccharomyces cerevisiae*. Microbiology 155(Pt 12):3827–3837

Kaup B, Bringer-Meyer S, Sahm H (2004) Metabolic engineering of *Escherichia coli*: construction of an efficient biocatalyst for D-mannitol formation in a whole-cell biotransformation. Appl Microbiol Biotechnol 64(3):333–339

Kaup B, Bringer-Meyer S, Sahm H (2005) D-Mannitol formation from D-glucose in a whole-cell biotransformation with recombinant *Escherichia coli*. Appl Microbiol Biotechnol 69(4):397–403

Kruger NJ, von Schaewen A (2003) The oxidative pentose phosphate pathway: structure and organisation. Curr Opin Plant Biol 6(3):236–246

Morita T, El-Kazzaz W, Tanaka Y, Inada T, Aiba H (2003) Accumulation of glucose 6-phosphate or fructose 6-phosphate is responsible for destabilization of glucose transporter mRNA in *Escherichia coli*. J Biol Chem 278(18):15608–15614

Nanchen A, Fuhrer T, Sauer U (2007) Determination of metabolic flux ratios from ^{13}C-experiments and gas chromatography-mass spectrometry data: protocol and principles. Methods Mol Biol 358:177–197

Panke S, Wubbolts M (2005) Advances in biocatalytic synthesis of pharmaceutical intermediates. Curr Opin Chem Biol 9(2):188–194

Parker C, Barnell WO, Snoep JL, Ingram LO, Conway T (1995) Characterization of the *Zymomonas mobilis* glucose facilitator gene product (*glf*) in recombinant *Escherichia coli*: examination of transport mechanism, kinetics and the role of glucokinase in glucose transport. Mol Microbiol 15(5):795–802

Peters-Wendisch PG, Schiel B, Wendisch VF, Katsoulidis E, Mockel B, Sahm H, Eikmanns BJ (2001) Pyruvate carboxylase is a major bottleneck for glutamate and lysine production by *Corynebacterium glutamicum*. J Mol Microbiol Biotechnol 3(2):295–300

Roehl RA, Vinopal RT (1976) Lack of glucose phosphotransferase function in phosphofructokinase mutants of *Escherichia coli*. J Bacteriol 126(2):852–860

Sambrook J, Russell DW (eds) (2001) Molecular cloning: a laboratory manual. Cold Spring Harbor Laboratory, Cold Spting Harbor

Sauer U, Canonaco F, Heri S, Perrenoud A, Fischer E (2004) The soluble and membrane-bound transhydrogenases UdhA and PntAB have divergent functions in NADPH metabolism of *Escherichia coli*. J Biol Chem 279(8):6613–6619

Schewe H, Kaup BA, Schrader J (2008) Improvement of P450 (BM-3) whole-cell biocatalysis by integrating heterologous cofactor regeneration combining glucose facilitator and dehydrogenase in *E. coli*. Appl Microbiol Biotechnol 78(1):55–65

Schroer K, Zelic B, Oldiges M, Lütz S (2009) Metabolomics for biotransformations: Intracellular redox cofactor analysis and enzyme kinetics offer insight into whole cell processes. Biotechnol Bioeng 104(2):251–260

Schweder T, Lin HY, Jürgen B, Breitenstein A, Riemschneider S, Khalameyzer V, Gupta A, Büttner K, Neubauer P (2002) Role of the general stress response during strong overexpression of a heterologous gene in *Escherichia coli*. Appl Microbiol Biotechnol 58(3):330–337

Seelbach K, Riebel B, Hummel W, Kula MR, Tishkov VI, Egorov AM, Wandrey C, Kragl U (1996) A novel, efficient regenerating method of NADPH using a new formate dehydrogenase. Tetrahedron Lett 37:1377–1380

Siedler S, Bringer S, Bott M (2011) Increased NADPH availability in *Escherichia coli*: improvement of the product per glucose ratio in reductive whole-cell biotransformation. Appl Microbiol Biotechnol. doi:10.1007/s00253-011-3374-4

Tan I (2006) Applications of whole cell biotransformations for the production of chiral alcohols. Rheinische Friedrich-Wilhelms University of Bonn, Bonn

Toya Y, Ishii N, Nakahigashi K, Hirasawa T, Soga T, Tomita M, Shimizu K (2010) ^{13}C-metabolic flux analysis for batch culture of *Escherichia coli* and its *pyk* and *pgi* gene knockout mutants based on mass isotopomer distribution of intracellular metabolites. Biotechnol Prog 26(4):975–992

Walton AZ, Stewart JD (2004) Understanding and improving NADPH-dependent reactions by nongrowing *Escherichia coli* cells. Biotechnol Prog 20(2):403–411

Weisser P, Krämer R, Sahm H, Sprenger GA (1995) Functional expression of the glucose transporter of *Zymomonas mobilis* leads to restoration of glucose and fructose uptake in *Escherichia coli* mutants and provides evidence for its facilitator action. J Bacteriol 177(11):3351–3354

Wichmann R, Vasic-Racki D (2005) Cofactor regeneration at the lab scale. Adv Biochem Eng Biotechnol 92:225–260

Wittmann C (2007) Fluxome analysis using GC-MS. Microb Cell Fact 6:6

Wittmann C, Weber J, Betiku E, Kromer J, Bohm D, Rinas U (2007) Response of fluxome and metabolome to temperature-induced

recombinant protein synthesis in *Escherichia coli*. J Biotechnol 132(4):375–384

Zamboni N, Fischer E, Muffler A, Wyss M, Hohmann HP, Sauer U (2005a) Transient expression and flux changes during a shift from high to low riboflavin production in continuous cultures of *Bacillus subtilis*. Biotechnol Bioeng 89(2):219–232

Zamboni N, Fischer E, Sauer U (2005b) FiatFlux—a software for metabolic flux analysis from ^{13}C-glucose experiments. BMC Bioinformatics 6:209

Zamboni N, Fendt SM, Ruhl M, Sauer U (2009) ^{13}C-based metabolic flux analysis. Nat Protoc 4(6):878–892

Own proportion to this work: 50 %

With exception of measuring the labeling distributions by GC-MS and calculation of the fluxes I performed the experimental work. I designed the study and wrote the draft of the manuscript.

Published in: Applied Microbiology and Biotechnology

Impact factor: 3.4

BIOTECHNOLOGICAL PRODUCTS AND PROCESS ENGINEERING

Reductive whole-cell biotransformation with *Corynebacterium glutamicum*: improvement of NADPH generation from glucose by a cyclized pentose phosphate pathway using *pfkA* and *gapA* deletion mutants

Solvej Siedler · Steffen N. Lindner · Stephanie Bringer ·
Volker F. Wendisch · Michael Bott

Abstract In this study, the potential of *Corynebacterium glutamicum* for reductive whole-cell biotransformation is shown. The NADPH-dependent reduction of the prochiral methyl acetoacetate (MAA) to the chiral (*R*)-methyl 3-hydroxybutyrate (MHB) by an alcohol dehydrogenase from *Lactobacillus brevis* (*Lbadh*) was used as model reaction and glucose served as substrate for the regeneration of NADPH. Since NADPH is mainly formed in the oxidative branch of the pentose phosphate pathway (PPP), *C. glutamicum* was engineered to redirect carbon flux towards the PPP. Mutants lacking the genes for 6-phosphofructokinase (*pfkA*) or glyceraldehyde 3-phosphate dehydrogenase (*gapA*) were constructed and analyzed with respect to growth, enzyme activities, and biotransformation performance. Both mutants showed strong growth defects in glucose minimal medium. For biotransformation of MAA to MHB using glucose as reductant, strains were transformed with an *Lbadh* expression plasmid. The wild type showed a specific MHB production rate of 3.1 $mmol_{MHB}$ h^{-1} g_{cdw}^{-1} and a yield of 2.7 mol_{MHB} $mol_{glucose}^{-1}$. The $\Delta pfkA$ mutant showed a similar MHB production rate, but reached a yield of 4.8 mol_{MHB} $mol_{glucose}^{-1}$, approaching the maximal value of 6 mol_{NADPH} $mol_{glucose}^{-1}$ expected for a partially cyclized PPP. The specific biotransformation rate of the $\Delta gapA$ mutant was decreased by 62 % compared to the other strains, but the yield was increased to 7.9 mol_{MHB} $mol_{glucose}^{-1}$, which to our knowledge is the highest one reported so far for this mode of NADPH regeneration. As one fourth of the glucose was converted to glycerol, the experimental yield was close to the theoretically maximal yield of 9 mol_{NADPH} $mol_{glucose}^{-1}$.

Keywords *Corynebacterium glutamicum* · Pathway engineering · NADPH yield · Pentose phosphate pathway · Resting cells · Reductive whole-cell biotransformation · Phosphofructokinase · Glyceraldehyde 3-phosphate dehydrogenase · *pfk* · *gap*

Introduction

Whole-cell biotransformation has become an important method in chemoenzymatic synthesis, e.g., for the production of amino acids and chiral alcohols (Ishige et al. 2005). *Corynebacterium glutamicum* is a Gram-positive, non-pathogenic soil bacterium which is predominantly used for the large-scale industrial production of the flavor enhancer L-glutamate and the food additive L-lysine (Pfefferle et al. 2003; Kimura 2003; Hermann 2003). Recent metabolic engineering studies have shown that *C. glutamicum* is also capable of producing a variety of other commercially interesting compounds, e.g., other L-amino acids (Wendisch et al. 2006), D-amino acids (Stäbler et al. 2011), organic acids such as succinate (Okino et al. 2008; Litsanov et al. 2012a, b), diamines such as cadaverine (Mimitsuka et al. 2007) or putrescine (Schneider and Wendisch 2010), biofuels such as ethanol or isobutanol (Inui et al. 2004; Smith et al. 2010; Blombach et al. 2011), or proteins (Meissner et al. 2007). An overview of the product spectrum of *C. glutamicum* can be found in a recent review (Becker and Wittmann 2011).

Solvej Siedler and Steffen N. Lindner contributed equally to this work.

S. Siedler · S. Bringer (✉) · M. Bott (✉)
Institut für Bio–und Geowissenschaften, IBG-1: Biotechnologie,
Forschungszentrum Jülich GmbH,
52425 Jülich, Germany
e-mail: st.bringer-meyer@fz-juelich.de
e-mail: m.bott@fz-juelich.de

S. N. Lindner · V. F. Wendisch
Faculty of Biology & CeBiTec, Bielefeld University,
33615 Bielefeld, Germany

C. glutamicum was also shown to be a suitable host for whole-cell biotransformation with resting cells for production of mannitol (Bäumchen and Bringer-Meyer 2007) and cyclohexanone derivatives (Doo et al. 2009; Yun et al. 2012). These reactions are often NAD(P)H dependent and cofactor recycling is crucial for profitable processes. For example, formate dehydrogenase or glucose dehydrogenase are used, but only 1 mol NAD(P)H can be generated from 1 mol formate or 1 mol glucose (Kaup et al. 2004, 2005; Ernst et al. 2005; Eguchi et al. 1992; Tan 2006). Use of metabolically active cells gives the opportunity to regenerate reduced cofactors via sugar metabolism and to gain a higher reduced cofactor to glucose ratio (Chin and Cirino 2011).

In *Escherichia coli*, several attempts were made for engineering cellular metabolism towards a higher NADPH per glucose yield (Fasan et al. 2011; Akinterinwa and Cirino 2011). NADPH is mainly generated in the oxidative branch of the pentose phosphate pathway (PPP), where glucose 6-phosphate dehydrogenase catalyzes the oxidation of glucose 6-phosphate to 6-phosphoglucono-δ-lactone and 6-phosphogluconate dehydrogenase, which catalyzes the oxidative decarboxylation of 6-phosphogluconate to ribulose 5-phosphate, yielding 2 mol NADPH (Fig. 1). Therefore, employment of the PPP is an interesting option for NADPH-dependent processes (Chin and Cirino 2011; Chemler et al. 2010). In a recent study with *E. coli*, we analyzed the NADPH-dependent reduction of the prochiral β-ketoester methyl acetoacetate (MAA) to the chiral hydroxy ester (*R*)-methyl 3-hydroxybutyrate (MHB) using glucose as substrate for the

generation of NADPH (Siedler et al. 2011, 2012). The reduction was catalyzed by an *R*-specific alcohol dehydrogenase (ADH) from *Lactobacillus brevis*. MHB serves as a building block of statins (Panke and Wubbolts 2005). Deletion of *pfkA* and *pfkB* encoding phosphofructokinase I and II, respectively, resulted in a partial cyclization of the PPP and a yield of 5.4 mol_{MHB} $mol_{glucose}^{-1}$, which was near the theoretically maximal yield of 6 (Kruger and von Schaewen 2003).

To determine whether this metabolic engineering strategy can be generalized, is e.g. transferable to *C. glutamicum*, was one major goal of this study. It has to be kept in mind that differences exist in the repertoires of metabolic enzymes of *E. coli* and *C. glutamicum*. Of relevance for the present work is the occurrence of only one gene encoding a 6-phosphofructo1-kinase (*pfkA*) and the absence of genes encoding transhydrogenases and the key enzymes of the Entner–Doudoroff-pathway in *C. glutamicum* (Yokota and Lindley 2005). To further improve the NADPH per glucose yield, deletion of the glyceraldehyde 3-phosphate dehydrogenase (*gapA*) gene would be beneficial, as it should result in a complete cyclization of the PPP. Deletion of *gapA* theoretically enables a yield of 12 mol NADPH per mole of glucose 6-phosphate by complete recycling of fructose 6-phosphate and triose 3-phosphate through the oxidative PPP (Kruger and von Schaewen 2003). The *gapB* gene encoding a second glyceraldehyde 3-phosphate dehydrogenase in *C. glutamicum* should not be relevant in this context, as GapB does not function in the glycolytic direction (Omumasaba et al. 2004).

Fig. 1 Scheme of the upper part of glycolysis and pentose phosphate pathway of *C. glutamicum*. Gene deletions and NADPH generating reactions are indicated. *PTS* phosphotransferase system, *IolT1/IolT2* alternative glucose import system, *Glk* ATP-dependent glucokinase, *PpgK* polyphosphate/ATP-dependent glucokinase, *Pgi* phosphoglucose isomerase, *PfkA* phosphofructokinase, *GapA* glyceraldehyde-3-phosphate dehydrogenase, *DHAP* dihydroxyacetone phosphate, *PEP* phosphoenolpyruvate

In this study, we analyzed *C. glutamicum* mutants lacking either *pfkA* or *gapA* for their behavior in reductive whole-cell biotransformation. The results supported the view that the PPP operates in cyclic manner, oxidizing glucose to CO_2 with concomitant reduction of $NADP^+$ to NADPH.

Materials and methods

Chemicals and enzymes

Chemicals were obtained from Sigma-Aldrich (Taufkirchen, Germany), Qiagen (Hilden, Germany), Merck (Darmstadt, Germany), and Roche Diagnostics (Mannheim, Germany).

Bacterial strains, plasmids, media, and growth conditions

Strains and plasmids used in this work are listed in Table 1. *E. coli* strains were transformed by the method described by Hanahan (1983) and cultivated in LB medium (Miller 1972). *E. coli* DH5α was used for cloning purposes and *C. glutamicum* ATCC 13032 and derivatives for gene expression and whole-cell biotransformation. When required, antibiotics were added to the medium at a final concentration of 50 μg kanamycin ml^{-1} (pEKEx2-LbADH) or 100 μg spectinomycin ml^{-1} (pEKEx3 derivatives).

For growth experiments with *C. glutamicum*, 50-ml LB overnight cultures were inoculated from LB plates, harvested by centrifugation (10 min, $3,220 \times g$), washed in CgXII medium (Eggeling and Bott 2005), and inoculated in CgXII medium containing 100 mM glucose to a final optical density at 600 nm (OD_{600}) of 1. When appropriate, 1 mM isopropyl-β-D-thiogalactopyranosid (IPTG), 25 μg ml^{-1} kanamycin, and 100 μg ml^{-1} spectinomycin was added. For all growth experiments, 500 ml baffled shake flasks with 50 ml CgXII medium were used and incubated at 30 °C and 120 rpm. Growth was followed by OD_{600} determination using a UV-1650 PC photometer (Shimadzu, Duisburg, Germany). The biomass concentration was calculated from OD_{600} values using an experimentally determined correlation factor of 0.25 g (dry weight) of cells (cdw) per liter for an OD_{600} of 1 (Kabus et al. 2007). For the determination of enzyme activity in cell-free extracts, 50 ml LB medium containing 1 mM IPTG and 100 μg ml^{-1} spectinomycin was inoculated from LB overnight cultures to an OD_{600} of 0.5. At an OD_{600} of 4, cells were harvested by centrifugation (10 min, $3,220 \times g$, 4 °C) and stored at −20 °C until use.

Recombinant DNA work

Standard methods like polymerase chain reaction (PCR), restriction, or ligation were carried out according to established protocols (Sambrook and Russell 2001). *E. coli* cells were transformed by the $CaCl_2$ method (Hanahan et al. 1991). DNA sequencing was performed by Eurofins MWG Operon (Germany). Oligonucleotides (listed in Table 2) were synthesized by Biolegio bv (Nijmegen, The Netherlands) and Eurofins MWG Operon (Germany).

Construction of deletion mutants and plasmids

C. glutamicum deletion mutants were constructed using pK19*mobsacB* (Schäfer et al. 1994) using the procedure described by Niebisch and Bott (2001). Upstream and downstream flanking regions of *pfkA* (cg1409), and *gapA* (cg1791) were amplified by PCR using the oligonucleotide pairs pfkA-Del-A/pfkA-Del-B and pfkA-Del-C/pfkA-Del-D for deletion of *pfkA*, and gapA-Del-A/gapA-Del-B and gapA-Del-C/gapA-Del-D for deletion of *gapA* (see Table 2 for primer sequences). The upstream and downstream flanking regions of each gene were fused by overlap extension PCR, resulting in a DNA fragment of about 1 kb. The resulting PCR products were cloned into SmaI-restricted vector pK19*mobsacB* resulting in pK19*mobsacBΔpfkA*, and pK19*mobsacBΔgapA*. The correctness of the cloned PCR fragments was confirmed by DNA sequencing. Transformation of *C. glutamicum* wild type with these plasmids and selection for the first and second homologous recombination was performed as described (Niebisch and Bott 2001; Rittmann et al. 2003). Kanamycin-sensitive and sucrose-resistant clones were analyzed by PCR using oligonucleotide pairs pfkA-Del-Ver-fw/pfkA-Del-Ver-rv or gapA-Del-Ver-fw/gapA-Del-Ver-rv.

For the complementation of deletion mutants, the genes *pfkA* (cg1409), and *gapA* (cg1791) from *C. glutamicum* and the genes *pfkA* (b3916) and *pfkB* (b3916) from *E. coli* were amplified via PCR from genomic DNA of *C. glutamicum* WT, which was prepared as described previously (Eikmanns et al. 1995), and *E. coli* MG1655 genomic DNA, which was prepared by using the DNA isolation kit (Roche, Mannheim, Germany). PCR was performed using the following oligonucleotide pairs: pfkA-cgl-fw/pfkA-cgl-rv, gapA-cgl-fw/gapA-cgl-rv, pfkA-eco-fw/pfkA-eco-rv, and pfkB-eco-fw/pfkB-eco-rv (see Table 2). To allow IPTG-inducible expression of *pfkA*, and *gapA* from *C. glutamicum* and *pfkA*, and *pfkB* from *E. coli* the corresponding PCR products were ligated into the SmaI-restricted vector pEKEx3 resulting in pEKEx3-*pfkA*^{Cgl}, pEKEx3-*gapA*^{Cgl}, pEKEx3-*pfkA*^{Eco}, and pEKEx3-*pfkB*^{Eco}.

For the construction of the expression plasmid pEKEx2-*Lbadh*, the *adh* gene of *L. brevis* was amplified together with a 9-bp linker and an artificial ribosome binding site (AAGGAG) using the oligonucleotides Lbadh_for and Lbadh_rev and the plasmid pBtac*Lbadh* as template (Ernst et al. 2005). The PCR product was digested with *BamH*I and *EcoR*I and cloned into the vector pEKEx2. The correctness

Table 1 Strains and plasmids used in this work

Strains and plasmids	Relevant characteristics	Reference
Strains		
E. coli DH5α	F⁻ ø80Δ*lacZ*ΔM15 Δ(*lacZYA-argF*) U169 *deoR recA*1 *endA*1 *hsdR*17 (rk⁻, mk⁺) *phoA* supE44 λ⁻ *thi*-1 *gyrA*96 *relA*1	(Hanahan 1983), Invitrogen
C. glutamicum ATCC13032	Wild type, biotin auxotrophic	(Abe et al. 1967)
Δ*pfkA*	*C. glutamicum* ATCC13032 Δ*pfkA* (cg1409)	This study
Δ*gapA*	*C. glutamicum* ATCC13032 Δ*gapA* (cg1791)	This study
WT/pEKEx3	*C. glutamicum* ATCC13032 with pEKEx3	This study
WT/pEKEx3-*pfkA*^Cgl	*C. glutamicum* ATCC13032 with pEKEx3-*pfkA*^Cgl	This study
WT/pEKEx3-*pfkA*^Eco	*C. glutamicum* ATCC13032 with pEKEx3-*pfkA*^Eco	This study
WT/pEKEx3-*pfkB*^Eco	*C. glutamicum* ATCC13032 with pEKEx3-*pfkB*^Eco	This study
WT/pEKEx3-*gapA*^Cgl	*C. glutamicum* ATCC13032 with pEKEx3-*gapA*^Cgl	This study
WT/pEKEx2-*Lbadh*	*C. glutamicum* ATCC13032 with pEKEx2-*Lbadh*	This study
Δ*pfkA*/pEKEx3	*C. glutamicum* ATCC13032 Δ*pfkA* with pEKEx3	This study
Δ*pfkA*/pEKEx3-*pfkA*^Cgl	*C. glutamicum* ATCC13032 Δ*pfkA* with pEKEx3-*pfkA*^Cgl	This study
Δ*pfkA*/pEKEx3-*pfkA*^Eco	*C. glutamicum* ATCC13032 Δ*pfkA* with pEKEx3-*pfkA*^Eco	This study
Δ*pfkA*/pEKEx3-*pfkB*^Eco	*C. glutamicum* ATCC13032 Δ*pfkA* with pEKEx3-*pfkB*^Eco	This study
Δ*pfkA*/pEKEx2-*Lbadh*	*C. glutamicum* ATCC13032 Δ*pfkA* with pEKEx2-*Lbadh*	This study
Δ*gapA*/pEKEx3	*C. glutamicum* ATCC13032 Δ*gapA* with pEKEx3	This study
Δ*gapA*/pEKEx3-*gapA*^Cgl	*C. glutamicum* ATCC13032 Δ*gapA* with pEKEx3-*gapA*^Cgl	This study
Δ*gapA*/pEKEx2-*Lbadh*	*C. glutamicum* ATCC13032 Δ*gapA* with pEKEx2-*Lbadh*	This study
Plasmids		
pEKEx2	Kan^r; *E. coli*–*C. glutamicum* shuttle vector for regulated gene expression (P_tac *lacI*^q pBL1 *oriV*_C.g. pUC18 *oriV*_E.c.)	(Eikmanns et al. 1991)
pEKEx2-*Lbadh*	Kan^r; pEKEx2 derivative with *adh* gene from *Lactobacillus brevis*	This study
pEKEx3	Spec^r; *C. glutamicum*/*E. coli* shuttle vector (P_tac, *lacI*^q; pBL1, *oriV*_C.g., *oriV*_E.c.)	(Stansen et al. 2005)
pEKEx3-*pfkA*^Cgl	Spec^r; derivative of pEKEx3 for regulated expression of *pfkA* (cg1409) of *C. glutamicum*	This study
pEKEx3-*gapA*^Cgl	Spec^r; derivative of pEKEx3 for regulated expression of *gapA* (cg1791) of *C. glutamicum*	This study
pEKEx3-*pfkA*^Eco	Spec^r; derivative of pEKEx3 for regulated expression of *pfkA* (b3916) of *E. coli*	This study
pEKEx3-*pfkB*^Eco	Spec^r; derivative of pEKEx3 for regulated expression of *pfkB* (b1723) of *E. coli*	This study
pK19*mobsacB*	Kan^r; mobilizable *E. coli* vector used for the construction of *C. glutamicum* insertion and deletion mutants (RP4 *mob*; *sacB*_B.sub.; *lacZα*; *oriV*_E.c.)	(Schäfer et al. 1994)
pK19*mobsacB*Δ*pfkA*	Kan^r; pK19*mobsacB* derivative containing a PCR product which covers the flanking regions of the *C. glutamicum pfkA* (cg1409) gene	This study
pK19*mobsacB*Δ*gapA*	Kan^r; pK19*mobsacB* derivative containing a PCR product which covers the flanking regions of the *C. glutamicum gapA* (cg1791) gene	This study

of the cloned PCR fragments in the plasmids was confirmed by DNA sequencing.

Enzyme activity assays

For the determination of alcohol dehydrogenase activity, cells were harvested by centrifugation (10,000×*g*, 4 °C, 5 min) 30 min after start of biotransformation and stored at −20 °C until use. The cells were resuspended in 100 mM potassium phosphate buffer, pH 6.5, with 1 mM dithiothreitol and 1 mM MgCl₂. Cells were disrupted at 4 °C by 3× 15 s bead-beating with 0.1-mm-diameter glass beads using a Silamat S5 (Ivoclar Vivadent GmbH, Germany) and crude extracts were centrifuged at 16,000×*g* (4 °C, 20 min) to remove intact cells and cell debris. The supernatants were used as cell-free extracts. Alcohol dehydrogenase activity was determined photometrically at 340 nm using a mixture of 10 mM methyl acetoacetate, 250 μM NADPH, and 1 mM MgCl₂ in 100 mM potassium phosphate buffer, pH 6.5. The reactions were started by adding different dilutions of the cell-free extract. For rate calculation, an extinction coefficient for NADPH at 340 nm of 6.22 mM⁻¹ cm⁻¹ was used. One unit of enzyme activity corresponds to 1 μmol NADPH consumed per minute.

For the determination of the specific activity of phosphofructokinase and glyceraldehyde 3-phosphate dehydrogenase, cells were harvested by centrifugation (3,220×*g*, 4 °C, 10 min) and washed in the appropriate buffer (see below)

Table 2 Sequences of oligonucleotide primers

Name	Sequence (5′–3′)	Function and relevant characteristics
pfkA-cgl-fw	**GGATCC***GAAAGGAGG*CCCTTCAG<u>ATG</u>GAAGACATGCGAATTGCTAC	OE of Cgl *pfkA*; <u>start</u>; ***Bam*Hi**; *RBS*
pfkA-cgl-rv	**GGATCC**<u>CTA</u>TCCAAACATTGCCTGGGC	OE of Cgl *pfkA*; <u>stop</u>; ***Bam*Hi**
gapA-cgl-fw	*AAGGAGA*TATAGAT<u>ATG</u>ACCATTCGTGTTGGTATTAAC	OE of Cgl *gapA*; <u>start</u>; *RBS*
gapA-cgl-rv	<u>TTA</u>GAGCTTGGAAGCTACGAGCTC	OE of Cgl *gapA*; <u>stop</u>
pfkA-eco-fw	CC**GGATCC***GAAAGGAGG*CCCTTCAG<u>ATG</u>ATTAAGAAAATCGGTGTGTTGAC	OE of Eco *pfkA*; <u>start</u>; ***Bam*Hl**; *RBS*
pfkA-eco-rv	CC**GGATCC**<u>TTA</u>ATACAGTTTTTTCGCGCAGTC	OE of Eco *pfkA*; <u>stop</u>; ***Bam*Hl**
pfkB-eco-fw	GA**CTGCAG***GAAAGGAGG*CCCTTCAG<u>ATG</u>GTACGTATCTATACGTTGACAC	OE of Eco *pfkB*; <u>start</u>; ***Pst*I**; *RBS*
pfkB-eco-rv	GG**CTGCAG**<u>TTA</u>GCGGGAAAGGTAAGCGTAA	OE of Eco *pfkB*; <u>stop</u>; ***Pst*I**
pfkA-Del-A	CCGGAATATCTCGACGCCACAGAACGC	Del of *pfkA*
pfkA-Del-B	*CCCATCCACTAAACTTAAACA*AATTCGCATGTCTTCCATATTAAACCCATCACAACACCCGC	Del of *pfkA*; *linker sequence*
pfkA-Del-C	*TGTTTAAGTTTAGTGGATGGG*GAACGCTGGGTTACTGCCCAGGCAATGTTT	Del of *pfkA*; *linker sequence*
pfkA-Del-D	CCGAAGGAATAGACGAGTTAACAAAACTACGGTCTG	Del of *pfkA*
pfkA-Del-Ver-fw	GCCAAAACTCGAGTAGCCCGG	Verification of *pfkA* Del
pfkA-Del-Ver-rv	CCACAGCTTCAGTCATGCCC	Verification of *pfkA* Del
gapA-Del-A	GGCTGATCCTCAAATGACCAAG	Del of *gapA*
gapA-Del-B	*CCCATCCACTAAACTTAAACA*ACCAACACGAATGGTCATGTTG	Del of *gapA*; *linker sequence*
gapA-Del-C	*TGTTTAAGTTTAGTGGATGGG*CTGCGTCTGACCGAGCTCGTAG	Del of *gapA*; *linker sequence*
gapA-Del-D	CACCGAAGCCGTCAGAAACGAATG	Del of *gapA*
gapA-Del-Ver-fw	CCAACTTCGACGATGCCAATC	Verification of *gapA* Del
gapA-Del-Ver-rv	CTCTGGTGATTCTGCGATCTTTC	Verification of *gapA* Del
lbADH_for	CAGT**GGATCC***GAAAGGAGG*CCCTTCAG<u>ATG</u>TCTAACCGTTTGGATGG	OE of Lb *adh*; <u>start</u>; ***Bam*Hl**; *RBS*
lbADH_rev	GTCT**GAATTC**<u>TA</u>TTGAGCAGTGTAGCCACC	OE of Lb *adh*; <u>stop</u>; ***Eco*RI**

Restriction sites are highlighted in bold; linker sequences for crossover PCR and ribosomal binding sites are shown in italics; stop and start codons are underlined

OE overexpression, *Del* deletion, *RBS* ribosomal binding site, *Cgl C. glutamicum*, *Eco E. coli*

and stored at −20 °C until use. Cells were resuspended in 1 ml of the buffer and cell-free extracts were prepared by sonication as described previously (Stansen et al. 2005). All enzyme activity measurements were carried out at 30 °C. Protein concentrations were determined with bovine serum albumin as standard using Bradford reagents (Sigma, Taufkirchen, Germany).

6-Phosphofructokinase activity was measured spectrophotometrically at 340 nm according to Babul (1978) by a coupled enzymatic assay with pyruvate kinase and lactate dehydrogenase. ADP formed in kinase reaction was used to convert phosphoenolpyruvate to pyruvate, which was subsequently reduced to lactate with concomitant oxidation of NADH to NAD^+. The assay solution contained 100 mM Tris–HCl pH 7.5, 0.2 mM NADH, 1 mM ATP, 10 mM $MgCl_2$, and 0.2 mM phosphoenolpyruvate. One unit of enzyme activity corresponds to 1 μmol NADH oxidized per minute.

Glyceraldehyde 3-phosphate dehydrogenase activity was measured according to Omumasaba et al. (2004). The assay contained 1 mM NAD^+, 50 mM Na_2HPO_4, 0.2 mM EDTA, and 0.5 mM glyceraldehyde 3-phosphate in 50 mM triethanolamine hydrochloride (TEA) buffer pH 8.5. One unit of enzyme activity corresponds to 1 μmol NADH formed per minute.

Whole-cell biotransformation

For cultivation of the different recombinant *C. glutamicum* strains carrying the pEKEx2-*Lbadh* plasmid, a single colony of each strain was inoculated into 10 ml BHIS medium (37 g l^{-1} brain heart infusion, 91 g l^{-1} sorbitol) containing the appropriate selection marker as described above and grown overnight at 30 °C and 120 rpm. These pre-cultures were used for inoculation of the main cultures to an optical density at 600 nm (OD$_{600}$) of 0.4. Main cultures were grown in 100 ml BHIS medium in shake flasks in the presence of the appropriate selection marker and 0.5 mM IPTG at 30 °C and 120 rpm. The cells were harvested at an OD$_{600}$ between 2.5 and 5 by centrifugation (4,000×*g*, 4 °C, 7 min) and resuspended in a solution containing 111 mM glucose, 2 mM MgSO$_4$, and 250 mM potassium phosphate buffer, pH 6.5, to a cell density of 3 g$_{cdw}$ l^{-1}. The biotransformation was started by adding 50 mM MAA and conducted in shake flasks at 30 °C and 120 rpm to prevent cell sedimentation. Specific productivities (mmol$_{MHB}$ h^{-1} g$_{cdw}$$^{-1}$) were determined by taking samples at 30–60-min time intervals over a period of 3 h. MHB and glucose concentrations of the samples were determined (see below). Specific productivities were calculated by dividing the slope of graphs showing MHB concentration vs. time by the cell dry weight, which remained constant.

Analysis of substrates and products

Methyl acetoacetate (MAA), (*R*)-methyl 3-hydroxybutyrate (MHB), glucose, and extracellular metabolites were analyzed by HPLC as described previously (Siedler et al. 2011).

Results

Growth behavior and in vitro enzyme activities of *C. glutamicum* wild-type and mutant strains

In a *C. glutamicum* mutant lacking 6-phosphofructokinase, glucose catabolism is forced to proceed via the pentose phosphate pathway. Fructose 6-phosphate formed in the PPP by transaldolase or transketolase has to re-enter the oxidative part of the PPP again and only glyceraldehyde 3-phosphate can be catabolized further via the lower part of the glycolytic pathway. Thus, the initial part of glucose catabolism in a Δ*pfkA* mutant can be described by the following equation: Glucose 6-phosphate + 6 NADP$^+$ → Glyceraldehyde 3-phosphate + 3 CO$_2$ + 6 NADPH + 6 H$^+$. Thus, 6 mol NADPH are formed per mole of glucose.

The deletion of the *pfkA* gene prevented growth in CgXII medium with 100 mM glucose (Table 3). The growth defect of the Δ*pfkA* mutant was complemented to levels of the WT

control (0.32 h^{-1}) by plasmid-based overexpression of either the homologous *pfkA* gene from *C. glutamicum* (0.32 h^{-1}) or of the heterologous *pfkA* gene from *E. coli* (0.33 h^{-1}) and increased to 0.16 h^{-1} by heterologous expression of *pfkB* from *E. coli*. The slow growth of Δ*pfkA*/pEKEx3-*pfkB*^{Eco} was accompanied by a significantly higher biomass yield of 10.8 g l^{-1} compared to 8.4 g l^{-1} of WT/pEKEx3 or 8.6 g l^{-1} of strain Δ*pfkA*/pEKEx3-*pfkA*^{Cgl}.

6-Phosphofructokinase activity was absent in the *pfkA* deletion strain (Table 3). Plasmid-borne expression of *C. glutamicum pfkA* or of *E. coli pfkA* or *pfkB* increased phosphofructokinase activity in the WT background from 0.04 U mg^{-1} to 0.12, 0.11, and 0.19 U mg^{-1}, respectively. In the Δ*pfkA* background, phosphofructokinase activities of 0.10 to 0.13 U mg^{-1} were determined when either *C. glutamicum pfkA* or *E. coli pfkA* or *pfkB* was overexpressed (Table 3).

C. glutamicum possesses two glyceraldehyde 3-phosphate dehydrogenases, GapA and GapB, but only GapA functions in the glycolytic direction as a Δ*gapA* deletion mutant was unable to grow in glucose minimal medium whereas a Δ*gapB* mutant showed no growth defect under these conditions (Omumasaba et al. 2004). A complete block of glyceraldehyde 3-phosphate conversion to 1,3-bisphosphoglycerate should lead to a complete oxidation of glucose in the PPP according to the equation: Glucose + 6 H$_2$O + 12 NADP$^+$ → 6 CO$_2$ + 12 NADPH + 12 H$^+$.

In agreement with previous results (Omumasaba et al. 2004), a deletion of the *gapA* gene in strain ATCC 13032 resulted in an inability to grow in glucose minimal medium. This defect was complemented by plasmid-based overexpression of the *gapA* gene. NAD$^+$-dependent glyceraldehyde-3-phosphate dehydrogenase activity of cell-free extracts was 0.15 U mg^{-1} in WT/pEKEx3

Table 3 Growth rates (μ) and biomass concentrations [cell dry weight (cdw) l^{-1}] in glucose minimal medium with 1 mM IPTG and 100 µg ml^{-1} spectinomycin, and specific phosphofructokinase (Pfk) activity in cell extracts of the indicated *C. glutamicum* strains after cultivation in LB medium with 1 mM IPTG and 100 µg ml^{-1} spectinomycin

C. glutamicum	μ (h^{-1})	cdw (g l^{-1})[a]	Pfk activity (µmol min^{-1} mg^{-1})
WT/pEKEx3	0.32±0.00	8.43±0.18	0.04±0.01
WT/pEKEx3-*pfkA*^{Cgl}	0.30±0.00	8.13±0.07	0.12±0.02
WT/pEKEx3-*pfkA*^{Eco}	0.32±0.00	7.53±0.02	0.11±0.02
WT/pEKEx3-*pfkB*^{Eco}	0.32±0.00	8.48±0.03	0.19±0.02
Δ*pfkA*/pEKEx3	0.00±0.00	0.14±0.01[b]	0.00±0.00
Δ*pfkA*/pEKEx3-*pfkA*^{Cgl}	0.32±0.01	8.63±0.07	0.10±0.01
Δ*pfkA*/pEKEx3-*pfkA*^{Eco}	0.33±0.00	7.93±0.33	0.10±0.02
Δ*pfkA*/pEKEx3-*pfkB*^{Eco}	0.16±0.00	10.80±0.10	0.13±0.01

[a] Determination of cdw at maximal biomass

[b] Determination of cdw after 24 h

and absent in strain $\Delta gapA$/pEKEx3. In strains WT/pEKEx3-*gapA* and $\Delta gapA$/pEKEx3-*gapA*, the glyceraldehyde 3-phosphate dehydrogenase activity with NAD$^+$ was found to be 0.26 and 0.13 U mg^{-1}, respectively (Table 4).

Biotransformation of MAA to MHB with the reference and the mutant strains

For biotransformation of MAA to MHB, the gene encoding the (R)-specific alcohol dehydrogenase of *L. brevis* (*Lbadh*) was overexpressed in *C. glutamicum* WT and in the deletion strains $\Delta pfkA$ and $\Delta gapA$ using plasmid pEKEx2-*Lbadh*. The specific NADPH-dependent MAA dehydrogenase activity in cell-free extracts of these strains was similar, ranging from 0.51 to 0.76 U mg^{-1} in independent experiments. Assuming that the in vivo activities are comparable, they are not limiting the biotransformation rate. The *C. glutamicum* wild type showed a MAA dehydrogenase activity below 0.01 U mg^{-1} with either NADPH or NADH as cofactor indicating that the biotransformation occurred only in the presence of the recombinant ADH from *L. brevis*. For the biotransformation, the strains were cultivated in BHIS medium to the exponential growth phase and then harvested and resuspended in 250 mM potassium phosphate buffer pH 6.5 containing 111 mM glucose and 2 mM MgSO$_4$ to a cell density of 3 g$_{cdw}$ l^{-1}. The resulting cell suspensions were incubated at 30 °C and 120 rpm and the biotransformation was started by adding 50 mM MAA.

The kinetics of MHB production and of glucose consumption of the wild-type and the two mutant strains carrying pEKEx2-*Lbadh* over a period of 180 min are shown in Fig. 2, and the rates and yields are listed in Table 5. It is evident from Fig. 2 that the rates of MHB production and glucose consumption were almost constant within the time period investigated and proportional to each other. The strain WT/pEKEx2-*Lbadh* showed an MHB production rate

Table 4 Growth rates (μ) and biomass concentrations [cell dry weight (cdw) l^{-1}] in glucose minimal medium with 1 mM IPTG and 100 μg ml^{-1} spectinomycin, and specific NAD$^+$-dependent glyceraldehyde 3-phosphate dehydrogenase (GAPDH) activity in cell extracts of the indicated *C. glutamicum* strains after cultivation in LB medium with 1 mM IPTG and 100 μg ml^{-1} spectinomycin

C. glutamicum	μ (h^{-1})	cdw (g l^{-1})[a]	GAPDH activity (μmol min^{-1} mg^{-1})
WT/pEKEx3	0.33±0.01	7.80±0.07	0.15±0.02
WT/pEKEx3-*gapA*^{Cgl}	0.31±0.00	8.08±0.11	0.26±0.03
$\Delta gapA$/pEKEx3	0.00±0.01	0.00±0.00[b]	0.00±0.00
$\Delta gapA$/pEKEx3-*gapA*^{Cgl}	0.27±0.01	7.99±0.30	0.13±0.02

[a] Determination of cdw at maximal biomass

[b] Determination of cdw after 24 h

of 3.14 mmol h^{-1} g$_{cdw}$$^{-1}$ and a glucose consumption rate of 1.17 mmol h^{-1} g$_{cdw}$$^{-1}$. This resulted in a MHB yield of 2.7 mol per mole of glucose, corresponding to an NADPH yield of 2.7 mol per mole of glucose. The strain $\Delta pfkA$/pEKEx2-*Lbadh* had an 8 % reduced MHB production rate and a 49 % reduced glucose consumption rate, resulting in a 78 % increased MHB yield of 4.8 mol per mole of glucose. The strain $\Delta gapA$/pEKEx2-*Lbadh* showed a 62 % decreased MHB production rate and an 87 % reduced glucose consumption rate, corresponding to a 193 % increase of the MHB yield of 7.9 mol per mole of glucose. As discussed below, the strongly reduced glucose uptake rate of the strain $\Delta gapA$/pEKEx2-*Lbadh* is most likely a consequence of the fact that the strain does not form PEP.

By-product formation of wild-type and mutant strains

During biotransformation, by-product formation was nearly constant and specific rates were calculated (Table 5). The strain WT/pEKEx2-*Lbadh* showed an acetate formation rate (1.19 mmol h^{-1} g$_{cdw}$$^{-1}$) comparable to the glucose consumption rate (1.17 mmol h^{-1} g$_{cdw}$$^{-1}$). In addition, WT/pEKEx2-*Lbadh* formed succinate as by-product with a rate of 0.19 mmol h^{-1} g$_{cdw}$$^{-1}$. A low acetate production rate of 0.05 mmol h^{-1} g$_{cdw}$$^{-1}$ was shown by the strain $\Delta pfkA$/pEKEx2-*Lbadh*, which corresponds to only 8 % of the glucose uptake rate. Succinate was not formed by $\Delta pfkA$/pEKEx2-*Lbadh*. The strain $\Delta gapA$/pEKEx2-*Lbadh* formed neither acetate nor succinate, but glycerol with a rate of 0.08 mmol h^{-1} g$_{cdw}$$^{-1}$, which corresponds to 53 % of the glucose consumption rate. As glyceraldehyde 3-phosphate cannot be catabolized to pyruvate in the $\Delta gapA$ mutant, reduction to glycerol presents an alternative pathway to oxidation in the cyclic PPP.

Discussion

For reductive whole-cell biotransformations requiring NADPH, attempts were made in this work to increase the NADPH yield per mole of glucose using *C. glutamicum* as host strain and the reduction of MAA to MHB as NADPH-requiring model reaction. Rerouting of glucose catabolism from glycolysis to the oxidative PPP was achieved by deletion of either the *pfkA* gene or the *gapA* gene.

C. glutamicum wild type carrying pEKEx2-*Lbadh* showed a 31 % lower specific MHB production rate compared to *E. coli* carrying pBtac-*Lbadh*, even when compared to an *E. coli* biotransformation conducted at 30 °C (unpublished data). This difference might be due to a lower glucose uptake capacity or to a generally lower metabolic flux capacity of *C. glutamicum*. Overexpression of the genes involved in glucose uptake and catabolism via glycolysis

Fig. 2 Kinetics of MHB production (*open squares*) and glucose consumption (*filled squares*) during biotransformation of MAA to MHB using resting cells (3 g_{cdw} l^{-1}) of the indicated *C. glutamicum* strains carrying the plasmid pEKEx2-*Lbadh*. The cell suspensions were incubated at 30 °C and 120 rpm. Mean values and standard deviations from three independent experiments are shown

or PPP could improve the rate of glucose catabolism, as shown recently for oxygen-deprived conditions (Yamamoto et al. 2012; Jojima et al. 2010). The MHB per glucose yield found for *C. glutamicum* WT/pEKEx2-*Lbadh* (2.7 mol/mol) was 10 % higher than the corresponding value determined for *E. coli* BL21(DE3)/pBtac-*Lbadh* (2.44 mol/mol) (Siedler et al. 2011), which might be due to slight differences in the partition of glucose 6-phosphate between glycolysis and the PPP.

Biotransformation studies with *E. coli* Δ*pfkA* and Δ*pfkA*Δ*pfkB* mutants expressing *Lbadh* showed yields of 4.8 and 5.4 mol_{MHB} $mol_{glucose}^{-1}$, respectively (Siedler et al. 2011). ^{13}C metabolic flux analysis demonstrated a negative net flux through phosphoglucose isomerase in the Δ*pfkA* mutant, in compliance with the proposed partial cyclization of the PPP (Siedler et al. 2012). The MHB yield per glucose of the *E. coli* strain Δ*pfkA*/pBtac-*Lbadh* was comparable to that of the *C. glutamicum* strain Δ*pfkA*/pEKEx2-*Lbadh* (4.8 mol_{MHB} $mol_{glucose}^{-1}$), indicating that a partial cyclization of the PPP occurred in the latter species, too. Furthermore, similarities were found when comparing by-product formation in *E. coli* and *C. glutamicum*. Less acetate and no succinate was produced in both Δ*pfkA* mutant strains compared to the reference strains within the experimental period, presumably as a consequence of a decreased carbon flux through the lower part of glycolysis and the TCA cycle in these mutants (Siedler et al. 2012).

C. glutamicum possesses two glyceraldehyde 3-phosphate dehydrogenases (GAPDH), but only GapA functions in the glycolytic direction (Omumasaba et al. 2004). Thus, a deletion of the corresponding gene theoretically should result in a cyclization of the PPP. The fact that the MHB per glucose yield of the strain Δ*gapA*/pEKEx2-*Lbadh* (7.9 mol/mol) was higher compared to the strain Δ*pfkA*/pEKEx2-*Lbadh* and corresponded to 66 % of the maximal value of 12 mol NADPH per mole of glucose indicated a more extended cyclic operation of the PPP in the Δ*gapA* mutant compared to the Δ*pfkA* mutant. The maximal value for a complete oxidation of glucose in the PPP was not reached because 25 % of the glucose carbon was lost by reduction of glyceraldehyde 3-phosphate to glycerol. Taking this loss into account, only 9 mol_{MHB} $mol_{glucose}^{-1}$ could be achieved maximally. The experimental yield of 7.9 mol_{MHB} $mol_{glucose}^{-1}$ corresponds to 88 % of this value and is 46 % above the best yields reported so far (Chin and Cirino 2011; Siedler et al. 2011, 2012). Future yield optimization could be achieved by deletion of the gene encoding glycerol 3-phosphatase. Such a deletion was recently shown to prevent glycerol formation, which predominantly occurs in fructose-utilizing *C. glutamicum* strains (Lindner et al. 2012).

The strongly reduced biotransformation rate of the strain Δ*gapA*/pEKEx2-*Lbadh* was probably a consequence of the diminished capability for glucose uptake. In a Δ*gapA* mutant, no PEP should be formed during glucose catabolism and consequently, glucose uptake via the PTS should be impossible. PTS-independent glucose uptake has recently been described for *C. glutamicum*. It involves the inositol transporters IolT1 and IolT2 which also function as low-affinity glucose permeases (Lindner et al. 2011). Subsequent phosphorylation of glucose to glucose 6-phosphate is

Table 5 Biotransformation parameters and by-product formation of *C. glutamicum* wild-type and deletion mutants carrying plasmid pEKEx2-*Lbadh*

C. glutamicum strain	Specific MHB production rate (mmol h^{-1} g$_{cdw}^{-1}$)	Specific glucose consumption rate (mmol h^{-1} g$_{cdw}^{-1}$)	Yield (mol$_{MHB}$ mol$_{Glucose}^{-1}$)	Specific acetate formation rate (mmol h^{-1} g$_{cdw}^{-1}$)	Specific succinate formation rate (mmol h^{-1} g$_{cdw}^{-1}$)	Specific glycerol formation rate (mmol h^{-1} g$_{cdw}^{-1}$)
WT/pEKEx2-*Lbadh*	3.14±0.13	1.17±0.07	2.7±0.1	1.19±0.01	0.19±0.01	0
Δ*pfkA*/pEKEx2-*Lbadh*	2.88±0.08	0.60±0.01	4.8±0.2	0.05±0.01	0	0
Δ*gapA*/pEKEx2-*Lbadh*	1.20±0.04	0.15±0.03	7.9±0.9	0	0	0.08±0.04

catalyzed either by an ATP-dependent glucokinase encoded by *glk* (Park et al. 2000) or by the polyphosphate- or ATP-dependent glucose kinase PpgK (Lindner et al. 2010). It can be assumed that glucose uptake during biotransformation with the $\Delta gapA$ mutant occurs via this alternative pathway, as the observed glucose consumption rate of 2.5 nmol min^{-1} mg$_{cdw}^{-1}$ (Table 5) at glucose concentrations >10-fold above the apparent K_s values of IolT1 and IolT2 (2.8 and 1.9 mM, respectively) is in the range determined for PTS-independent glucose uptake at 1 mM glucose (0.7 nmol min^{-1} mg$_{cdw}^{-1}$) (Lindner et al. 2011). Overexpression of either *iolT1* or *iolT2* together with *ppgK* was shown to allow almost wild-type growth rates in a PTS-negative mutant (Lindner et al. 2011) and thus would probably also allow higher biotransformation rates of a $\Delta gapA$ mutant. Alternatively, expression of the glucose facilitator gene *glf* from *Zymomonas mobilis* could help to increase glucose uptake (Weisser et al. 1995; Parker et al. 1995).

Overall, we could demonstrate the potential of *C. glutamicum* for NADPH-dependent reductive whole-cell biotransformation and show that deletion of either *pfkA* or *gapA* is beneficial to improve the NADPH per glucose yield, presumably by cyclization of the PPP.

References

Abe S, Takayarna K, Kinoshita S (1967) Taxonomical studies on glutamic acid producing bacteria. J Gen Appl Microbiol 13 (3):279–301

Akinterinwa O, Cirino PC (2011) Anaerobic obligatory xylitol production in *Escherichia coli* strains devoid of native fermentation pathways. Appl Environ Microbiol 77(2):706–709

Babul J (1978) Phosphofructokinases from *Escherichia coli*. Purification and characterization of the nonallosteric isozyme. J Biol Chem 253 (12):4350–4355

Bäumchen C, Bringer-Meyer S (2007) Expression of *glf* $_{Z.m.}$ increases D-mannitol formation in whole cell biotransformation with resting cells of *Corynebacterium glutamicum*. Appl Microbiol Biotechnol 76(3):545–552

Becker J, Wittmann C (2011) Bio-based production of chemicals, materials and fuels—*Corynebacterium glutamicum* as versatile cell factory. Curr Opin Biotechnol. doi:10.1016/j.copbio.2011.11.012

Blombach B, Riester T, Wieschalka S, Ziert C, Youn JW, Wendisch VF, Eikmanns BJ (2011) *Corynebacterium glutamicum* tailored for efficient isobutanol production. Appl Environ Microbiol 77 (10):3300–3310

Chemler JA, Fowler ZL, McHugh KP, Koffas MA (2010) Improving NADPH availability for natural product biosynthesis in *Escherichia coli* by metabolic engineering. Metab Eng 12(2):96–104

Chin JW, Cirino PC (2011) Improved NADPH supply for xylitol production by engineered *Escherichia coli* with glycolytic mutations. Biotechnol Prog 27(2):333–341

Doo EH, Lee WH, Seo HS, Seo JH, Park JB (2009) Productivity of cyclohexanone oxidation of the recombinant *Corynebacterium glutamicum* expressing *chnB* of *Acinetobacter calcoaceticus*. J Biotechnol 142(2):164–169

Eggeling L, Bott M (eds) (2005) Handbook of *Corynebacterium glutamicum*. CRC, Boca Raton, pp 535–568

Eguchi T, Kuge Y, Inoue K, Yoshikawa N, Mochida K, Uwajima T (1992) NADPH regeneration by glucose dehydrogenase from *Gluconobacter scleroides* for l-leucovorin synthesis. Biosci Biotechnol Biochem 56(5):701–703

Eikmanns BJ, Kleinertz E, Liebl W, Sahm H (1991) A family of *Corynebacterium glutamicum/Escherichia coli* shuttle vectors for cloning, controlled gene expression, and promoter probing. Gene 102(1):93–98

Eikmanns BJ, Rittmann D, Sahm H (1995) Cloning, sequence analysis, expression, and inactivation of the *Corynebacterium glutamicum icd* gene encoding isocitrate dehydrogenase and biochemical characterization of the enzyme. J Bacteriol 177(3):774–782

Ernst M, Kaup B, Müller M, Bringer-Meyer S, Sahm H (2005) Enantioselective reduction of carbonyl compounds by whole-cell biotransformation, combining a formate dehydrogenase and a (*R*)-specific alcohol dehydrogenase. Appl Microbiol Biotechnol 66 (6):629–634

Fasan R, Crook NC, Peters MW, Meinhold P, Buelter T, Landwehr M, Cirino PC, Arnold FH (2011) Improved product-per-glucose yields in P450-dependent propane biotransformations using engineered *Escherichia coli*. Biotechnol Bioeng 108(3):500–510

Hanahan D (1983) Studies on transformation of *Escherichia coli* with plasmids. J Mol Biol 166(4):557–580

Hanahan D, Jessee J, Bloom FR (1991) Plasmid transformation of *Escherichia coli* and other bacteria. Methods Enzymol 204:63–113

Hermann T (2003) Industrial production of amino acids by coryneform bacteria. J Biotechnol 104(1–3):155–172

Inui M, Kawaguchi H, Murakami S, Vertes AA, Yukawa H (2004) Metabolic engineering of *Corynebacterium glutamicum* for fuel ethanol production under oxygen-deprivation conditions. J Mol Microbiol Biotechnol 8(4):243–254

Ishige T, Honda K, Shimizu S (2005) Whole organism biocatalysis. Curr Opin Chem Biol 9(2):174–180

Jojima T, Fujii M, Mori E, Inui M, Yukawa H (2010) Engineering of sugar metabolism of *Corynebacterium glutamicum* for production of amino acid L-alanine under oxygen deprivation. Appl Microbiol Biotechnol 87(1):159–165

Kabus A, Niebisch A, Bott M (2007) Role of cytochrome *bd* oxidase from *Corynebacterium glutamicum* in growth and lysine production. Appl Environ Microbiol 73(3):861–868

Kaup B, Bringer-Meyer S, Sahm H (2004) Metabolic engineering of *Escherichia coli*: construction of an efficient biocatalyst for D-mannitol formation in a whole-cell biotransformation. Appl Microbiol Biotechnol 64(3):333–339

Kaup B, Bringer-Meyer S, Sahm H (2005) D-Mannitol formation from D-glucose in a whole-cell biotransformation with recombinant *Escherichia coli*. Appl Microbiol Biotechnol 69(4):397–403

Kimura E (2003) Metabolic engineering of glutamate production. Adv Biochem Eng Biotechnol 79:37–57

Kruger NJ, von Schaewen A (2003) The oxidative pentose phosphate pathway: structure and organisation. Curr Opin Plant Biol 6 (3):236–246

Lindner SN, Knebel S, Pallerla SR, Schoberth SM, Wendisch VF (2010) Cg2091 encodes a polyphosphate/ATP-dependent glucokinase of *Corynebacterium glutamicum*. Appl Microbiol Biotechnol 87(2):703–713

Lindner SN, Seibold GM, Henrich A, Krämer R, Wendisch VF (2011) Phosphotransferase system-independent glucose utilization in *Corynebacterium glutamicum* by inositol permeases and glucokinases. Appl Environ Microbiol 77(11):3571–3581

Lindner SN, Meiswinkel TM, Panhorst M, Youn JW, Wiefel L, Wendisch VF (2012) Glycerol-3-phosphatase of *Corynebacterium glutamicum*. J Biotechnol. doi:10.1016/j.jbiotec.2012.02.003

Litsanov B, Brocker M, Bott M (2012a) Towards homosuccinate fermentation: metabolic engineering of *Corynebacterium glutamicum* for anaerobic succinate production from glucose and formate. Appl Environ Microbiol. doi:10.1128/AEM.07790-11

Litsanov B, Kabus A, Brocker M, Bott M (2012b) Efficient aerobic succinate production from glucose in minimal medium with *Corynebacterium glutamicum*. Microb Biotechnol 5(1):116–128

Meissner D, Vollstedt A, van Dijl JM, Freudl R (2007) Comparative analysis of twin-arginine (Tat)-dependent protein secretion of a heterologous model protein (GFP) in three different Gram-positive bacteria. Appl Microbiol Biotechnol 76(3):633–642

Miller JH (ed) (1972) Experiments in molecular genetics. Cold Spring Harbor Laboratory, New York

Mimitsuka T, Sawai H, Hatsu M, Yamada K (2007) Metabolic engineering of *Corynebacterium glutamicum* for cadaverine fermentation. Biosci Biotechnol Biochem 71(9):2130–2135

Niebisch A, Bott M (2001) Molecular analysis of the cytochrome bc_1-aa_3 branch of the *Corynebacterium glutamicum* respiratory chain containing an unusual diheme cytochrome c_1. Arch Microbiol 175(4):282–294

Okino S, Noburyu R, Suda M, Jojima T, Inui M, Yukawa H (2008) An efficient succinic acid production process in a metabolically engineered *Corynebacterium glutamicum* strain. Appl Microbiol Biotechnol 81(3):459–464

Omumasaba CA, Okai N, Inui M, Yukawa H (2004) *Corynebacterium glutamicum* glyceraldehyde-3-phosphate dehydrogenase isoforms with opposite, ATP-dependent regulation. J Mol Microbiol Biotechnol 8(2):91–103

Panke S, Wubbolts M (2005) Advances in biocatalytic synthesis of pharmaceutical intermediates. Curr Opin Chem Biol 9(2):188–194

Park SY, Kim HK, Yoo SK, Oh TK, Lee JK (2000) Characterization of *glk*, a gene coding for glucose kinase of *Corynebacterium glutamicum*. FEMS Microbiol Lett 188(2):209–215

Parker C, Barnell WO, Snoep JL, Ingram LO, Conway T (1995) Characterization of the *Zymomonas mobilis* glucose facilitator gene product (*glf*) in recombinant *Escherichia coli*: examination of transport mechanism, kinetics and the role of glucokinase in glucose transport. Mol Microbiol 15(5):795–802

Pfefferle W, Möckel B, Bathe B, Marx A (2003) Biotechnological manufacture of lysine. Adv Biochem Eng Biotechnol 79:59–112

Rittmann D, Schaffer S, Wendisch VF, Sahm H (2003) Fructose-1, 6-bisphosphatase from *Corynebacterium glutamicum*: expression and deletion of the *fbp* gene and biochemical characterization of the enzyme. Arch Microbiol 180(4):285–292

Sambrook J, Russell DW (eds) (2001) Molecular cloning: a laboratory manual. Cold Spring Harbor Laboratory, Cold Spring Harbor

Schäfer A, Tauch A, Jäger W, Kalinowski J, Thierbach G, Pühler A (1994) Small mobilizable multi-purpose cloning vectors derived from the *Escherichia coli* plasmids pK18 and pK19: selection of defined deletions in the chromosome of *Corynebacterium glutamicum*. Gene 145(1):69–73

Schneider J, Wendisch VF (2010) Putrescine production by engineered *Corynebacterium glutamicum*. Appl Microbiol Biotechnol 88 (4):859–868

Siedler S, Bringer S, Bott M (2011) Increased NADPH availability in *Escherichia coli*: improvement of the product per glucose ratio in reductive whole-cell biotransformation. Appl Microbiol Biotechnol 92(5):929–937

Siedler S, Bringer S, Blank LM, Bott M (2012) Engineering yield and rate of reductive biotransformation in *Escherichia coli* by partial cyclization of the pentose phosphate pathway and PTS-independent glucose transport. Appl Microbiol Biotechnol 93 (4):1459–1467

Smith KM, Cho KM, Liao JC (2010) Engineering *Corynebacterium glutamicum* for isobutanol production. Appl Microbiol Biotechnol 87(3):1045–1055

Stäbler N, Oikawa T, Bott M, Eggeling L (2011) *Corynebacterium glutamicum* as a host for synthesis and export of D-amino acids. J Bacteriol 193(7):1702–1709

Stansen C, Uy D, Delaunay S, Eggeling L, Goergen JL, Wendisch VF (2005) Characterization of a *Corynebacterium glutamicum* lactate utilization operon induced during temperature-triggered glutamate production. Appl Environ Microbiol 71(10):5920–5928

Tan I (2006) Applications of whole cell biotransformations for the production of chiral alcohols. Rheinische Friedrich-Wilhelms University of Bonn, Bonn, Dissertation

Weisser P, Krämer R, Sahm H, Sprenger GA (1995) Functional expression of the glucose transporter of *Zymomonas mobilis* leads to restoration of glucose and fructose uptake in *Escherichia coli* mutants and provides evidence for its facilitator action. J Bacteriol 177(11):3351–3354

Wendisch VF, Bott M, Eikmanns BJ (2006) Metabolic engineering of *Escherichia coli* and *Corynebacterium glutamicum* for biotechnological production of organic acids and amino acids. Curr Opin Microbiol 9(3):268–274

Yamamoto S, Gunji W, Suzuki H, Toda H, Suda M, Jojima T, Inui M, Yukawa H (2012) Overexpression of glycolytic genes enhances *Corynebacterium glutamicum* glucose metabolism and alanine production under oxygen-deprived conditions. Appl Environ Microbiol. doi:10.1128/AEM.07998-11

Yokota A, Lindley ND (2005) Central metabolism: sugar uptake and conversion. In: Eggeling L, Bott M (eds) Handbook of *Corynebacterium glutamicum*. CRC, Boca Raton, pp 215–240

Yun JY, Lee JE, Yang KM, Cho S, Kim A, Kwon YE, Park JB (2012) Ethambutol-mediated cell wall modification in recombinant *Corynebacterium glutamicum* increases the biotransformation rates of cyclohexanone derivatives. Bioprocess Biosyst Eng 35(1–2):211–216

Own proportion to this work: 40%

Steffen Lindner created all *C. glutamicum* mutant strains and analyzed their growth behaviors and enzyme activities. I performed the biotransformation experiments and wrote a draft of the manuscript.

Published in: Applied Microbiology and Biotechnology

Impact factor: 3.4

NADPH-dependent reductive biotransformation with *Escherichia coli* and its *pfkA* deletion mutant: influence on global gene expression and role of oxygen supply

Solvej Siedler, Stephanie Bringer, Tino Polen, Michael Bott

Institut für Bio- und Geowissenschaften, IBG-1: Biotechnologie, Forschungszentrum Jülich, D-52425 Jülich, Germany

KEYWORDS: *Escherichia coli*, NADPH yield, phosphofructokinase, SthA transhydrogenase, DNA microarrays, resting cells, reductive whole-cell biotransformation

Short running title: Aerobic and anaerobic reductive biotransformation

Correspondence to:

Dr. Stephanie Bringer, Prof. Dr. Michael Bott

Institut für Bio- und Geowissenschaften, IBG-1: Biotechnologie, Forschungszentrum Jülich GmbH, D-52425 Jülich

E-mail: st.bringer-meyer@fz-juelich.de, m.bott@fz-juelich.de

Tel.: +49 2461 613476, +49 2461 613294

Fax: +49 2461 612710

ABSTRACT: We recently demonstrated that an *Escherichia coli* $\Delta pfkA$ mutant lacking the major phosphofructokinase possesses a partially cyclized pentose phosphate pathway leading to an increased NADPH per glucose ratio. This effect is favorable in reductive biotransformations, such as the NADPH-dependent reduction of methyl acetoacetate (MAA) to (*R*)-methyl 3-hydroxybutyrate (MHB) catalyzed by an alcohol dehydrogenase from *Lactobacillus brevis*, as it decreases the amount of glucose required for NADPH regeneration. Here, global transcriptional analyses were performed to study regulatory responses of the $\Delta pfkA$ mutant and the reference strain during biotransformation. Comparative DNA microarray analysis revealed differences of mRNA levels of several genes which are regulated by the ArcAB two-component system, pointing to different redox states of the respiratory QH_2/Q pools. This prompted us to compare yields and productivities of the reductive biotransformation under defined aerobic and anaerobic conditions. Under anaerobic conditions, the specific MHB production rates of both strains were similar (7.4 ± 0.2 mmol$_{MHB}$ h^{-1} g$_{cdw}^{-1}$). Under aerobic conditions, yields and rates were markedly increased and the rate of the $\Delta pfkA$ mutant (11.0 ± 0.3 mmol$_{MHB}$ h^{-1} g$_{cdw}^{-1}$) was 14% lower compared to that of the reference strain (12.8 ± 0.01 mmol$_{MHB}$ h^{-1} g$_{cdw}^{-1}$). While the oxygen transfer rate (OTR) of the reference strain increased after addition of MAA, the OTR of $\Delta pfkA$ drastically decreased instead, indicating a limited respiration. This limitation in $\Delta pfkA$ can likely be attributed to reduced NADH generation from NADPH via soluble transhydrogenase SthA, which in the presence of MAA competed with the recombinant ADH for NADPH.

Introduction

Microbial whole-cell biotransformation is implemented in industry for the production of chiral alcohols (Ishige et al. 2005). A variety of dehydrogenases catalyzes the enantio- and regioselective reduction of ketones and depends on nicotinamide adenine dinucleotide coenzymes (NADH or NADPH) for hydride transfer (Goldberg et al. 2007). Efficient coenzyme recycling by engineered strains transforming the oxidized coenzyme back to its reduced form is essential for efficient reductive whole-cell biotransformations and different possibilities for catching reducing power have been reported (Goldberg et al. 2007).

Recently, glucose was used as electron donor for cofactor regeneration under anaerobic as well as aerobic conditions using metabolically engineered *Escherichia coli* strains (Akinterinwa and Cirino 2011, Chin and Cirino 2011, Siedler et al. 2011, 2012). Partial cyclization of the pentose phosphate pathway (PPP) by deletion of the phosphofructokinase genes (*pfkA*, *pfkB*) resulted in an increased NADPH per glucose ratio and in an improved product to glucose yield of the NADPH-dependent biotransformation of the β-keto ester methyl acetoacetate (MAA) to the chiral hydroxy ester (*R*)-methyl 3-hydroxybutyrate (MHB), which is catalyzed by an alcohol dehydrogenase from *Lactobacillus brevis* (Fig. 1) (Siedler et al. 2011). The partially cyclized PPP was confirmed by ^{13}C metabolic flux analysis, which revealed a positive net flux from fructose 6-phosphate to glucose 6-phosphate in the *E. coli* Δ*pfkA* mutant (Siedler et al. 2012). Moreover, the carbon flux through the lower part of the Embden-Meyerhof pathway (EMP) and through the tricarboxylic acid cycle (TCA) was reduced in the Δ*pfkA* mutant to $^1/_4$ of that of the reference strain (Siedler et al. 2012). *E. coli* possesses two pyridine nucleotide transhydrogenases for adjustment of the relative concentrations of NADPH and NADH, the cytoplasmic SthA and the membrane-bound PntAB (Jackson 2003). While PntAB drives NADPH generation from NADH by using the proton-motive force, SthA catalyzes the reduction of NAD$^+$ by NADPH (Sauer et al. 2004). In the ^{13}C metabolic flux analysis mentioned above, a significantly higher flux through the

SthA-catalyzed reaction was observed during growth of the Δ*pfkA* mutant, pointing to an important role of SthA in this mutant (Siedler et al. 2012).

In this work we analyzed the influence of reductive biotransformation on global gene expression by DNA microarrays. As in our previous studies, we used *E. coli* BL21(DE3) or its Δ*pfkA* mutant, both expressing the *L. brevis* ADH, and the NADPH-dependent reduction of MAA to MHB as model reaction. The results obtained in the transcriptome studies prompted us to perform whole-cell biotransformation experiments under controlled conditions of oxygen availability. In the course of these studies the role of the soluble transhydrogenase (SthA) was unraveled, as well as potential bottlenecks in the reference strain and its Δ*pfkA* mutant.

Materials and Methods

Bacterial strains and plasmids, media and growth conditions

Strains and plasmids used in this work are listed in Table I. The Δ*pfkA* mutant strain was constructed as described previously (Siedler et al. 2011). *E. coli* strains were transformed by the method described by Hanahan (Hanahan et al. 1991) and cultivated in 2xYT medium (16 g L^{-1} tryptone, 10 g L^{-1} yeast extract, 5 g L^{-1} sodium chloride). The media contained 100 µg mL^{-1} ampicillin to maintain plasmid pBtac-*Lbadh.*

Whole cell biotransformation

For cultivation of the recombinant *E. coli* Star BL21(DE3) strain and its Δ*pfkA* derivative, both carrying the plasmid pBtac-*Lbadh*, a single colony of each strain was inoculated into 20 mL of 2xYT medium containing 100 µg mL^{-1} ampicillin and grown overnight at 37°C and 140 rpm. These pre-cultures were used for inoculation of the main cultures to an OD_{600} of 0.05. Main

cultures were grown in 600 mL of 2xYT medium containing 100 μg mL^{-1} ampicillin at 37°C and 130 rpm to an OD_{600} of 0.3, then *Lbadh* expression was induced with 1 mM of IPTG and the cultures incubated for another 3 h at 37 °C and 130 rpm. Then the cells having an OD_{600} between 2 and 4.5, which had been determined as the optimal cell density for subsequent whole-cell biotransformation, were harvested by centrifugation (4,000 *g*, 7 min) and resuspended in 190 ml reaction buffer containing 111 mM glucose, 2 mM $MgSO_4$, and 250 mM potassium phosphate buffer, pH 6.5, to a cell density of 3 g cell dry weight (cdw) per liter. Biotransformations were performed at 37°C in a bioreactor system (Dasgip, Jülich, Germany) composed of four 400-ml vessels, each equipped with electrodes for measuring the dissolved oxygen concentration (DO) and the pH. The system allows to constantly control these two parameters. The carbon dioxide concentration in the exhaust air was measured continuously by an infrared spectrometer. The oxygen availability was kept constant at 15% DO by mixing air, O_2 and N_2. Calibration was performed by gassing with air (100% DO) and N_2 (0% DO). Anaerobic conditions were provided by gassing with 100% N_2. The agitation speed was kept constant at 900 rpm. Controlling and recording of all data as well as calculation of oxygen transfer rates (OTR) and CO_2 transfer rates (CTR) was carried out by the software "Fedbatch Pro" (Dasgip, Jülich, Germany).

The biotransformation was started by adding 60 mM MAA after the DO was constant. Specific productivities (mmol MHB per hour per gram cdw) were determined by taking samples at 15-min time intervals over a period of 2 h. MHB and glucose concentrations of the samples were determined (see below). Specific productivities were calculated by dividing the slopes of graphs showing MHB concentration versus time by the cell dry weight.

Analysis of substrates and products

Methyl acetoacetate (MAA), (*R*)-methyl 3-hydroxybutyrate (MHB), glucose and extracellular metabolites were analyzed by HPLC as described previously (Siedler et al. 2011). Glucose concentrations were in addition determined enzymatically by using the glucose Gluc-DH FS* Kit according to the instructions of the manufacturer (DiaSys, Holzheim, Germany).

RNA preparation, cDNA synthesis and DNA microarray analysis

For RNA preparation, *E. coli* strains were harvested 10 min after resuspension in biotransformation buffer before addition of MAA and 10 min after the addition of MAA. For cell harvest 20 ml of the cultures were poured into precooled (-20°C) tubes containing 15 g of ice and centrifuged (3 min, 4200 x g, 4°C). The cell pellets were frozen in liquid nitrogen and stored at -70 °C until RNA isolation as described before (Polen et al. 2003). DNA microarrays for *E. coli* were obtained from Microarrays Inc. (Huntsville, USA). The array design includes 9308 longmer oligonucleotide (70 mer) probes, representing genomes of four *E. coli* strains and three plasmids (4269 ORFs in K12, 5306 ORFs in O157:H7, 5251 ORFs in O157:H7, 5366 ORFs in CFT073, 3 genes in OSAK1, 10 genes in pO157_Sakai, 97 genes in pO157_EDL933). Some genes are represented by different gene-specific oligonucleotides (e.g. *guaD*). Only genes of *E. coli* K12 were analyzed. We applied the available K-12 DNA microrrays since comparisons of the B and K-12 genome sequences and the annotated protein coding genes showed >99% sequence identity over ~92% of their genomes with a total of ~4039 coding sequences in the genome of the common ancestor, of which 97.6% remain evident in K and 96.5% in B (Jeong et al. 2009, Studier et al, 2009). The comparisons of the responses to the addition of MAA of the two strains were performed in duplicate, respectively, while the analysis of the differences of the two strains was done from three independent biological replicates. The details for handling of the

microarrays, data processing and data analysis were described before (Hanke et al. 2012). Lists of differentially expressed genes were obtained by filtering the data using the following criteria: i) Flags>=0 (GenePix Pro 6.0); ii) Signal-Noise >=3 for red (F635med/B635med, GenePixPro 6.0) or green (F532med/B532med, GenePixPro 6.0) and iii) averaged mRNA level change of >=2-fold (strain comparison, Table II) or >=2.5-fold (influence of MAA, Table III) and p-values ≤0.05. Processed and normalized data, as well as experimental details according to the MIAME guidelines (Brazma et al. 2001), were stored in the in-house microarray database (Polen and Wendisch 2004).

Results and discussion

Influence on global gene expression of NADPH-dependent whole-cell biotransformation by resting cells of *E. coli* using glucose as reductant

In order to study the influence of an NADPH-dependent whole-cell biotransformation on global gene expression, we analyzed the reduction of MAA to MHB by resting cells of *Escherichia coli* and its Δ*pfkA* mutant, both carrying plasmid pBTac-*Lbadh* encoding an alcohol dehydrogenase from *Lactobacillus brevis*. Cells resuspended to 3 g cell dry weight/l in a phosphate buffer (pH 6.5) containing 110 mM glucose were incubated at 37 °C and 130 rpm for 10 min in a shake flask. Then biotransformation was started by addition of 60 mM MAA. Directly before and 10 minutes after MAA addition samples were taken for RNA isolation. The resulting RNA preparations were then used for comparative DNA microarray analyses and the mRNA ratios (after vs. before MAA addition) were determined for both the reference strain and the Δ*pfkA* mutant. The number of detectable genes (signal to noise ratio >3 for red or green) were about 91% and together with the distribution in MA plots indicate that basically RNA from resting cells at the early time point of the biotransformation can also be applied to global gene expression analysis as RNA from growing or early stationary cells (e.g. Neusser et al. 2010, and Fig. S1). Thus, DNA microarray experiments represent an efficient tool to analyze resting cells under biotransformation conditions with respect to global gene expression.

In both strains, less than 20 genes showed an mRNA ratio ≥2.5 (lower ones allowed in the case of operons and for comparison of the two experiments) or ≤0.4 (higher ones allowed in the case of operons and for comparison of the two experiments). These genes are listed in Table II. Most interesting was a set of four genes whose expression was elevated in both strains after addition of MAA, but 2- to 5-fold more strongly in the Δ*pfkA* mutant: *soxS* (24.38 vs. 4.59), *yqhC* (mRNA ratio 7.90 vs. 3.70), *yqhD* (36.24 vs. 12.70), and *dkgA* (16.18 vs. 7.36).

The *soxS* gene encodes an AraC-type transcriptional regulator which controls genes involved in the response to oxidative stress (Greenberg et al. 1990; Pomposiello et al. 2001; Tsaneva and Weiss 1990). Under stress conditions, expression of *soxS* is activated by SoxR, a dimeric transcriptional regulator of the MerR family with two [2Fe-2S] clusters (Hidalgo et al. 1998). SoxR itself becomes activated by oxidation of the [2Fe-2S] cluster. Inactivation of oxidized SoxR occurs via NADPH-dependent reduction, which requires *rseC* and *rsxABCDGE* genes (Koo et al. 2003). The intrinsic instability of the SoxS protein allows the response to be turned off once SoxR is reduced (Griffith et al. 2004). The SoxRS system has been intensively studied in *E. coli* and there are multiple ways to induce the regulon. Evidence has been provided that the NADPH availability plays a crucial role in the induction of the SoxRS response (Krapp et al. 2011; Liochev and Fridovich 1992). In our biotransformation experiments, cells face a very high NADPH demand when MAA, the substrate for the *L. brevis* alcohol dehydrogenase, is present and the NADPH/NADP$^+$ ratio is decreased (Siedler et al. 2011). The strong NADPH consumption by MAA reduction is likely to impede the NADPH-dependent reduction of oxidized SoxR, causing activation of *soxS* expression. The 5.3-fold higher *soxS* mRNA ratio in the Δ*pfkA* mutant compared to the reference strain (24.4 vs. 4.6) might reflect the stronger decrease of the NADPH/NADP$^+$ ratio upon substrate addition. Whereas expression of *soxS* was increased in our experiments, experimentally confirmed SoxS target genes, like *zwf* encoding glucose 6-phosphate dehydrogenase, did not show increased mRNA levels. We assume that the non-induction of the SoxS target genes is a consequence of the resting cell conditions, which hinder SoxS protein synthesis.

The *yqhC* gene encodes a transcriptional regulator of the AraC family which was shown to activate transcription of *yqhD* and *dkgA*, which are located divergent to *yqhC* (Lee et al. 2010; Turner et al. 2011). The *yqhD* gene product functions as broad-substrate range NADPH-dependent aldehyde reductase (Jarboe 2011). The *dkgA* gene (previously named *yqhE*) was originally characterized as an NADPH-dependent 2,5-diketo-D-gluconate reductase (Yum et al.

1999) and later shown to reduce also ethyl acetoacetate and other 2-substituted derivatives (Habrych et al. 2002; Jeudy et al. 2006). Possibly MAA can function as a co-activator which binds to YqhC and switches this regulator to its active state.

Transcriptome comparison of an *E. coli* Δ*pfkA* mutant and its parent during MAA reduction by resting cells

In order to support the DNA microarray results described above, a direct transcriptome comparison of the two strains was performed using RNA isolated 10 min after MAA addition. In this series of DNA microarray experiments, 85 genes with ≥2-fold increased mRNA levels and 49 genes with ≥2-fold decreased mRNA levels were observed in the Δ*pfkA* mutant (Table III). The *soxS* gene showed a 6-fold higher mRNA level in the Δ*pfkA* mutant, confirming the results described above.

Elevated mRNA levels were observed in the Δ*pfkA* mutant for the genes encoding succinate dehydrogenase (*sdhCDAB*, mRNA ratios 3.0-15.5), genes involved in fatty acid synthesis (*fadB*, *fadH*, *fadhl*, mRNA ratios 3.7-13.4), as well as genes for stress responses, like osmotic stress (*betBIT*, mRNA ratios 3.8-7.4) and oxidative stress (*soxS*, mRNA ratio 6.3;*iscR*, mRNA ratio 2.5). 30 genes encoding ribosomal proteins showed 3- to 16-fold increased mRNA levels and also 8 flagellar genes (ECD_01067-74) displayed 2.4- to 3.2-fold elevated expression in the Δ*pfkA* mutant. The *sthA* gene encoding a soluble transhydrogenase displayed a more than 3-fold increased mRNA level in the Δ*pfkA* mutant,,indicating an imbalanced redox ratio of the NAD(P)H pools. This result is coherent with a high flux through SthA transhydrogenase in the Δ*pfkA* mutant (Siedler et al. 2012) (see below).

The strongest decreased mRNA levels in the Δ*pfkA* mutant besides *pfkA* itself were found for genes involved in tryptophan biosynthesis, possibly due to the higher carbon flux through the PPP resulting in an increased availability of precursors of tryptophan and possibly an increased

tryptophan synthesis. High tryptophan levels are known to cause repression of the tryptophan biosynthesis operon *trpEDCBA* by activation of the repressor TrpR (Klig et al. 1988; Sarsero et al. 1991). The *rseC* gene (ECD_02464, mRNA ratio 0.5), encoding a protein involved in the NADPH-dependent reduction of the iron sulfur cluster of SoxR (see above), displayed a decreased mRNA level in the $\Delta pfkA$ mutant. In concert with a lowered NADPH availability after addition of MAA (Siedler et al. 2011), reduced *rseC* expression might reinforce a shift of SoxR to the active oxidized state. As a consequence, the *soxS* RNA level was 6-fold higher in the $\Delta pfkA$ mutant compared to the reference strain.

Several expression differences which were revealed by the microarray analysis can be assigned to the regulon of the ArcAB two-component system, which is sensing microaerobic conditions (Green and Paget 2004). All genes highlighted in Table III are regulated by ArcAB (Cho et al. 2006; Lamark et al. 1996; Liu and De Wulf 2004). For example, the genes for the cytochrome bo_3 ubiquinol oxidase (*cyoB*, *cyoA*, mRNA ratios 2.8-5.3) showed elevated mRNA levels, while a cytochrome *bd* terminal oxidase gene (*cydA*, mRNA ratio 0.3) displayed a lower relative mRNA level (Spiro and Guest 1991). ArcAB was reported to recognize microaerobic conditions by the QH_2 to Q ratio of the respiratory chain (Malpica et al. 2006). This ratio is correlated with the NADH to NAD^+ ratio. In fact, a 30% lower NADH to NAD^+ ratio was measured in the $\Delta pfkA$ mutant compared to that of the reference strain after 120 min of biotransformation in a shake flask experiment (Siedler et al. 2011). The question of the causes and effects of a higher NADH/NAD^+ ratio and consequently a stronger activity of the ArcAB two-component system in the reference strain than that in $\Delta pfkA$ in shake flask experiments prompted us to analyze aerobic and anaerobic biotransformations under controlled conditions of oxygen availability.

Comparison of biotransformations under anaerobic and aerobic conditions

Biotransformations with the Δ*pfkA* mutant and the reference strain were conducted in a DASGIP bioreactor under defined aerobic and anaerobic conditions. Under anaerobic conditions both strains showed comparable MHB production rates (7.4 mmol h^{-1} g$_{cdw}$$^{-1}$, Table IV, whereas the glucose uptake rate of the Δ*pfkA* deletion mutant (2.4 mmol h^{-1} g$_{cdw}$$^{-1}$) was much lower than that of the reference strain (3.5 mmol h^{-1} g$_{cdw}$$^{-1}$). This resulted in a 48% higher yield (mol MHB per mol glucose) of the mutant compared to the reference strain (Table IV). Despite the reduced glucose uptake rate of the Δ*pfkA* mutant, its CO_2 transfer rate was comparable to that of the reference strain (Fig. 2), which probably is due to the increased carbon dioxide formation via 6-phosphogluconate dehydrogenase caused by the partially cyclized flux within the pentose phosphate pathway (Siedler et al. 2012). Formation of the mixed acid fermentation products acetate, formate and succinate by the Δ*pfkA* mutant and the reference strain was similar, but lactate formation by the Δ*pfkA* mutant was reduced by almost 90% (Table V). The latter result can be explained by the fact that less NADH is synthesized in the *pfkA* mutant due to the altered glucose metabolism and additionally part of NADH might be used to reduce NADP$^+$ via transhydrogenase, as there is a strong NADPH demand for the biotransformation. The carbon balances were closed for both strains under anaerobic conditions (Table V).

Under aerobic conditions, the MHB production rates of the reference strain (12.8 mmol h^{-1} g$_{cdw}$$^{-1}$) and of the Δ*pfkA* mutant (11.0 mmol h^{-1} g$_{cdw}$$^{-1}$) were 73% and 49% higher than the rates observed under anaerobic conditions, respectively (Table IV). Again, the glucose uptake rate of the *pfkA* mutant (2.3 mmol h^{-1} g$_{cdw}$$^{-1}$) was significantly lower than that of the reference strain (3.8 mmol h^{-1} g$_{cdw}$$^{-1}$), resulting in 41% increased molar MHB/glucose yield.

To ensure steady-state aerobic conditions in the bioreactor, cells were first incubated for 30 min in the absence of the substrate MAA. During this adaptation time, no significant differences were observed either for the oxygen transfer rates (OTR) or for the carbon dioxide transfer rates

(CTR) of the reference strain and the Δ*pfkA* mutant (Fig. 3). The similar OTR values might be explained by a high flux through the transhydrogenase SthA in the Δ*pfkA* mutant (Siedler et al. 2012), resulting in the conversion of NADPH generated in the cyclized pentose phosphate pathway to NADH, which then drives respiration. After start of the biotransformation by the addition of MAA to the cell suspensions, both the OTR and the CTR markedly increased in the reference strain and later on decreased again (Fig. 3). In contrast, the OTR of the Δ*pfkA* mutant rapidly dropped to zero and the CTR remained at the level observed immediately before MAA addition (Fig. 3). The strongly decreased respiration of the Δ*pfkA* mutant can partially be explained by the fact that in the presence of MAA the NADPH generated in the cyclized pentose phosphate pathway is almost exclusively used by *L. brevis* ADH (about 20 U mg protein^{-1}) for MAA reduction to MHB and no longer available for NADH generation by the soluble transhydrogenase SthA. This assumption was supported by the observation that the OTR of the Δ*pfkA* mutant increased again when MAA was completely reduced to MHB about 100 min after MAA addition (Fig. 3).

As the Δ*pfkA* mutant can in principle still form NADH via glyceraldehyde 3-phosphate dehydrogenase, pyruvate dehydrogenase or 2-oxoglutarate dehydrogenase, the OTR drop zero after MAA addition indicates that either the flux through these reactions is rather low or that the NADH generated in these reactions is used by the membrane-bound transhydrogenase PntAB for proton-motive force-driven NADPH synthesis. However, the latter reaction can also occur in the reference strain and therefore the differences in OTR after MAA addition between the Δ*pfkA* mutant and the reference strain must have other reasons. A likely explanation is offered by the observation that the reference strain, but not the Δ*pfkA* mutant accumulated acetate during the 30 min adaptation period before addition of MAA. This acetate was consumed by reference strain in the first 30 min after MAA addition (data not shown) and probably contributes to the increased OTR in this period. In particular, the succinate dehydrogenase and malate:ubiquinone oxidoreductase reactions, which form ubiquinol rather than NADH, might be the drivers of the

OTR increase. Acetate oxidation by the reference strain can also explain the increased CTR observed after MAA addition.

When comparing the MHB production rates and MHB/glucose yield under aerobic and anaerobic conditions, it is evident that oxygen has a positive influence on both parameters and in both the reference strain and the Δ*pfkA* mutant. In the case of the reference strain, the yield under aerobic conditions in the bioreactor (3.4 mol/mol) is 62% higher than under anaerobic conditions and still 36% higher than under shake flask conditions, indicating oxygen-limiting conditions in the latter. In the case of the Δ*pfkA* mutant, the yield under aerobic conditions in the bioreactor (4.8 mol/mol) was 55% higher than under anaerobic conditions and identical to the yield observed in shake flasks. A reason for the positive effect of aerobic conditions might be an improved proton-motive force as driver of the membrane-bound transhydrogenase PntAB. Future studies using a *pntAB* deletion mutant are necessary to test this hypothesis.

Conclusions

The present work has shown that the MHB production rate of a whole-cell biotransformation process conducted with resting cells at high densities in shake flasks was oxygen-limited. Global gene expression analyses conducted with resting *E. coli* cells revealed expression changes in response to biotransformation conditions which were specific for the strain background. The ArcAB two-component system was more active in the reference strain, pointing to different redox states of the respiratory QH_2/Q pool of the reference and the Δ*pfkA* mutant strains. These differences could be explained by the different abilities of the strains to reduce oxygen aerobically in the presence of MAA. The ADH competed with the SthA for NADPH and appeared to be predominant; hence less NADH was formed and could be used for respiration. Presumably, the ADH is so strongly more active than the SthA that deletion of the

transhydrogenase gene in this case of a whole-cell biotransformation would not be beneficial for a higher MHB per glucose yield.

References

Akinterinwa O, Cirino PC. 2011. Anaerobic obligatory xylitol production in *Escherichia coli* strains devoid of native fermentation pathways. Appl Environ Microbiol 77(2):706-9.

Brazma A, Hingamp P, Quackenbush J, Sherlock G, Spellman P, Stoeckert C, Aach J, Ansorge W, Ball CA, Causton HC and others. 2001. Minimum information about a microarray experiment (MIAME)-toward standards for microarray data. Nat Genet 29(4):365-371.

Chin JW, Cirino PC. 2011. Improved NADPH supply for xylitol production by engineered *Escherichia coli* with glycolytic mutations. Biotechnol Prog 27(2):333-341.

Cho BK, Knight EM, Palsson BO. 2006. Transcriptional regulation of the *fad* regulon genes of *Escherichia coli* by ArcA. Microbiol 152(Pt 8):2207-2219.

Ernst M, Kaup B, Müller M, Bringer-Meyer S, Sahm H. 2005. Enantioselective reduction of carbonyl compounds by whole-cell biotransformation, combining a formate dehydrogenase and a (*R*)-specific alcohol dehydrogenase. Appl Microbiol Biotechnol 66(6):629-634.

Goldberg K, Schroer K, Lütz S, Liese A. 2007. Biocatalytic ketone reduction--a powerful tool for the production of chiral alcohols-part II: whole-cell reductions. Appl Microbiol Biotechnol 76(2):249-255.

Green J, Paget MS. 2004. Bacterial redox sensors. Nat Rev Microbiol 2(12):954-966.

Greenberg JT, Monach P, Chou JH, Josephy PD, Demple B. 1990. Positive control of a global antioxidant defense regulon activated by superoxide-generating agents in *Escherichia coli*. Proc Natl Acad Sci U S A 87(16):6181-6185.

Griffith KL, Wolf RE, Jr. 2004. Genetic evidence for pre-recruitment as the mechanism of transcription activation by SoxS of Escherichia coli: the dominance of DNA binding mutations of SoxS. J Mol Biol 344(1):1-10.

Habrych M, Rodriguez S, Stewart JD. 2002. Purification and identification of an *Escherichia coli* beta-keto ester reductase as 2,5-diketo-D-gluconate reductase YqhE. Biotechnol Prog 18(2):257-261.

Hanahan D, Jessee J, Bloom FR. 1991. Plasmid transformation of *Escherichia coli* and other bacteria. Meth Enzymol 204:63-113.

Hanke T, Richhardt J, Polen T, Sahm H, Bringer S, Bott M. 2012. Influence of oxygen limitation, absence of the cytochrome bc_1 complex and low pH on global gene expression in *Gluconobacter oxydans* 621H using DNA microarray technology. J Biotechnol 157(3):359-372.

Hidalgo E, Leautaud V, Demple B. 1998. The redox-regulated SoxR protein acts from a single DNA site as a repressor and an allosteric activator. EMBO J 17(9):2629-2636.

Ishige T, Honda K, Shimizu S. 2005. Whole organism biocatalysis. Curr Opin Chem Biol 9(2):174-180.

Jackson JB. 2003. Proton translocation by transhydrogenase. FEBS Lett 545(1):18-24.

Jarboe LR. 2011. YqhD: a broad-substrate range aldehyde reductase with various applications in production of biorenewable fuels and chemicals. Appl Microbiol Biotechnol 89(2):249-257.

Jeong H, Barbe V, Lee CH, Vallenet D, Yu DS, Choi SH, Couloux A, Lee SW, Yoon SH, Cattolico L and others. 2009. Genome sequences of *Escherichia coli* B strains REL606 and BL21(DE3). J Mol Biol 394(4):644-652.

Jeudy S, Monchois V, Maza C, Claverie JM, Abergel C. 2006. Crystal structure of *Escherichia coli* DkgA, a broad-specificity aldo-keto reductase. Proteins 62(1):302-307.

Klig LS, Carey J, Yanofsky C. 1988. *trp* repressor interactions with the *trp aroH* and *trpR* operators. Comparison of repressor binding *in vitro* and repression *in vivo*. J Mol Biol 202(4):769-777.

Koo MS, Lee JH, Rah SY, Yeo WS, Lee JW, Lee KL, Koh YS, Kang SO, Roe JH. 2003. A reducing system of the superoxide sensor SoxR in *Escherichia coli*. EMBO J 22(11):2614-2622.

Krapp AR, Humbert MV, Carrillo N. 2011. The *soxRS* response of *Escherichia coli* can be induced in the absence of oxidative stress and oxygen by modulation of NADPH content. Microbiol 157(Pt 4):957-965.

Lamark T, Rokenes TP, McDougall J, Strom AR. 1996. The complex *bet* promoters of *Escherichia coli*: regulation by oxygen (ArcA), choline (BetI), and osmotic stress. J Bacteriol 178(6):1655-1662.

Lee C, Kim I, Lee J, Lee KL, Min B, Park C. 2010. Transcriptional activation of the aldehyde reductase YqhD by YqhC and its implication in glyoxal metabolism of *Escherichia coli* K-12. J Bacteriol 192(16):4205-4214.

Liochev SI, Fridovich I. 1992. Fumarase C, the stable fumarase of *Escherichia coli*, is controlled by the *soxRS* regulon. Proc Natl Acad Sci U S A 89(13):5892-5896.

Liu X, De Wulf P. 2004. Probing the ArcA-P modulon of *Escherichia coli* by whole genome transcriptional analysis and sequence recognition profiling. J Biol Chem 279(13):12588-12597.

Malpica R, Sandoval GR, Rodriguez C, Franco B, Georgellis D. 2006. Signaling by the Arc two-component system provides a link between the redox state of the quinone pool and gene expression. Antioxid Redox Signal 8(5-6):781-795.

Neusser T, Polen T, Geissen R, Wagner R. 2010. Depletion of the non-coding regulatory 6S RNA in *E. coli* causes a surprising reduction in the expression of the translation machinery. BMC Genomics 11:165.

Polen T, Rittmann D, Wendisch VF, Sahm H. 2003. DNA microarray analyses of the long-term adaptive response of *Escherichia coli* to acetate and propionate. Appl Environ Microbiol 69(3):1759-1774.

Polen T, Wendisch VF. 2004. Genomewide expression analysis in amino acid-producing bacteria using DNA microarrays. Appl Biochem Biotechnol 118(1-3):215-232.

Pomposiello PJ, Bennik MH, Demple B. 2001. Genome-wide transcriptional profiling of the *Escherichia coli* responses to superoxide stress and sodium salicylate. J Bacteriol 183(13):3890-3902.

Sarsero JP, Wookey PJ, Pittard AJ. 1991. Regulation of expression of the *Escherichia coli* K-12 *mtr* gene by TyrR protein and Trp repressor. J Bacteriol 173(13):4133-4143.

Sauer U, Canonaco F, Heri S, Perrenoud A, Fischer E. 2004. The soluble and membrane-bound transhydrogenases UdhA and PntAB have divergent functions in NADPH metabolism of *Escherichia coli*. J Biol Chem 279(8):6613-6619.

Siedler S, Bringer S, Blank LM, Bott M. 2012. Engineering yield and rate of reductive biotransformation in *Escherichia coli* by partial cyclization of the pentose phosphate pathway and PTS-independent glucose transport. Appl Microbiol Biotechnol 93(4):1459-1467.

Siedler S, Bringer S, Bott M. 2011. Increased NADPH availability in *Escherichia coli*: improvement of the product per glucose ratio in reductive whole-cell biotransformation. Appl Microbiol Biotechnol 92(5):929-937.

Spiro S, Guest JR. 1991. Adaptive responses to oxygen limitation in *Escherichia coli*. Trends Biochem Sci 16(8):310-314.

Studier FW, Daegelen P, Lenski RE, Maslov S, Kim JF. 2009. Understanding the differences between genome sequences of *Escherichia coli* B strains REL606 and BL21(DE3) and comparison of the *E. coli* B and K-12 genomes. J Mol Biol 394(4):653–680.

Tsaneva IR, Weiss B. 1990. *soxR*, a locus governing a superoxide response regulon in *Escherichia coli* K-12. J Bacteriol 172(8):4197-4205.

Turner PC, Miller EN, Jarboe LR, Baggett CL, Shanmugam KT, Ingram LO. 2011. YqhC regulates transcription of the adjacent *Escherichia coli* genes *yqhD* and *dkgA* that are involved in furfural tolerance. J Ind Microbiol Biotechnol 38:431-439.

Yum DY, Lee BY, Pan JG. 1999. Identification of the *yqhE* and *yafB* genes encoding two 2, 5-diketo-D-gluconate reductases in *Escherichia coli*. Appl Environ Microbiol 65(8):3341-3346.

List of Figures

Figure 1. Reduction of methyl acetoacetate catalyzed by an alcohol dehydrogenase from *Lactobacillus brevis*.

Figure 2. Parameters of anaerobic biotransfomation. CO_2 transfer rates (CTR) of reference strain (black) and Δ*pfkA* mutant (grey), respectively. MAA was added at time 0. Two biological replicates of each strain are shown.

Figure 3. Parameters of aerobic biotransfomation. A) Oxygen transfer rates (OTR) and B) CO_2 transfer rates (CTR) of reference strain (black) and Δ*pfkA* mutant (grey), respectively. After adaptation of the process and constant conditions, MAA was added as indicated with the arrow. Two biological replicates of each strain are shown.

Table I. Strains and plasmids used in this work.

Strains / Plasmids	Relevant characteristics	Reference
Strains		
Escherichia coli BL21(DE3) Star	F$^-$ *omp*T *hsdS*$_B$(r$_B^-$, m$_B^-$) *gal dcm rne*131 (DE3)	Invitrogen
Reference strain	*E. coli* BL21(DE3) Star with pBtac*Lbadh*	(Siedler et al. 2011)
$\Delta pfkA$	*E. coli* BL21(DE3) Star $\Delta pfkA$ with pBtac*Lbadh*	(Siedler et al. 2011)
Plasmids		
pBtac1	Amp^R, P$_{tac}$, *lacI*; expression vector for *E. coli*	Boehringer Mannheim GmbH
pBTac-*Lbadh*	pBtac1 derivative with *adh* gene from *Lactobacillus brevis*	X-Zyme, (Ernst et al. 2005)

Table II. Genes showing a 2.5-fold increased or decreased mRNA level 10 min after starting NADPH-dependent MAA reduction by resting cells of *E. coli* or its Δ*pfkA* mutant using glucose as reductant. For experimental details see Materials and Methods. The genes with an mRNA ratio (after vs. before MAA addition) ≥2.5 (lower ones allowed in the case of operons and for comparison of the two experiments) or ≤0.4 (higher ones allowed in the case of operons and for comparison of the two experiments) and a *p*-value of ≤0.05 are listed. The data shown represent mean values from two biological replicates. The genes are ordered according to their locus tag.

Locus tag	Gene	Annotation	Reference + MAA/- MAA	Δ*pfkA* + MAA /- MAA
		Transport		
ECD_02533-34	*proVW*	Glycine betaine transporter subunit	2.47 - 2.90	0.74 - 0.85
ECD_00778	*glnH*	Glutamine ABC transporter periplasmic protein	0.40	0.34
		Stress response		
ECD_03934	*soxS*	DNA-binding transcriptional dual regulator	4.59	24.38
ECD_02420	*iscA*	Iron-sulfur cluster assembly protein	2.05	1.81
ECD_02421	*iscU*	Scaffold protein	1.76	3.14
ECD_02422	*iscS*	Cysteine desulfurase	2.24	3.04
ECD_02423	*iscR*	DNA-binding transcriptional repressor	1.67	5.83
ECD_10012	*ybcC*	DLP12 prophage; predicted exonuclease	2.54	0.79
ECD_01323	*ydaQ*	Rac prophage, Putative exisionase	0.35	1.16
		Metabolism		
ECD_02883	*yqhC*	DNA-binding transcriptional regulator of *dkgA*, *yqhD*	3.70	7.89
ECD_02884	*yqhD*	Alcohol dehydrogenase, NAD(P)-dependent	12.70	36.24
ECD_02885	*dkgA*	2,5-diketo-D-gluconate reductase A	7.36	16.18
ECD_03288	*gntK*	Gluconate kinase 2	4.40	2.74
ECD_01236	*trpC*	Bifunctional indole-3-glycerol phosphate synthase	3.74	1.14
ECD_03591	*tnaL*	Tryptophanase leader peptide	2.85	no signal
ECD_03754-55	*glnLA*	Sensory histidine kinase in two-component regulatory system with GlnG; Glutamine synthetase	0.76	0.30 - 0.50
		Regulation		
ECD_02467	*rpoE*	RNA polymerase, sigma 24 (sigma E) factor	3.56	1.36
ECD_01489	*marR*	DNA-binding transcriptional repressor of multiple antibiotic resistance	2.07	2.63
ECD_01490	*marA*	DNA-binding transcriptional activator of multiple antibiotic resistance	1.40	2.44
		Hypothetical/predicted function		
ECD_01108	*ycfR*	Hypothetical protein	7.25	5.25
ECD_01025	*ycdR*	Predicted enzyme associated with biofilm formation	0.39	1.06

Table III.   Selected genes of a genome-wide comparison of mRNA levels of *E. coli* Δ*pfkA* versus the reference strain under biotransformation conditions in the presence of the substrate MAA. Cells were suspended at a cell density of 3 g_{cdw} L^{-1} for 10 min in biotransformation medium and samples were taken for RNA isolation. Genes with an mRNA ratio ≥2.0 (lower ones allowed in the case of operons and for comparison of the two experiments) or ≤0.5 (higher ones allowed in the case of operons and for comparison of the two experiments) and a *p*-value of ≤0.05 are listed. All genes highlighted in red were repressed by the ArcA, ArcB two component system and the gene highlighted in green was induced by ArcA, ArcB. The data shown represent mean values from three biological replicates. The genes were grouped into different functional categories within which they were ordered according to their mRNA ratios except in the case of operons, which were ordered according to their locus tag.

Locus tag	Gene	Annotation	Δ*pfkA*/reference mRNA ratio
		Metabolism	
ECD_00681-84	sdhCDAB	Succinate dehydrogenase	3.04 - 15.46
ECD_02266, ECD_02950, ECD_03737	fadBHI	Fatty acid synthesis	3.71 - 13.37
ECD_03905-08	malFEKM; lamB	Maltose operon	3.31 - 6.78
ECD_01164	dadA	D-Amino acid dehydrogenase small subunit	5.43
ECD_00115	lpdA	Dihydrolipoamide dehydrogenase	2.34
ECD_00112	pdhR	Transcriptional regulator of pyruvate dehydrogenase complex	0.39
ECD_03637	rbsB	Ribose transporter / kinase	0.34
ECD_03028	mtr	Tryptophan transporter	0.14
ECD_01234-39,	trpABCDL	Tryptophan synthesis	0.05 - 0.17
ECD_03592-93	tnaAB	Tryptophanase/L-cysteine desulfhydrase	0.02 - 0.23
ECD_03801	pfkA	6-Phosphofructokinase	0.05
		Osmotic stress response	
ECD_00268-70	betBIT	Betaine aldehyde dehydrogenase, cholin transporter	3.78 - 7.44
		Respiration and oxidative stress	
ECD_03934	soxS	DNA-binding transcriptional dual regulator	6.25

ECD_00382-83	*cyoBA*	Cytochrome bo_3 ubiquinol oxidase	2.80 - 5.26
ECD_02423	*iscR*	FeS, O_2-regulation	2.49
ECD_02464-65	*rseCB*	RseC protein involved in reduction of the SoxR iron-sulfur cluster	0.45
ECD_00692	*cydA*	Cytochrome *bd* terminal oxidase, SU I	0.27
ECD_00693	*cydB*	Cytochrome *bd* terminal oxidase, SU II	0.38
		Other functions	
		30 Ribosomal proteins	3.19 - 15.97
ECD_03847	*sthA*	Soluble transhydrogenase	3.05
ECD_01067-74	*flgMABCDEFG*	Flagellar genes	2.44 - 3.21

Table IV.   Parameters of whole-cell biotransformation of MAA to MHB with glucose as donor of reducing equivalents with *E. coli* reference strain and mutant Δ*pfkA*. The detailed conditions are described in the Materials and methods section. Mean values from two independent experiments are shown.

Strain *E. coli*	Condition	MHB production rate $mmol\ h^{-1}\ g_{cdw}^{-1}$	Glucose uptake rate $mmol\ h^{-1}\ g_{cdw}^{-1}$	Yield $mol_{MHB}\ mol_{Glucose}^{-1}$
Reference	anaerobic	7.4	3.5	2.1
Δ*pfkA*	anaerobic	7.4	2.4	3.1
Reference	aerobic	12.8	3.81	3.4
Δ*pfkA*	aerobic	11.0	2.3	4.8
Reference	shake flask*	8.6	3.4	2.5
Δ*pfkA*	shake flask*	9.1	1.8	4.8

*(Siedler et al. 2011)

Table V. Formation of by-products, carbon dioxide, uptake of glucose and carbon balances of the *E. coli* BL21(DE3) reference strain and the $\Delta pfkA$ mutant during aerobic and anaerobic biotransformations. Mean values from two independent experiments are shown.

Strain	Condition	By-products				CO$_2$	Glucose uptake	Balance
E. coli		Acetate	Formate	Lactate	Succinate			
		(mmol h^{-1} g$_{cdw}^{-1}$)					(mmol h^{-1} g$_{cdw}^{-1}$)	(% C)
Reference	anaerobic	3.3	3.1	2.6	0.5	2.8	3.5	106
$\Delta pfkA$	anaerobic	3.2	3.1	0.3	0.4	2.7	2.4	102
Reference	aerobic	*	0	0	0	21.7	3.8	95
$\Delta pfkA$	aerobic	0	0	0	0	13.8	2.3	100

* Acetate was formed during adaptation of the process and later on consumed

Figure 1.   Reduction of methyl acetoacetate catalyzed by an alcohol dehydrogenase from

Lactobacillus brevis.

Figure 2.   Parameters of anaerobic biotransfomation. CO_2 transfer rates (CTR) of reference strain (black) and Δ*pfkA* mutant (grey), respectively. MAA was added at time zero. Two biological replicates of each strain are shown.
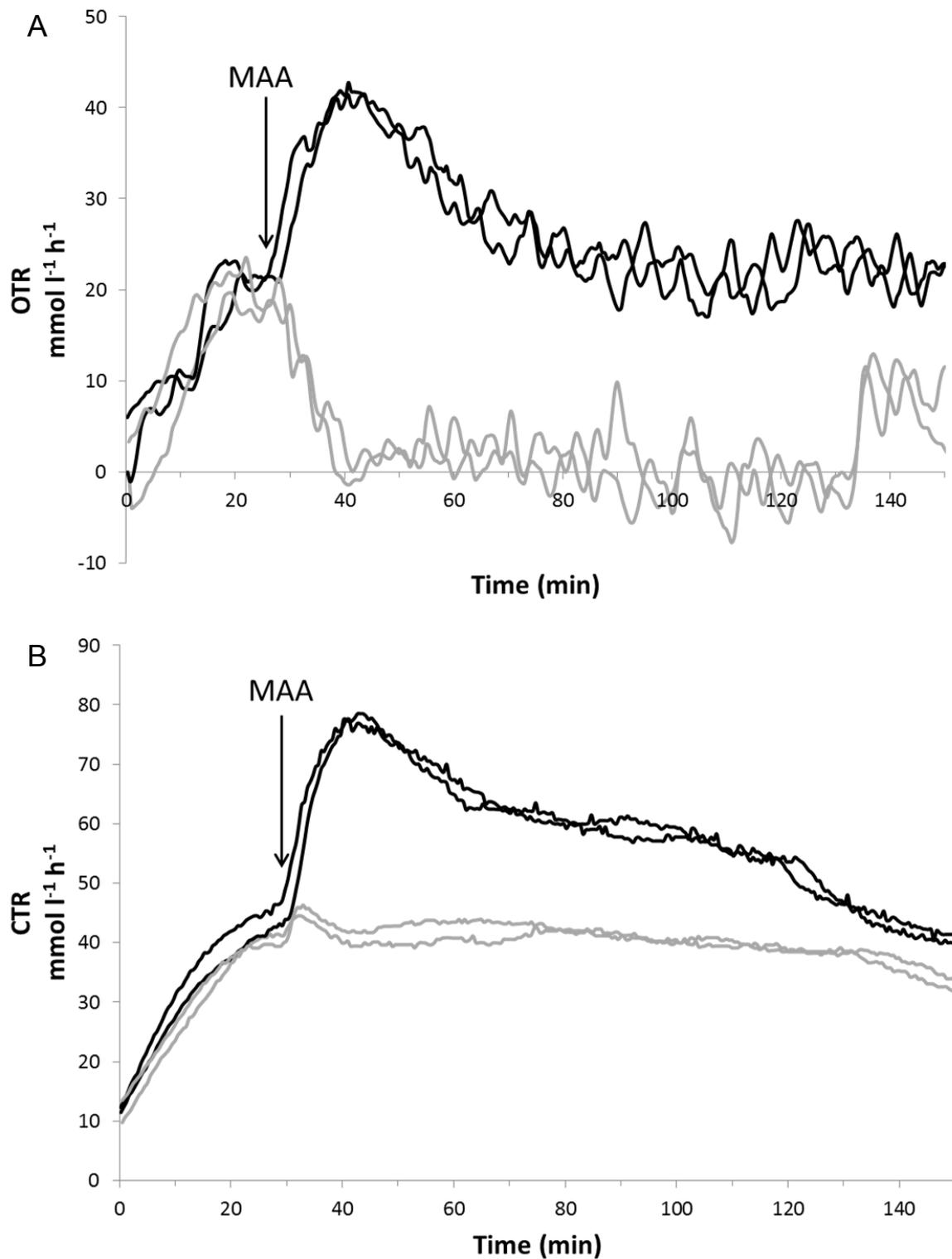
Figure 3. Parameters of aerobic biotransfomation. A) Oxygen transfer rates (OTR) and B) CO_2 transfer rates (CTR) of reference strain (black) and Δ*pfkA* mutant (grey), respectively. After

adaptation of the process and constant conditions, MAA was added as indicated with the arrow.

Two biological replicates for each strain are shown.

Figure 2. Parameters of anaerobic biotransfomation. CO_2 transfer rates (CTR) of reference strain (black) and Δ*pfkA* mutant (grey), respectively. MAA was added at time zero. Two biological replicates of each strain are shown.

A)

B)
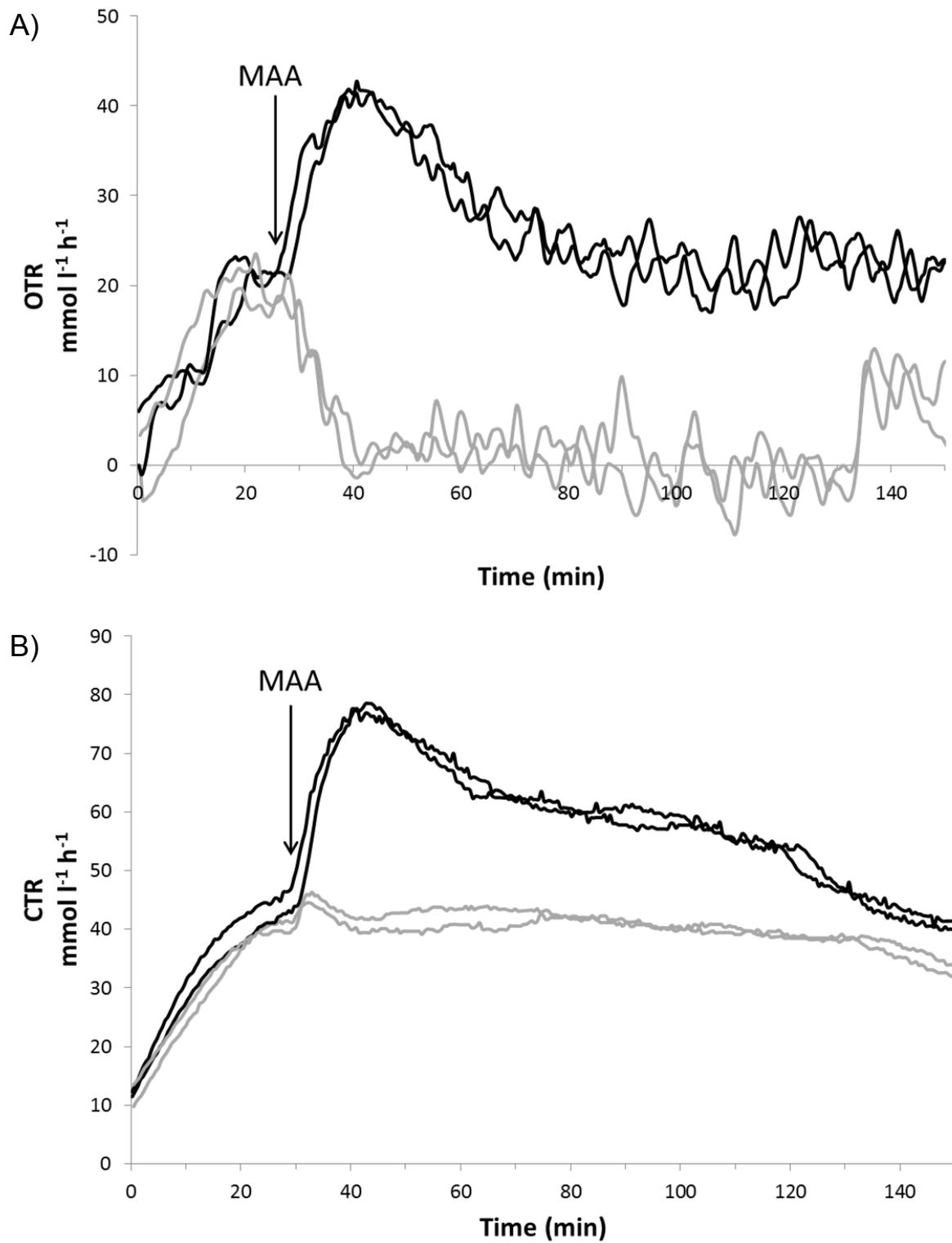
Figure 3.   Parameters of aerobic biotransfomation. A) Oxygen transfer rates (OTR) and B) CO_2 transfer rates (CTR) of reference strain (black) and Δ*pfkA* mutant (grey), respectively. After adaptation of the process and constant conditions, MAA was added as indicated with the arrow. Two biological replicates for each strain are shown.

I performed the experimental work and wrote a draft of the manuscript.

Own proportion to this work: 60%

To be submitted

SoxR as Single-Cell Biosensor for NADPH-Consuming Enzymes in *Escherichia coli*

Solvej Siedler[#], Georg Schendzielorz, Stephan Binder, Lothar Eggeling, Stephanie Bringer, and Michael Bott[*]

IBG-1: Biotechnology, Institute of Bio- and Geosciences, Forschungszentrum Jülich, D-52425 Jülich, Germany

[*]Corresponding author; m.bott@fz-juelich.de; phone +49 2461 613294; fax +49 2461 612710

[#] Current address: Technical University of Denmark, Novo Nordisk Foundation Center for Biosustainability, Fremtidsvej 3, DK - 2970 Hørsholm, Denmark

ABSTRACT: An ultra-high throughput screening system for NADPH-dependent enzymes, such as stereospecific alcohol dehydrogenases, was established. It is based on the [2Fe-2S] cluster-containing transcriptional regulator SoxR of *Escherichia coli* that activates expression of *soxS* in the oxidized, but not in the reduced state of the cluster. As SoxR is kept in its reduced state by NADPH-dependent reductases, an increased NADPH demand of the cell counteracts SoxR reduction and increases *soxS* expression. We have taken advantage of these properties by placing the *eyfp* gene under the control of the *soxS* promoter and analysed the response of *E. coli* cells expressing an NADPH-dependent alcohol dehydrogenase from *Lactobacillus brevis* (*Lb*Adh), which reduces methyl acetoacetate to (*R*)-methyl 3-hydroxybutyrate. Remarkably, the specific fluorescence of the cells correlated with the substrate concentration added and with *Lb*Adh enzyme activity, confirming the NADPH-responsiveness of the sensor. These properties enabled sorting of single cells harboring wild-type *Lb*Adh from those with lowered or without *Lb*Adh activity by fluorescence-activated cell sorting (FACS). In a first application the system was used successfully to screen a mutant *Lb*Adh library for variants showing improved activity with the substrate 4-methyl-2-pentanone.

KEYWORDS: *NADPH biosensor, alcohol dehydrogenases, enzyme evolution, single-cell analysis, FACS*

Redox reactions are at the core of cellular metabolic processes and about one quarter of the known enzymes are oxidoreductases.[1] A feature of many of these enzymes is their stereo- and regiospecificity. The pharmaceutical industry takes advantage of these properties, as well as from the mild and environmentally friendly conditions at which enzyme-catalyzed reactions proceed. Among such processes, alcohol dehydrogenases are of particular interest.[2, 3] They are employed in the reduction of various ketones to produce enantiopure secondary alcohols. These enzymes are frequently NADPH-dependent, and there is a need for continuous supply of the reduced cofactor for the reaction to proceed.[2, 4, 5] This applies both for isolated enzymes and for whole-cell processes.[6, 7]

In our studies with *Escherichia coli* on the reductive biotransformation of methyl acetoacetate (MAA) to (*R*)-methyl 3-hydroxybutyrate (MHB) by an NADPH-dependent alcohol dehydrogenase from *Lactobacillus brevis* (*Lb*Adh)[6, 8] we noticed a significantly increased mRNA level of the *soxS* gene in cells catalyzing MAA reduction. SoxS is a transcription factor whose expression is activated under conditions of oxidative stress by SoxR[9-12] . The genes of the SoxRS regulon mediate the cellular response to superoxide, to diverse redox-cycling drugs like paraquat, or to nitric oxide.[13, 14] SoxR is a homodimer with each subunit containing an [2Fe-2S] cluster.[15, 16] Only when oxidized to [2Fe–2S]$^{2+}$ they confer transcriptional activity to SoxR, which in turn results in expression of *soxS*.[17, 18] SoxS then activates expression of the SoxRS regulon, which includes e.g. the genes for superoxide dismutase (*sodA*), glucose 6-phosphate dehydrogenase (*zwf*), or fumarase C (*fumC*).[19] Inactivation of SoxR involves its NADPH-dependent reduction catalyzed by the *rsxABCDGE* and *rseC* products.[20]

The nature of the cellular signal sensed by SoxR is still a matter of debate.[21-23] Besides direct oxidation of the iron-sulfur centers by superoxide[24] and redox cycling drugs[22], Liochev and Fridovich first suggested that the *soxRS* regulon is responsive to the NADPH/NADP$^+$ ratio[25], which was supported by recent studies.[26] Here, we provide further evidence that SoxR senses NADPH availability and utilized this finding to develop a sensor for the *in vivo* analysis of NADPH-dependent reactions, offering a number of exiting possibilities for high-throughput analysis and development of NADPH-dependent enzymes.

RESULTS AND DISCUSSION

SoxR as an NADPH sensor. Previous studies had indicated that the transcriptional regulator SoxR of *E. coli* becomes active when the NADPH availability of the cell is decreased[26], such as during reductive biotransformations with an NADPH-dependent alcohol dehydrogenase, and then triggers expression of its target gene *soxS*. To evaluate and apply the function of SoxR as an NADPH sensor, we constructed plasmid pSenSox, in which *soxR* of *E. coli* DH5α together with the *soxR-soxS* intergenic region and a small part of the *soxS* coding region followed by a stop codon were cloned in front of *eyfp*, thereby placing synthesis of the autofluorescent protein eYFP under transcriptional control of the *soxS* promoter (Figure 1). The sensor plasmid also encodes the NADPH-dependent alcohol dehydrogenase of *L. brevis*, *Lb*Adh, under the control of an isopropyl β-D-thiogalactoside-inducible promoter. *Lb*Adh was previously shown by us and others to efficiently convert MAA stoichiometrically to MHB.[6, 8, 27, 28]

E. coli BL21(DE3) was transformed with plasmid pSenSox and whole-cell biotransformation assays were performed using 10 - 70 mM MAA as *Lb*Adh substrate.[27, 28] NADPH was provided by the metabolism of components present in yeast extract and tryptone. Fluorescence of the cultures was recorded online using a BioLector system (Figure 2a). Upon addition of MAA the cultures started to emit fluorescence with the initial slope of the fluorescence increase being independent of the MAA concentration added (Figure 2a). For the lowest MAA concentration of 10 mM, the specific fluorescence maximum was achieved already after 1 h, when MAA reduction to MHB was complete.[27] Increasing concentrations of MAA led to increased fluorescence maxima, which were reached at later time points (Figure 2a). This correlates with the increased time required for MAA reduction to MHB, during which the NADPH demand is increased. Importantly, the maximal fluorescence intensity obtained for different initial MAA concentrations remained constant for several hours, due to the high stability of eYFP. When the specific fluorescence achieved after 10 h was plotted against the initial MAA concentration, an almost linear relationship was obtained for MAA concentrations up to 60 mM (Figure 2b). In the absence of MAA, constant background fluorescence was observed. Similarly, in biotransformation experiments with

cells carrying plasmid pSenNeg encoding an inactive *Lb*Adh fragment only background fluorescence was detectable independent of the MAA concentration added. These controls confirm that the fluorescence increase was strictly dependent on the NADPH-dependent reduction of MAA to MHB. The increased fluorescence obtained with increased MAA concentrations was also visible at the single cell level by epifluorescence microscopy (Figure 2c) as well as by flow cytometry.

These data support the view that SoxR of *E. coli* is activated under conditions of increased NADPH demand, as obtained by the reduction of MAA to MHB by *Lb*Adh. By coupling SoxR activity to the expression of *eyfp* via the *soxS* promoter, we could show that the specific fluorescence of *E. coli* cells correlates with the concentration of MAA reduced to MHB (Figure 2). At a constant *Lb*Adh activity, the time required for complete MAA reduction and thus the period of high NADPH demand increases linearly with the MAA concentration. To explain the observed correlation, we propose that SoxR is subject to permanent oxidation under aerobic conditions even in the absence of oxidative stress, but kept in its reduced form by NADPH-dependent reduction via the *rsxABCDGE* and *rseC* gene products. Under conditions of high NADPH-demand, SoxR reduction is reduced, thus favoring the presence of oxidized, active SoxR. Regarding the discussion on the nature of the signal sensed by SoxR, our data support the concept of Liochev and Fridovich[25] that there are multiple ways to induce the SoxRS regulon, which ultimately shift the equilibrium of oxidized and reduced SoxR to the oxidized form. This can either happen by increasing the oxidation of reduced SoxR or by decreasing the reduction of oxidized SoxR, as exemplified in our study.

Correlation between fluorescence and *Lb*Adh activity. In a next series of experiments the influence of varying *Lb*Adh activities on fluorescence output at a constant MAA concentration was tested (Table 1). For this purpose, strains with a specific *Lb*Adh activity between 0.03 U (mg protein)$^{-1}$ (background activity) and 15.2 U (mg protein)$^{-1}$ were used in biotransformations with 40 mM MAA. The different *Lb*Adh activities were achieved either by varying the expression level of the wild-type enzyme by induction or repression or by using mutant *Lb*Adh proteins with the amino acid exchanges Leu194Ser and Leu194Ala. In the biotransformation assays, constant fluorescence was achieved after 10 h. As shown in

Table 1, higher *Lb*Adh activities led to higher maximal specific fluorescence. This suggests that increasing specific *Lb*Adh activities cause increased NADPH consumption rates which in turn reduce the rate of NADPH-dependent reduction of oxidized SoxR, leading to an increased SoxR activity. Thus, the pSenSox system in the living cell offers the remarkable possibility to distinguish NADPH-dependent enzymes with varying specific activity.

Application of SoxR for high-throughput screening of NADPH-dependent enzymes. Recently, metabolite-activated transcription factors controlling *eypf* expression were used to monitor the cytosolic concentration of the respective metabolites in single bacterial cells, which allowed high-throughput screening and isolation of single producer cells using fluorescence-activated cell sorting (FACS).[29-31] Based on these results we tested whether also single cells differing in their specific *Lb*Adh activity can be analyzed and sorted via FACS. For this purpose, *E. coli* cells carrying either pSenSox (6.2 U mg^{-1} *Lb*Adh activity), pSen-L194A (2.7 U mg^{-1}), or pSenNeg (0.03 U mg^{-1}) were used for biotransformation of 70 mM MAA for 19 h and then subjected to FACS. The resulting combined histogram (Figure 3a) showed three well resolved peaks of eYFP fluorescence indicating that the three strains differing in their specific *Lb*Adh activities form homogeneous populations. Using an appropriate gate (P1), where 0% of the cells with background fluorescence (carrying pSenNeg) would be selected, still 80.8% of the population of cells with high fluorescence (carrying pSenSox) and 1.5% of the cells with lower fluorescence (carrying pSen-L194A) could be isolated.

These results encouraged us to test the suitability of the NADPH sensor for HT-screening of alcohol dehydrogenase mutant libraries. To do this we introduced mutations in *Lb*Adh by saturation mutagenesis at positions Ala93, Leu152, and Val195 and randomly by error-prone PCR. The cells of the mutant library were then used for reductive biotransformation of 20 mM 4-methyl-2-pentanone (4M2P). This prochiral ketone was chosen since the reduced product (*R*)-4-methyl-2-pentanol is of economic interest, and wild-type *Lb*Adh has only ~12% activity with this substrate as compared to MAA (15.5 μmol min^{-1} (mg protein)$^{-1}$). After 3 h of biotransformation, the cells were subjected to FACS. We performed a sort on the

library, in which the lower bound of the sorting gate was set by cells with wild-type *Lb*adh after biotransformation of 4M2P and the higher bound by the same strain after biotransformation of MAA instead of 4MP (Figure 3b). 10^6 cells of the *Lb*Adh mutant library were analyzed and 250 cells showing high fluorescence were selected and spotted on plates, of which 123 grew up to colonies. 96 of them were analyzed in a microtiter plate for fluorescence intensity after 2 h incubation with 4M2P. From 6 selected clones with high specific fluorescence the specific *Lb*Adh activity was determined and one clone was identified having a 36% increased activity with the substrate 4M2P accompanied by an 8-fold increased K_M value (Table 2). The plasmid of this mutant clone was fully sequenced and found to contain a single mutation in the *adh* gene leading to an Ala93Met exchange.

In conclusion, the correlation between NADPH consumption and fluorescence was visible at the single-cell level and suitable for FACS analysis, allowing the highest throughput assays currently possible. As we could demonstrate a correlation between the specific activity of the NADPH-consuming enzyme and the specific fluorescence of the cells, the SoxR sensor provides a generalized high-throughput screening system for this type of enzymes. We demonstrated this potential by the rapid isolation of an *Lb*Adh variant via FACS with an improved activity towards the substrate 4-methyl-2-pentanone (Table 2). As long as educts and products can enter and leave the sensor-containing cells libraries of NADPH-dependent dehydrogenases or P450-monooxygenases can now be assayed in a high-throughput format without development of specific assays. This novel technology is expected to expedite the availability of new enzymes for the synthesis of chiral compounds significantly.

METHODS

Bacterial strains, media and growth conditions. Bacterial strains and plasmids are listed in Table 3. *E. coli* strains were transformed by the method described by Hanahan[32] and cultivated in LB medium[33] or in 2xYT medium (16 g l^{-1} tryptone, 10 g l^{-1} yeast extract, 5 g l^{-1} sodium chloride). *E. coli* DH5α[32] was used for cloning and screening purposes and *E. coli* BL21 Star (DE3) (Invitrogen, Karlsruhe, Germany) and derivatives for gene expression and whole-cell biotransformation for sensor establishment. Plasmids

were selected by adding antibiotics to the medium at a final concentration of 100 μg ampicillin ml^{-1} (pSenSox and derivatives) and 50 μg kanamycin ml^{-1} (pET28a).

Recombinant DNA work. Standard methods including PCR, DNA restriction or ligation were carried out according to standard protocols.[34] Oligonucleotides were synthesized by Biolegio ev (Nijmegen, The Netherlands) and are listed in Table 3. For construction of the plasmid-based biosensor pSenSox, the *E. coli* DNA region encompassing the *soxR* open reading frame, the *soxR-soxS* intergenic region, and the first 21 codons of *soxS* were amplified with Phusion DNA polymerase (Thermo Scientific) from chromosomal DNA of *E. coli* BL21(DE3) by PCR using oligonucleotides SoxS_for_SphI and SoxR_rev_SalI, which introduce SphI and SalI restriction sites as well as a stop codon after codon 21 of *soxS*. Additionally, the *eyfp* gene was amplified by PCR with oligonucleotides EYFP_for_SphI, containing a ribosome binding site, and EYFP_rev_ClaI using the vector pSenlys [29] as template, thereby introducing restriction sites for SphI and ClaI digestion. Both PCR products were cloned into the plasmid pBtac*Lb*adh [8], resulting in plasmid pSenSox. For the construction of pSenNeg, a 221 bp region of the *adh* gene of *L. brevis* was amplified with the oligonucleotides ADH_negK_for and ADH_negK_rev introducing EcoRI and HindIII restriction sites. The PCR product was cut with EcoRI and HindIII and used to replace the functional *adh* gene in plasmid pSenSox by a non-functional *adh* fragment. For saturation mutagenesis of codons Ala93, Leu152 and Val195 within the intact *adh* gene, the oligonucleotide pairs Ala93_for/Ala93_rev, Leu152_for/Leu152_rev, and Val195_for/Val195_rev were used according to the Stratagene site-directed mutagenesis kit with the following modifications: DpnI (Fermentas) and pfx polymerase (Invitrogen) were used. For random mutagenesis of the entire *adh* gene, error-prone PCR (ep-PCR) was performed using the oligonuelotide pair ADH_mut_for/ADH_mut_rev, plasmid pSenSox as template and Phusion DNA polymerase using the protocol described by Wilson and Keefe 2001 [35]. The PCR products were cut with EcoRI and HindIII and used to replace the native *adh* gene in pSenSox.

Whole cell biotransformation in microtiter plates. For biotransformation experiments with *E. coli* cells harboring pSenSox or a derivative, 5 ml 2xYT medium containing the appropriate antibiotic(s) was

inoculated with a single colony of the respective strain and incubated overnight at 37°C and 130 rpm. These pre-cultures were used for inoculation of the main cultures to an optical density at 600 nm (OD_{600}) of 0.05. Main cultures were grown in 50 ml 2xYT medium in the presence of the appropriate selection marker at 37°C and 130 rpm to an OD_{600} of 0.3, induced with 1 mM IPTG when required, and incubated for another 3 h to an OD_{600} between 5 and 6. For online monitoring of fluorescence during biotransformation, 900 µl portions of the cultures were transferred into 48 well microtiter Flowerplates, supplemented with 100 µl of the biotransformation substrate dissolved in water, and incubated in a BioLector cultivation system (m2plabs GmbH, Aachen, Germany) at 30°C and 1200 rpm (shaking diameter 3 mm). During cultivation biomass was measured as backscattered light intensity (620 nm, signal gain factor of 15). The eYFP fluorescence of the cultures was measured at an excitation wavelength of 485 nm and an emission wavelength of 520 nm (signal gain factor of 70). The specific fluorescence was calculated as the ratio of eYFP fluorescence/scattered light intensity (given in a.u.).[36]

96-well screening system. For screening of ADH activity, *E. coli* DH5α was transformed with the pSenSox derivatives subjected to site-directed mutagenesis and plated on LB agar plates containing 100 µg ml^{-1} ampicillin. Single colonies were inoculated into 200 µl of 2xYT medium in a 96-well plate and grown overnight at 37°C and 800 rpm. For the main culture 5 µl of the preculture was inoculated into 145 µl 2xYT medium in a 96-well plate. After 5 h 40 mM methyl acetoacetate (MAA) was added to the cells and the fluorescence and the OD_{600} was measured every hour for 4 h using a plate reader (TECAN, Infinite 200 PRO). The specific fluorescence was defined as the fluorescence per OD_{600}.

Fluorescence-activated cell sorting. Flow cytometric measurements were performed with a FACS AriaII (Becton Dickinson, San Jose, USA) with 488 nm excitation (blue solid-state laser). Forward-scatter characteristics (FSC) and side-scatter characteristics (SSC) were detected as small-angle and large-angle scatters of the 488-nm laser, respectively. eYFP fluorescence was detected using a 502-nm long-pass and a 530/30-nm band-pass filter set. Data were analyzed using BD DIVA 6.1.3 software. The sheath fluid was sterile filtered phosphate-buffered saline (137 mM NaCl, 2.7 mM KCl, 10 mM Na_2HPO_4, and 1.8 mM KH_2PO_4). Electronic gating was set to exclude nonbacterial particles on the basis of forward versus

side scatter area. For sorting of eYFP-positive cells the next level of electronic gating was set to exclude

non-fluorescent cells. Background was estimated using cells with pSenSox (wild-type *Lb*Adh) for sorting

of eYFP-positive cells. For screening of cells having increased Adh activity with the substrate 4-methyl-2-

pentanone, *E. coli* DH5α was transformed with a pSenSox library containing either site-directed or

randomly via epPCR mutagenized *Lbadh*. After transformation, plating on LB agar plates containing

ampicillin and incubation for 18 h at 37°C, the colonies were resuspended in 10 ml 2xYT medium and

diluted by a factor of 10 using 2xYT medium. Cells containing non-mutagenized pSenSox were used as

background control. After 4 h of growth at 37°C and 130 rpm, 20 mM 4-methyl-2-pentanone was added to

the cells and incubation was continued for 2.5 h, after which the cells were subjected to FACS.

Determination of alcohol dehydrogenase activity. *E. coli* strains carrying the desired plasmids were

cultured for 5 h at 37°C and 130 rpm in 50 ml 2xYT medium. Cells were harvested by centrifugation for 5

min at 10,000 g and 4°C. The cells were resuspended in 100 mM potassium phosphate buffer, pH 6.5,

with 1 mM dithiothreitol and 1 mM MgCl$_2$. Cells were disrupted at 4°C by 3×15 s bead-beating with glass

beads (diameter 0.1 mm) using a Silamat S5 (Ivoclar Vivadent GmbH, Germany) and crude extracts were

centrifuged for 20 min at 16,000 g and 4°C to remove intact cells and cell debris. The supernatants were

used as cell-free extracts. Adh activity was measured photometrically at 340 nm using different dilutions

of the cell-free extract using a mixture of 10 mM MAA, 250 μM NADPH, and 1 mM MgCl$_2$ in 100 mM

potassium phosphate buffer, pH 6.5. Reactions were started by addition of cell-free extract. One unit of

enzyme activity was defined as the amount of enzyme catalyzing the oxidation of 1 μmol min^{-1} NADPH

at 30°C under the specified conditions. Protein concentrations were determined by the method of

Bradford[37] using bovine serum albumin as standard. For the determination of the K_m values, the substrate

4-methyl-2-pentanone was used in concentrations of 0.1‑10 mM. K_m and V_{max} values were calculated

using Lineweaver‑Burk plots of the experimental data.[38]

AUTHOR INFORMATION

Corresponding Author

*E-mail: m.bott@fz-juelich.de.

Author Contributions

S.S., G.S. and S.Bi. performed the experiments, S.Br., L.E. and M.B. provided guidance for experimental set-ups, and S.Br., L.E. and M.B. wrote the paper.

Notes

The authors declare no competing financial interest.

REFERENCES

(1) McDonald, A. G., Boyce, S., and Tipton, K. F. (2009) ExplorEnz: the primary source of the IUBMB enzyme list, *Nucleic Acids Res. 37*, D593-D597.

(2) Hall, M., and Bommarius, A. S. (2011) Enantioenriched compounds via enzyme-catalyzed redox reactions, *Chem. Rev. 111*, 4088-4110.

(3) Bornscheuer, U. T., Huisman, G. W., Kazlauskas, R. J., Lutz, S., Moore, J. C., and Robins, K. (2012) Engineering the third wave of biocatalysis, *Nature 485*, 185-194.

(4) Reetz, M. T. (2011) Laboratory evolution of stereoselective enzymes: a prolific source of catalysts for asymmetric reactions, *Angew. Chem. Int. Ed. Engl. 50*, 138-174.

(5) Huisman, G. W., Liang, J., and Krebber, A. (2010) Practical chiral alcohol manufacture using ketoreductases, *Curr. Opin. Chem. Biol. 14*, 122-129.

(6) Schroer, K., Mackfeld, U., Tan, I. A., Wandrey, C., Heuser, F., Bringer-Meyer, S., Weckbecker, A., Hummel, W., Daussmann, T., Pfaller, R., Liese, A., and Lütz, S. (2007) Continuous asymmetric ketone reduction processes with recombinant *Escherichia coli*, *J. Biotechnol. 132*, 438-444.

(7) Hummel, W. (1999) Large-scale applications of NAD(P)-dependent oxidoreductases: recent developments, *Trends Biotechnol. 17*, 487-492.

(8) Ernst, M., Kaup, B., Müller, M., Bringer-Meyer, S., and Sahm, H. (2005) Enantioselective reduction of carbonyl compounds by whole-cell biotransformation, combining a formate dehydrogenase and a (*R*)-specific alcohol dehydrogenase, *Appl. Microbiol. Biotechnol. 66*, 629-634.

(9) Greenberg, J. T., Monach, P., Chou, J. H., Josephy, P. D., and Demple, B. (1990) Positive control of a global antioxidant defense regulon activated by superoxide-generating agents in *Escherichia coli*, *Proc. Natl. Acad. Sci. U S A 87*, 6181-6185.

(10) Tsaneva, I. R., and Weiss, B. (1990) *soxR*, a locus governing a superoxide response regulon in *Escherichia coli* K-12, *J. Bacteriol. 172*, 4197-4205.

(11) Wu, J., and Weiss, B. (1991) Two divergently transcribed genes, *soxR* and *soxS*, control a superoxide response regulon of *Escherichia coli*, *J. Bacteriol. 173*, 2864-2871.

(12) Amábile-Cuevas, C. F., and Demple, B. (1991) Molecular characterization of the *soxRS* genes of *Escherichia coli*: two genes control a superoxide stress regulon, *Nucleic Acids Res. 19*, 4479-4484.

(13) Chiang, S. M., and Schellhorn, H. E. (2012) Regulators of oxidative stress response genes in *Escherichia coli* and their functional conservation in bacteria, *Arch. Biochem. Biophys. 525*, 161-169.

(14) Imlay, J. A. (2008) Cellular defenses against superoxide and hydrogen peroxide, *Annu. Rev. Biochem. 77*, 755-776.

(15) Watanabe, S., Kita, A., Kobayashi, K., and Miki, K. (2008) Crystal structure of the [2Fe-2S] oxidative-stress sensor SoxR bound to DNA, *Proc. Natl. Acad. Sci. U S A 105*, 4121-4126.

(16) Hidalgo, E., and Demple, B. (1994) An iron-sulfur center essential for transcriptional activation by the redox-sensing SoxR protein, *EMBO J. 13*, 138-146.

(17) Ding, H., Hidalgo, E., and Demple, B. (1996) The redox state of the [2Fe-2S] clusters in SoxR protein regulates its activity as a transcription factor, *J. Biol. Chem. 271*, 33173-33175.

(18) Gaudu, P., and Weiss, B. (1996) SoxR, a [2Fe-2S] transcription factor, is active only in its oxidized form, *Proc. Natl. Acad. Sci. U S A 93*, 10094-10098.

(19) Blanchard, J. L., Wholey, W. Y., Conlon, E. M., and Pomposiello, P. J. (2007) Rapid changes in gene expression dynamics in response to superoxide reveal SoxRS-dependent and independent transcriptional networks, *PLoS One 2*, e1186.

(20) Koo, M. S., Lee, J. H., Rah, S. Y., Yeo, W. S., Lee, J. W., Lee, K. L., Koh, Y. S., Kang, S. O., and Roe, J. H. (2003) A reducing system of the superoxide sensor SoxR in *Escherichia coli*, *EMBO J. 22*, 2614-2622.

(21) Liochev, S. I., Benov, L., Touati, D., and Fridovich, I. (1999) Induction of the *soxRS* regulon of *Escherichia coli* by superoxide, *J. Biol. Chem. 274*, 9479-9481.

(22) Gu, M., and Imlay, J. A. (2011) The SoxRS response of *Escherichia coli* is directly activated by redox-cycling drugs rather than by superoxide, *Mol. Microbiol. 79*, 1136-1150.

(23) Liochev, S. I., and Fridovich, I. (2011) Is superoxide able to induce SoxRS?, *Free Radic. Biol. Med. 50*, 1813.

(24) Fujikawa, M., Kobayashi, K., and Kozawa, T. (2012) Direct oxidation of the [2Fe-2S] cluster in SoxR protein by superoxide: distinct differential sensitivity to superoxide-mediated signal transduction, *J. Biol. Chem. 287*, 35702-35708.

(25) Liochev, S. I., and Fridovich, I. (1992) Fumarase C, the stable fumarase of *Escherichia coli*, is controlled by the *soxRS* regulon, *Proc. Natl. Acad. Sci. U S A 89*, 5892-5896.

(26) Krapp, A. R., Humbert, M. V., and Carrillo, N. (2011) The *soxRS* response of *Escherichia coli* can be induced in the absence of oxidative stress and oxygen by modulation of NADPH content, *Microbiology 157*, 957-965.

(27) Siedler, S., Bringer, S., and Bott, M. (2011) Increased NADPH availability in *Escherichia coli*: improvement of the product per glucose ratio in reductive whole-cell biotransformation, *Appl. Microbiol. Biotechnol. 92*, 929-937.

(28) Siedler, S., Bringer, S., Blank, L. M., and Bott, M. (2012) Engineering yield and rate of reductive biotransformation in *Escherichia coli* by partial cyclization of the pentose phosphate pathway and PTS-independent glucose transport, *Appl. Microbiol. Biotechnol. 93*, 1459-1467.

(29) Binder, S., Schendzielorz, G., Stäbler, N., Krumbach, K., Hoffmann, K., Bott, M., and Eggeling, L. (2012) A high-throughput approach to identify genomic variants of bacterial metabolite producers at the single-cell level, *Genome Biol. 13*, R40.

(30) Mustafi, N., Grünberger, A., Kohlheyer, D., Bott, M., and Frunzke, J. (2012) The development and application of a single-cell biosensor for the detection of l-methionine and branched-chain amino acids, *Metab. Eng. 14*, 449-457.

(31) Grünberger, A., Paczia, N., Probst, C., Schendzielorz, G., Eggeling, L., Noack, S., Wiechert, W., and Kohlheyer, D. (2012) A disposable picolitre bioreactor for cultivation and investigation of industrially relevant bacteria on the single cell level, *Lab Chip 12*, 2060-2068.

(32) Hanahan, D. (1983) Studies on transformation of *Escherichia coli* with plasmids, *J. Mol. Biol. 166*, 557-580.

(33) Miller, J. (1972) Experiments in Molecular Genetics, *Cold Spring Harbor Laboratory, Cold Spring Harbor, New York*, 352-355.

(34) Sambrook, J., and Russell, D. W. (2001) Molecular cloning: a laboratory manual, 3rd ed. Cold Spring Harbor Laboratory Press, Cold Spring Harbor, N.Y.

(35) Wilson, D. S., and Keefe, A. D. (2001) Random mutagenesis by PCR, *Curr. Protoc. Mol. Biol. Chapter 8*, Unit8 3.

(36) Funke, M., Diederichs, S., Kensy, F., Müller, C., and Büchs, J. (2009) The baffled microtiter plate: increased oxygen transfer and improved online monitoring in small scale fermentations, *Biotechnol. Bioeng. 103*, 1118-1128.

(37) Bradford, M. M. (1976) A rapid and sensitive method for the quantitation of microgram quantities of protein utilizing the principle of protein-dye binding, *Anal. Biochem. 72*, 248-254.

(38) Lineweaver, H., and Burk, D. (1934) The determination of enzyme dissociation constants, *J. Am. Chem. Soc. 56*, 658-666.

Table 1. Dependence of the maximal specific fluorescence from the specific *Lb*Adh activity of cells

E. coli BL21(DE3) strains	IPTG[a]	*Lb*Adh activity[b]	Maximal specific fluorescence[c]
pSenNeg	-	0.03 ± 0.01	0.07 ± 0.01
pSenSox + pET28a	-	0.5 ± 0.1	0.09 ± 0.01
pSen-L194S	-	0.7 ± 0.3	0.11 ± 0.01
pSen-L194A	-	2.7 ± 0.6	0.18 ± 0.04
pSenSox	-	6.3 ± 0.6	0.38 ± 0.02
pSenSox	+	15.2 ±2.0	0.46 ± 0.04

[a]IPTG was added to 1 mM. [b]*Lb*Adh activity of cell-free extracts is given in μmol min^{-1} (mg protein)$^{-1}$. [c]Values were measured after 19 h of biotransformation with 40 mM MAA.

Table 2. Properties of wild-type *Lb*Adh and the variant *Lb*Adh-A93M for the substrate 4-methyl-2-pentanone.

Enzyme[a]	V$_{max}$[b] (μmol min^{-1} mg^{-1})	K_M[b] (mM)
*Lb*Adh	1.94 ± 0.02	0.11 ± 0.01
*Lb*Adh-A93M	2.62 ± 0.03	0.88 ± 0.07

[a]Enzyme activities were determined with crude extracts of the respective strains carrying either pSenSox or pSen-LA93M. [b]Mean values and standard deviation from three replicates are given.

Table 3. Strains, plasmids and oligonucleotides used in this work[a]

Strains, plasmids and oligonucleotides	Relevant characteristics or 5′–3′ sequence	Reference or restriction site
Strains		
Escherichia coli BL21 Star (DE3)	F⁻ *omp*T *hsdS*$_B$(r$_B$⁻, m$_B$⁻) *gal dcm rne*131 (DE3)	Invitrogen
Escherichia coli DH5α	F⁻ ø80Δ*lacZ*ΔM15 Δ(*lacZYA-argF*) U169 *deoR recA*1 *endA*1 *hsdR*17 (rk⁻, mk⁺) *phoA supE*44 λ⁻ *thi*-1 *gyrA*96 *relA*1	(1)
Plasmids		
pBTac-*Lbadh*	Amp^R; pBtac1 derivative with *adh* gene from *Lactobacillus brevis*	(4)
pSenSox	Amp^R; pBtac-*Lbadh* derivative containing *soxRS*-based biosensor	This study
pSenNeg	Amp^R; pSensox derivative encoding an inactive *Lb*Adh fragment	This study
pSen-L194S	Amp^R; pSensox derivative encoding *Lb*Adh-L194S	This study
pSenL194A	Amp^R; pSensox derivative encoding adh L194A	This study
pSenA93M	Amp^R; pSensox derivative with mutated adh A93M	This study
pET28a	Kan^R; plasmid used for provision of IPTG-inducible *lacI* gene	Novagen
pSenLys	Kan^R; pJC1 derivative containing *lysGE*-based biosensor	(5)
Oligonucleotides*		
SoxS_for_SphI	ATCT<u>GCATGC</u>***TTA***CGGCTGGTCAATATGCTCGTC	SphI
SoxR_rev_SalI	GCTA<u>GTCGAC</u>CAAACTAAAGCGCCCTTGTG	SalI
EYFP_for_SphI	AGAG<u>GCATGC</u>AAGGAGAATTAC***ATG***GTGAGCAAGGGCGAGG	SphI
EYFP_rev_ClaI	GCGC<u>ATCGAT</u>TTATTACTTGTACAGCTCGTCCATG	ClaI
ADH_negK_for	ACAA<u>GAATTC</u>GCTAAGAGTGTCGGCACTCC	EcoRI
ADH_negK_rev	GGCC<u>AAGCTT</u>CCGAAGAAGACACCATCAAG	HindIII
Ala93_for	GTTAATAACGCTGGGATCNNKGTTAACAAGAGTGTC	
Ala93_rev	GACACTCTTGTTAACMNNGATCCCAGCGTTATTAAC	
Leu152_for	GATCCTAGCTTAGGGGCNNKCAACGCATC	
Leu152_rev	GATGCGTTGMNNGCCCCTAAGCTAGGATC	
Val195_for	GACACCATTGGNNKATGACCTACCAGGGGC	
Val195_rev	GCCCCTGGTAGGTCATCAACMNNTGGTGTC	
ADH_mut_for	ATAC<u>GAATTC</u>***ATG***TCTAACCGTTTGGATGG	EcoRI
ADH_mut_rev	GTGTG<u>AAGCTT</u>A***CTA***TTGAGCAGTGTAG	HindIII

[a]Restriction sites are underlined, coding sequences are shown in italics, start or stop codons in bold face.
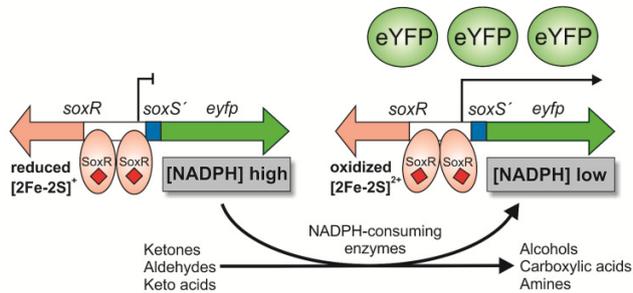
Figure 1. NADPH biosensor based on the transcriptional regulator SoxR of *E. coli*. Dimeric SoxR with two Fe–S clusters binds to the *soxR-soxS* intergenic region. At sufficient NADPH levels, the Fe-S clusters are kept in the reduced state and SoxR is inactive. Enhanced activity of NADPH-consuming enzymes impedes SoxR reduction and the oxidized Fe-S clusters trigger a conformational change of SoxR, causing transcription of its target gene *soxS*. In the NADPH biosensor pSenSox, *soxS* has been replaced by *eyfp* coding for the auto- fluorescent protein eYFP, which allows identifying cells with a low NADPH level by their increased fluorescence.
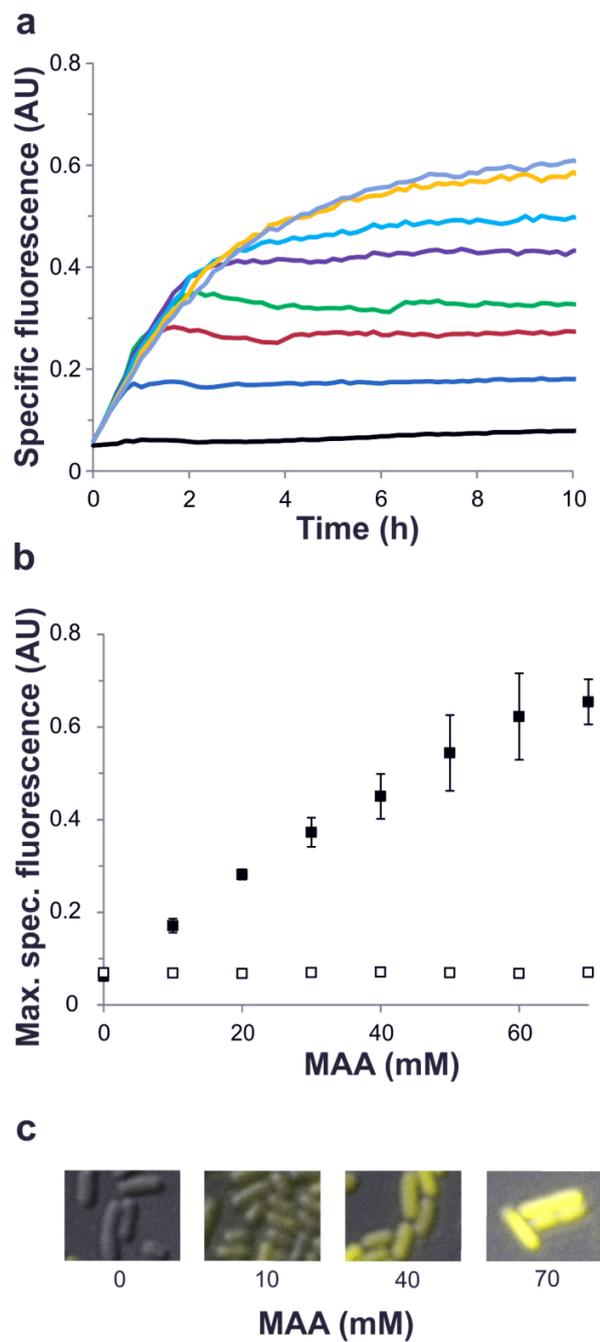
Figure 2. (a) Specific fluorescence of *E. coli* carrying the NADPH biosensor pSenSox during biotransformation of 10 mM (dark blue), 20 mM (brown), 30 mM (green), 40 mM (purple), 50 mM (light blue), 60 mM (yellow) and 70 mM (grey) MAA

to MHB via the NADPH-dependent alcohol dehydrogenase *Lb*Adh. In black a control without MAA is shown. (b) The specific fluorescence obtained after 10 h of biotransformation was plotted against the initial MAA concentration (■). The empty squares (□) show the values obtained with the control plasmid pSenNeg encoding an inactive *Lb*Adh fragment. (c) Epifluorescence of cells from biotransformations with 0, 10, 40, or 70 mM MAA.
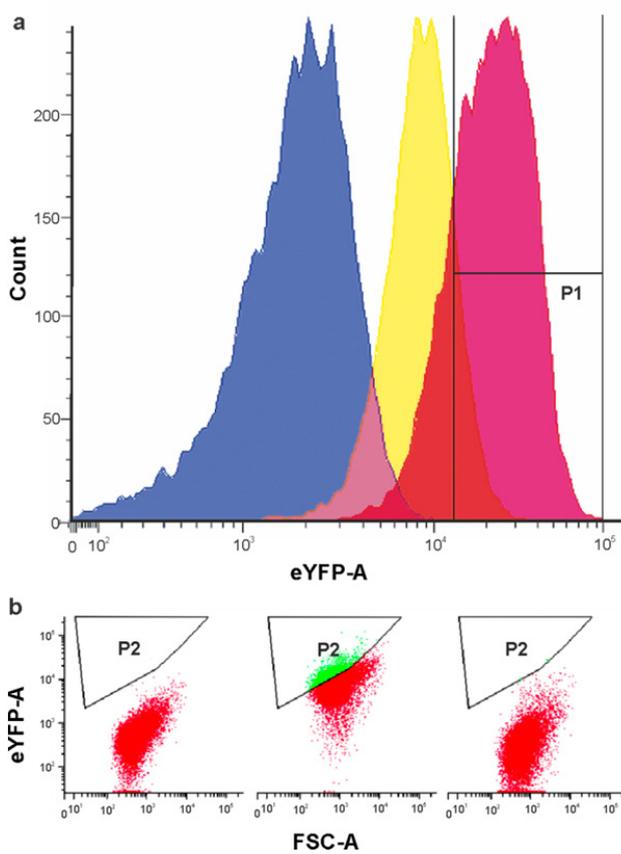
Figure 3. Flow cytometric analysis of *E. coli* cells with the *soxR-soxS*-based NADPH sensor and different NADPH-dependent *Lb*Adh activities. (a) Combined fluorescence histograms of three *E. coli* strains carrying either pSenNeg (blue, 0.03 U mg^{-1} *Lb*Adh acitivity), pSen-L194S (yellow, 0.70 U mg^{-1} *Lb*Adh activity), or pSenSox (red, 6.28 U mg^{-1} *Lb*Adh activity) after biotransformation for 19 h with 70 mM MAA. Gate P1 was used for differentiation of pSenNeg and mutant or wild type populations. (b) FACS-generated dot plots displaying the FSC signal (forward scatter) and the eYFP signal of *E. coli* cells carrying pSenSox after reductive biotransformation of

20 mM 4M2P (left side) or of 20 mM MAA (middle). On the right side, the library of mutant *Lb*Adhs was used for biotransformation of 20 mM 4M2P and then subjected to FACS. Gate P2 was used for mutant screening.

TOC figure
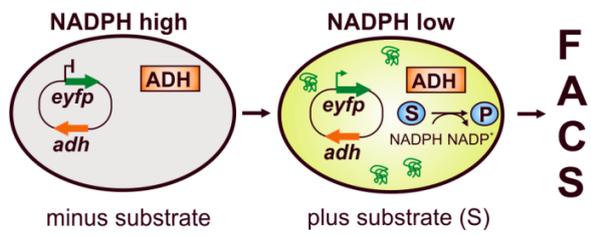
Own proportion to this work: 60%

I designed the study and performed the experimental work. FACS analysis was done together with either Stefan Binder or Georg Schendzielorz. I wrote the draft of the manuscript.

Submitted to ACS Synthetic Biology

4. Discussion

4.1 Whole-cell biotransformation

Whole-cell biotransformation is an important method in chemo-enzymatic synthesis and optimization is of great interest. The optimization of the NADPH per glucose yield was focused in this work. The model reaction of the reduction of MAA to MHB catalyzed by an ADH from *L. brevis* was chosen as a model reaction. The ADH was not limiting because in vitro measurements showed high activities which would principally enable a 40 times higher specific biotransformation rate. In a recent work higher specific biotransformation rates of 33 mmol MHB h^{-1} g_{cdw}^{-1} were achieved using a substrate-coupled biotransformation strategy with ADH catalyzing both, the reduction of MAA and the regeneration of NADPH by oxidation of 2-propanol (Schroer et al. 2009). For the conversion of MAA to MHB, it was shown that there is no substrate and product inhibition, and neither substrate nor product were toxic to the cells under the chosen conditions (Tan 2006). Taken together, enzyme activity, substrate and product transport as well as toxicity can be ruled out as limiting factors.

The effects of a linear flux through the PPP by deletion of *pgi*, the partial cyclization of the PPP by deletion of *pfkA* and the complete cyclization of the PPP by deletion of *gapA* was analyzed in this study.

4.1.1 Linear flux through the PPP in *Escherichia coli*

The Δ*pgi* mutant of *E. coli* BL21(DE3) showed a strong growth defect with a growth rate of 0.1 h^{-1} in glucose minimal media, in agreement with previous studies (Sauer et al. 2004; Nanchen et al. 2007). A 76 % lower glucose consumption rate of 2.7 mmol glucose h^{-1} g_{cdw}^{-1} was detected, compared to the reference strain. Several reasons for the lower glucose consumption rate have already been discussed in literature. The Δ*pgi* mutant has a high glucose 6-phosphate pool, which was reported to destabilize the *ptsG* mRNA and therefore decreases the glucose uptake capacity of the cell (Morita et al. 2003). Additionally, a connection between the reoxidation rate of NADPH and the

glucose uptake rate was shown (Sauer et al. 2004). A Δpgi mutant showed a growth defect, while a $\Delta pgi\Delta udhA$ double deletion mutant, lacking in addition to phosphoglucose isomerase the soluble transhydrogenase UdhA, did not grow on glucose at all. Under our biotransformation conditions, the NADPH level was kept low by the recombinant alcohol dehydrogenase, as shown by the decrease of the NADPH/NADP$^+$ ratio after addition of the substrate MAA. But the glucose uptake rate was similar under biotransformation conditions with 2.3 mmol glucose h^{-1} g_{cdw}^{-1} showing a different limitation as discussed above.

Deletion of *pgi* should result in a linear complete flux through the PPP which was confirmed by flux analysis consistent to previous studies. Glucose catabolism proceeds almost completely via the PPP in the Δpgi mutant (Canonaco et al. 2001). This linear flux through the PPP should result in a higher NADPH per glucose yield because theoretically 2 mol NADPH were generated in the PPP from each glucose molecule (Kruger and von Schaewen 2003).

A 55% higher MHB per glucose yield of 3.8 mol_{MHB} $mol_{glucose}^{-1}$ in a biotransformation with resting cells was achieved with the Δpgi mutant. The intracellular NADPH/NADP$^+$ ratio under biotransformation conditions before the addition of MAA was two-times higher compared to the reference strain. In independent studies deletion of *pgi* resulted in a 39% higher NADPH/NADP$^+$ ratio which led to a 4-times higher thymidine per glucose yield compared to the reference strain without *pgi* deletion (Lee et al. 2010). The deletion of *pgi* was also beneficial for a higher yield of 3.8 mol xylitol per mol glucose with an only 30% higher NADPH/NADP$^+$ ratio under resting cell conditions without xylitol (Chin and Cirino 2011). Summarized, deletion of *pgi* results in a higher NADPH/NADP$^+$ ratio and this is beneficial for the reduction of several substrates.

Theoretical approaches showed an increase of 300% in NADPH production rate in a Δpgi mutant, but although the production of catechin and leucocyanidin reached a higher final concentration the production rate did not increase (Chemler et al. 2010). This was also shown in this study were the specific MHB production rate did not alter in the Δpgi mutant compared to the reference strain.

4.1.2 Partial cyclization of the PPP in *Escherichia coli*

Deletion of *pfkA* in *E. coli* BL21(DE3) resulted in 23% residual phosphofructokinase activity. This was consistent with the ^{13}C flux analysis with a flux of 32% from fructose 6-phosphate to triose 3-phosphate in relation to the glucose uptake rate set to 100%. The main result from ^{13}C flux analysis was the verification of the partial cyclization of the PPP. A negative net flux from glucose 6-phosphate to fructose 6-phosphate was present in the $\Delta pfkA$ mutant strain indicating a cyclic operating PPP. Under resting cell conditions, this partial cyclization resulted in a significant increase of the whole-cell biotransformation yield. The theoretical value of 6 mol_{NADPH} $mol_{glucose}^{-1}$ by a partial cyclization of the PPP was nearly reached with a value of 4.8 and 5.5 mol_{MHB} $mol_{glucose}^{-1}$ with $\Delta pfkA$ mutant and $\Delta pfkA\Delta pfkB$ mutant, respectively. The values were similar to those of an independent study where a yield of 5.1 and 5.4 mol xylitol per mol glucose was accomplished with a with a $\Delta pfkA$ mutant and $\Delta pfkA\Delta sthA$ mutant, respectively (Chin and Cirino 2011).
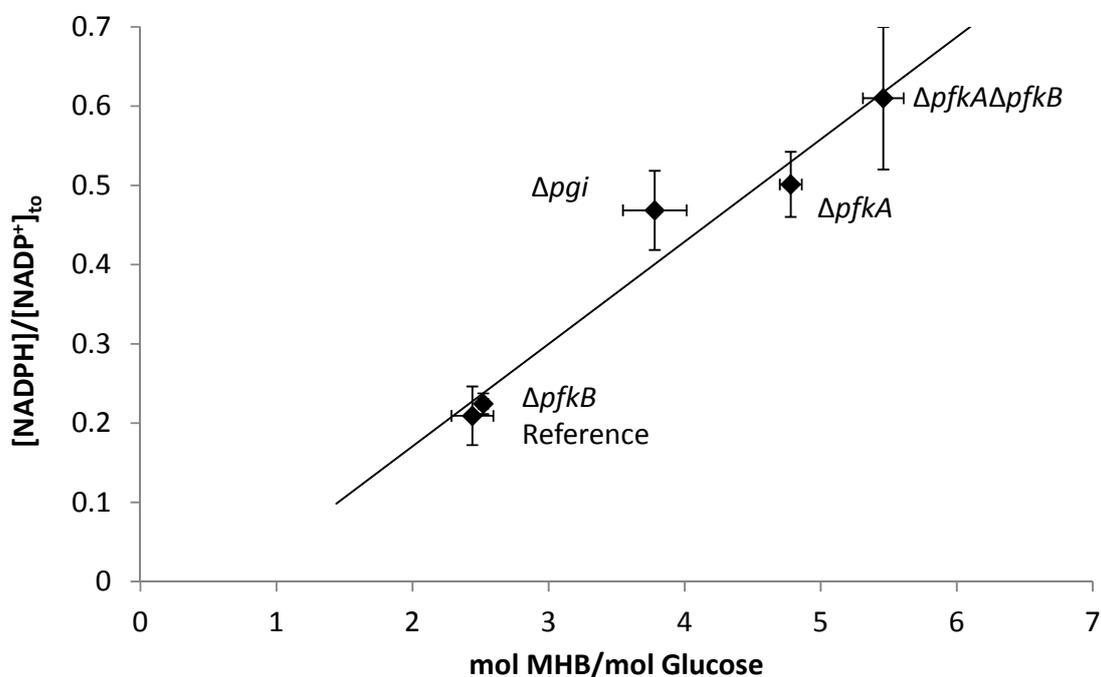
Fig. 5: Correlation of the [NADPH]/[NADP$^+$] ratios before MAA addition to the biotransformation test mixtures (t_0) and the biotransformation yield (mol MHB/mol glucose)

The intracellular NADPH/NADP$^+$ ratio increased by 238% in the $\Delta pfkA$ compared to the reference strain when analyzed during biotransformation before the addition of the substrate MAA. A linear correlation between the NADPH/NADP$^+$ ratio to the MHB/glucose yield was detected (Fig. 5).

The $\Delta pfkA$ mutant showed a strong growth defect in glucose minimal media with a 70% lower growth rate compared to the reference strain BL21(DE3) of 0.18 h^{-1}. This was in line with the lower glucose uptake rate of 4 mmol h^{-1} g$_{cdw}^{-1}$ which was 65% lower than the glucose uptake rate of the reference strain. Roehl and Vinopal had assumed a limitation of the glucose uptake rate by the lowered phosphoenolpyruvate (PEP) concentration, a compound which is essential for the phosphoenolpyruvate transferase system (PTS) (Roehl and Vinopal 1976). This assumption was validated by the ^{13}C flux analysis results received in this work, because the flux through pyruvate kinase was nearly absent in the $\Delta pfkA$ mutant.

Glucose uptake independent of the PTS system by overexpression of glucose facilitator (*glf*) and glucokinase (*glk*) from *Zymomonas mobilis* (Weisser et al. 1995; Parker et al. 1995) increased the glucose uptake rate in whole-cell biotransformation under resting cell conditions by 41%. This higher glucose uptake rate resulted in a 20% higher specific MHB production rate in the $\Delta pfkA$ mutant but not in the reference strain. This gave evidence that the limitation occurred only in the mutant strain.

4.1.3 Partial cyclization of the PPP in *Corynebacterium glutamicum*

To find out if the effects of cyclization of the PPP are equivalent in *C. glutamicum* was another aim of this study. It has to be kept in mind that differences exist in the repertoires of metabolic enzymes of *E. coli* and *C. glutamicum*. Of relevance for the present work is the occurrence of only one gene encoding a 6-phosphofructo 1-kinase (*pfkA*) and the absence of genes encoding transhydrogenases and the two enzymes of the Entner-Doudoroff-pathway in *C. glutamicum*.

The MHB yield per glucose of the *E. coli* $\Delta pfkA$ mutant was comparable to that of the *C. glutamicum* $\Delta pfkA$ mutant (4.8 mol MBH per mol glucose), both overexpressing *adh* from *L. brevis*, indicating that partial cyclization of the PPP occurred in the latter species, too. Furthermore, similarities were found by comparison of by-product formation in *E.*

coli and *C. glutamicum*. Less acetate and no succinate was produced in the Δ*pfkA* mutant strains compared to the reference strains in the experimental period. This is a consequence of the decreased carbon flux through the lower part of glycolysis and the TCA in the Δ*pfkA* mutant.

The strong growth defect of the *C. glutamicum* Δ*pfkA* mutant in glucose minimal medium may be caused by several effects. In *E. coli*, increased levels of glucose 6-phosphate or fructose 6-phosphate caused by deletion of *pgi* or *pfkA* were shown to stimulate RNase E-dependent degradation of *ptsG* mRNA, thereby decreasing the glucose uptake capacity of the cell (Morita et al. 2003; Kimata et al. 2001). Additionally, for a Δ*pfkA* mutant of *E. coli* was assumed that a reduced availability of phosphoenolpyruvate (PEP) decreases PEP-dependent glucose uptake (Roehl and Vinopal 1976; Siedler et al. 2012). Similar mechanisms might work in *C. glutamicum* and could be responsible for the growth defect of the Δ*pfkA* mutant. This defect could be eliminated by expression of the *pfkA* genes of *C. glutamicum* or of *E. coli*, but not by the *pfkB* gene of *E. coli*, even though phosphofructokinase activity was high *in vitro*. Surprisingly, the final cell density of the Δ*pfkA* mutant containing plasmid pEKEx3-*pfkB*^{Eco} was 29% higher compared to the wild type containing the empty plasmid. *E. coli* contains two non-homologues phosphofructokinases, PfkA (= Pfk I) and PfkB (= Pfk II) (Fraenkel et al. 1973). About 90–95% of the total phosphofructokinase activity of *E. coli* is contributed by PfkA under physiological conditions (Vinopal et al. 1975; Vinopal and Fraenkel 1975). An *E. coli* mutant containing no PfkA activity and high PfkB activity showed a similar effect as the Δ*pfkA* mutant of *C. glutamicum* containing *E. coli* PfkB, i.e. a 31% lower doubling time and a 12% higher cell yield (Robinson and Fraenkel 1978). *E. coli* PfkA and PfkB are regulated by different allosteric effectors. While PfkA is activated by ADP and inhibited by PEP (Blangy et al. 1968), PfkB is not influenced by PEP and ADP but inhibited by high fructose 1,6-bisphosphate concentrations (Babul 1978). If overexpression of *pfkB* causes elevated fructose 1,6-bisphosphate levels, PfkB would be feedback inhibited and this could be responsible for the slow growth rate despite high in vitro phosphofructokinase activity. The reason for the increased biomass yield of the Δ*pfkA* mutants of *E. coli* and *C. glutamicum* overexpressing *pfkB* is still unclear.

4.1.4 Cyclization of the PPP in *Corynebacterium glutamicum*

Complete oxidation of glucose via a cyclic PPP, which requires complete recycling of both fructose 6-phosphate and triose phosphate, theoretically affords the generation of 12 mol reduction equivalents per mol glucose 6-phosphate (Kruger and von Schaewen 2003). The fact that the MHB per glucose yield of the $\Delta gapA$ mutant (7.9 mol mol^{-1}) was higher compared to $\Delta pfkA$ mutant and corresponded to 66% of the maximal value of 12 mol NADPH per mol glucose 6-phosphate indicated a more expanded cyclic operation of the PPP in the *gapA* mutant compared to the *pfkA* mutant. The maximal value of a complete cyclic PPP was not reached because 25% of carbon was lost by conversion of glyceraldehyde 3-phosphate reduction to glycerol. Taking this loss into account, only 9 mol$_{MHB}$ mol$_{glucose}$$^{-1}$ could be achieved maximally and the experimental yield of 7.9 mol mol^{-1} corresponds to 88% of this value. A strongly reduced specific biotransformation rate was shown by the $\Delta gapA$ mutant, which was probably a consequence of the diminished capability for glucose uptake. In a $\Delta gapA$ mutant, no PEP should be formed during glucose catabolism and consequently, glucose uptake via the PTS should be impossible. For *C. glutamicum* PTS-independent glucose uptake has recently been described. The inositol transporters IolT1 and IolT2 function also as low-affinity glucose permeases (Lindner et al. 2011). Subsequent phosphorylation of glucose to glucose 6-phosphate is catalyzed either by an ATP-dependent glucokinase enocoded by *glk* (Park et al. 2000) or by the polyphosphate- or ATP-dependent glucose kinase PpgK (Lindner et al. 2010). During biotransformation the $\Delta gapA$ mutant showed a glucose consumption rate of 2.5 nmol^{-1} mg$_{cdw}$$^{-1}$ which is in the range of determined PTS-independent glucose uptake of 0.7 nmol min^{-1} mg$_{cdw}$$^{-1}$ measured at low external glucose concentrations (1 mM) (Lindner et al. 2011). Because glucose concentrations during biotransformation are >10-fold above the apparent Ks values of IolT1 and IolT2 (2.8 and 1.9 mM, respectively) (Lindner et al. 2011), it can be assumed that glucose uptake occurs via this alternative pathway in the $\Delta gapA$ mutant. Overexpression of either *iolT1* or *iolT2* together with *ppgK* was shown to allow almost wild-type growth rates in a PTS-negative mutant (Lindner et al. 2011) and thus would probably also allow higher biotransformation rates of a $\Delta gapA$ mutant. Alternatively, expression of the glucose facilitator gene *glf* from *Zymomonas*

mobilis could help to increase glucose uptake (Weisser et al. 1995; Parker et al. 1995; Bäumchen and Bringer-Meyer 2007).

4.1.5 The role of transhydrogenase in the Δ*pfkA* mutant of *E. coli*

The effects of the Δ*pfkA* mutant in whole-cell biotransformation were analyzed regarding to gene expression changes and the influence of oxygen on the biotransformation rate and physiological parameters. During biotransformation gene expression analysis revealed a different regulation between the BL21(DE3) and the Δ*pfkA* mutant. While the reference strain was influenced by the ArcAB two component system this influence was less in the Δ*pfkA* mutant. Phosphorylated, active ArcA activates or represses many of the genes that are involved in respiration and metabolism, including terminal oxidases, tricarboxylic acid cycle enzymes and glyoxylate shunt enzymes (Liu and De Wulf 2004) The ArcAB two component system is sensing microarobic conditions by the QH_2 to Q ratio of the respiratory chain (Georgellis et al. 2001; Malpica et al. 2004; Malpica et al. 2006). This ratio is linked to the $NADH/NAD^+$ ratio in the respiratory chain. The differences on the gene transcription level fitted to a 30% lower NADH to NAD^+ ratio in the Δ*pfkA* mutant compared to that of the reference strain after 120 min of biotransformation in a shake flask experiment. The differences can be explained by the results of anaerobic and aerobic biotransformation. Under anaerobic biotransformation conditions similar specific MHB production rates (7.4 mmol h^{-1} g_{cdw}^{-1}) and CO_2 transfer rates (2.4 mmol h^{-1} g_{cdw}^{-1}) were achieved with reference strain and Δ*pfkA* mutant. Additionally, the production of byproducts were similar with exception of a much lower lactate formation in the Δ*pfkA* mutant pointing to an adjusted $NADH/NAD^+$ ratio in the absence of oxygen. Under aerobic conditions a markedly increased carbon dioxide transfer rate (CTR) and oxygen transfer rate (OTR) were observed with the reference strain while a constant CTR and a much lower OTR were observed with the Δ*pfkA* mutant after addition of MAA. Under aerobic conditions and after the addition of MAA the ADH competed with the transhydrogenase SthA for NADPH and less H^- was transferred from NADPH to NAD^+ and consequently less NADH could be used for respiration in the mutant. That could explain the lower OTR in the presence of MAA in the mutant. These dissimilar responses were due to the different abilities of the two strains to use oxygen.

The Δ*pfkA* mutant was not able to use oxygen effectively for respiration, because conversion of NADPH to NADH by SthA seemed to be discontinued after addition of MAA. Under these conditions less oxygen could be used and on that account the cells were not as oxygen limited as the cells of the reference strain as was also indicated by the gene expression changes.

4.2 NADPH/NADP$^+$ redox sensor

In this study we have analyzed the SoxRS response to low intracellular NADPH/NADP$^+$ ratios in detail for the application of high throughput screening systems for NADPH dependent enzymes.

Formerly, it was assumed that SoxRS is sensing superoxide stress because the gene expression of *soxS* is activated by redox-cycling agents like paraquat (PQ), menadione and plumbagin (Nunoshiba et al. 1992; Wu and Weiss 1991). However, these reagents produce superoxide at the expense of the oxidation of NADPH, decreasing the reducing capacity of the cell. The first authors who proposed the view that SoxRS senses the NADPH state of *E. coli* were Liochev and Friedovich (1992), but their theory was neglected. Twenty years after this hypothesis the activation of the SoxRS system dependent of the NADPH/NADP$^+$ ratio was shown: overexpression of NADPH producing enzymes reduced the transcription of the *soxS* gene and vice versa expression of NADPH consuming enzymes enhanced the *soxS* transcription, due to the altered NADPH/NADP$^+$ ratio (Krapp et al. 2011; Gu and Imlay 2011). Physiologically, the SoxRS sensing low intracellular NADPH concentrations is reasonable because SoxS is regulating the gene expression of *zwf*, encoding the glucose-6-phosphate dehydrogenase (Li and Demple 1994) which is the first and under physiological conditions limiting step of the PPP. Paraquat-induced superoxide stress (resulting in lower NADPH content) increases the flux through the PPP supporting the regulatory theory (Rui et al. 2010).

The results of this thesis contribute to the view that SoxRS senses the NADPH state of *E. coli*. In principal, due to the unnaturally high activity of an overexpressed enzyme catalyzing a NADPH dependent reaction, low intracellular NADPH concentrations exist. This effect can be used for screening of a desired enzyme activity. Microarray analysis

before and after addition of MAA showed a 4.5 fold higher transcribed *soxS* gene after addition of MAA in the reference strain. A correlation between the lower NADPH/NADP$^+$ and the *soxS* gene transcription was assumed (Fig. 6). SoxR is kept in its inactive state by a NADPH dependent reduction, e.g. catalyzed by the proteins RseC and RsxBC (Koo et al. 2003). If low NADPH concentrations are present less SoxR can be reduced and thereupon oxidized SoxR is activating *soxS* gene expression.
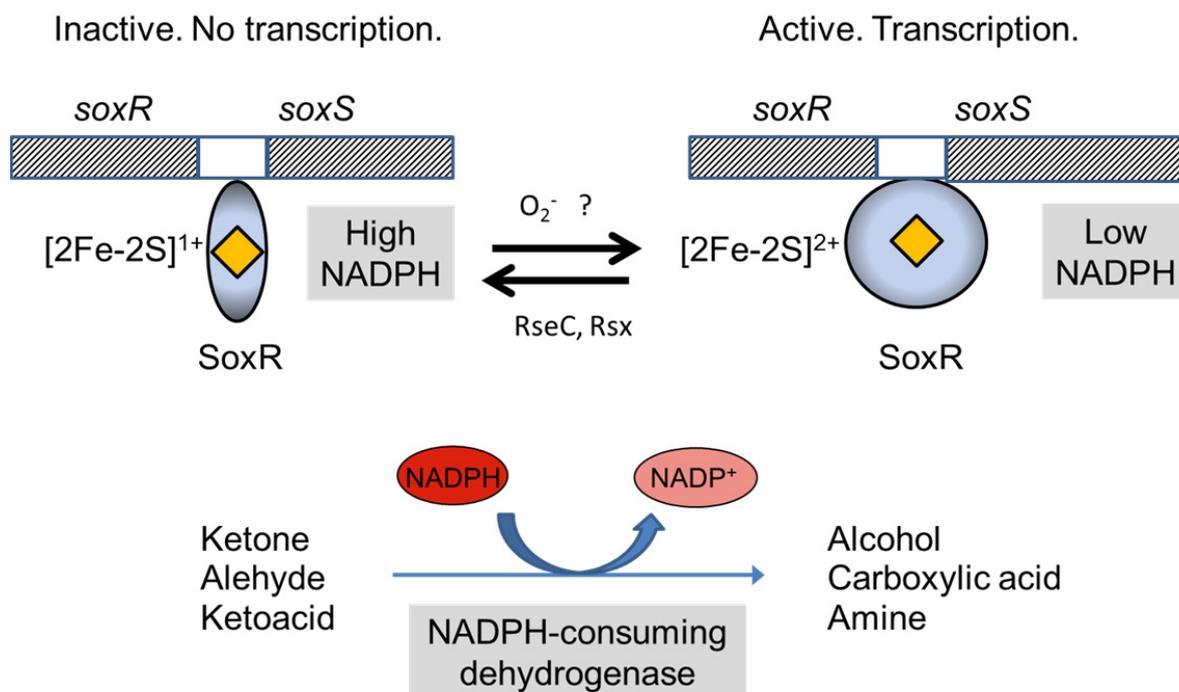
Fig. 6: Scheme of the transcription of *soxS* mediated by oxidized SoxR. SoxR is held in its reduced state by NADPH dependent reductases. If low intracellular NADPH concentrations are present SoxR cannot be reduced back to its inactive form and *soxS* gene transcription is activated. High activity of an NADPH-consuming dehydrogenase lowers the intracellular NADPH/NADP$^+$ ratio and indirectly activates SoxR.

We used this finding to develop a sensor for the in vivo analysis of NADPH-dependent reactions offering a number of exciting possibilities for high-throughput (HT) analysis and development of NADPH-dependent enzymes. The *soxS* gene transcription was coupled to the transcription of the enhanced yellow fluorescent protein (*eyfp*). The specific fluorescence output of the sensor is dependent on substrate concentration and ADH activity. The eYFP protein is stable (Tsien 1998) and the fluorescence signal stays constant over a period of >10 hours which is an advantage for screening of enzymes

because no kinetics need to be determined. FACS analysis revealed the applicability of this system for high throughput screening systems. None of 10^6 wild type cells were selected due to the sorting gate after 3 hours incubation with 4-methyl-2-pentanone (MP). In an analysis of the cells harboring the mutated ADH an inhomogeneity is visible with sorting of 2 cells out of 10^6 analyzed cells (Fig. 7).
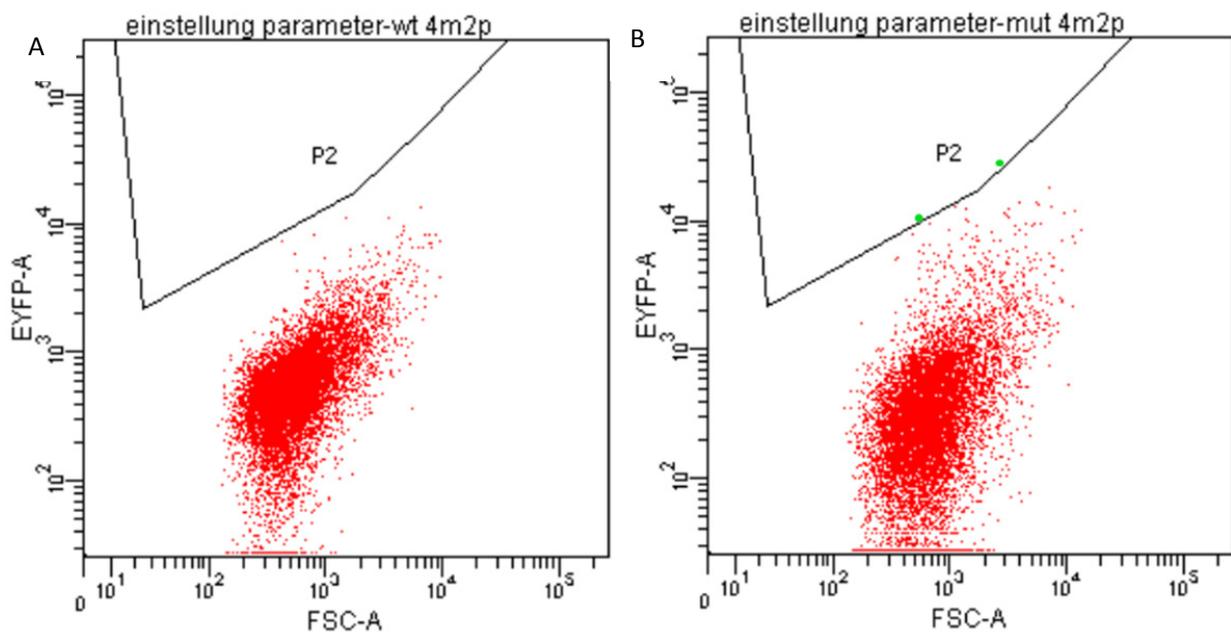
Fig. 7: Example of a FACS analysis of cells three hours after induction with 20 mM MP. Cells falling into the gate P2 were selected and further analyzed. A) *E. coli* cells expressing wild type ADH; B) *E. coli* cells expressing mutated library of the ADH

Six of the sorted cells were selected due to their higher fluorescence intensity in 96-well plates three hours after addition of MP compared to cells expressing the wild type enzyme. One enzyme turned out to have a 35 % higher maximum of specific enzyme activity. The enzyme has an amino acid exchange from alanine 93 to methionine. Ala93 is involved in acetophenone substrate binding (Schlieben et al. 2005) and it can be assumed that the exchange to methionine somehow favors correct binding of the smaller molecule MP, compared to acetophenone, resulting in a higher maximal velocity. Methionine is larger and reduces the binding pocket; this can be an explanation for the lower K_M of the mutated ADH.

4.3   Conclusion and perspectives

This thesis shows the potential of metabolic engineering of the PPP for cofactor regeneration. Taking advantage of the metabolism of the cell with a cyclized PPP enables a NADPH per glucose yield of up to 7.9 mol/mol. Further studies should aim at the elucidation of bottlenecks and diminishing of glycerol byproduct formation.

In case of the redox sensor a generalized HT screen is available for NADPH-consuming enzymes of interest. As long as educts and products are diffusible through the cytoplasmic membrane, libraries of dehydrogenases requiring NADPH, or P450-monooxygenases where NADPH is part of the catalytic cycle can now be assayed in HT screening approaches without development of specific assays. This novel technology is expected to expedite the availability of new enzymes for the synthesis of chiral compounds enormously.

References

Appel D, Lutz-Wahl S, Fischer P, Schwaneberg U, Schmid RD (2001) A P450 BM-3 mutant hydroxylates alkanes, cycloalkanes, arenes and heteroarenes. J Biotechnol 88 (2):167-171.

Babul J (1978) Phosphofructokinases from *Escherichia coli*. Purification and characterization of the nonallosteric isozyme. J Biol Chem 253 (12):4350-4355.

Bäumchen C, Bringer-Meyer S (2007) Expression of *glf* $_{z.m.}$ increases D-mannitol formation in whole cell biotransformation with resting cells of *Corynebacterium glutamicum*. Appl Microbiol Biotechnol 76 (3):545-552.

Bäumchen C, Roth AH, Biedendieck R, Malten M, Follmann M, Sahm H, Bringer-Meyer S, Jahn D (2007) D-mannitol production by resting state whole cell biotransformation of D-fructose by heterologous mannitol and formate dehydrogenase gene expression in *Bacillus megaterium*. Biotechnol J 2 (11):1408-1416.

Binder S, Schendzielorz G, Stäbler N, Krumbach K, Hoffmann K, Bott M, Eggeling L (2012) A high-throughput approach to identify genomic variants of bacterial metabolite producers at the single-cell level. Genome Biol 13 (5):R40.

Blanchard JL, Wholey WY, Conlon EM, Pomposiello PJ (2007) Rapid changes in gene expression dynamics in response to superoxide reveal SoxRS-dependent and independent transcriptional networks. PLoS One 2 (11):e1186.

Blangy D, Buc H, Monod J (1968) Kinetics of the allosteric interactions of phosphofructokinase from *Escherichia coli*. J Mol Biol 31 (1):13-35.

Boddupalli SS, Estabrook RW, Peterson JA (1990) Fatty acid monooxygenation by cytochrome P-450$_{BM-3}$. J Biol Chem 265 (8):4233-4239.

Canonaco F, Hess TA, Heri S, Wang T, Szyperski T, Sauer U (2001) Metabolic flux response to phosphoglucose isomerase knock-out in *Escherichia coli* and impact of overexpression of the soluble transhydrogenase UdhA. FEMS Microbiol Lett 204 (2):247-252.

Chemler JA, Fowler ZL, McHugh KP, Koffas MA (2010) Improving NADPH availability for natural product biosynthesis in *Escherichia coli* by metabolic engineering. Metab Eng 12 (2):96-104.

Chin JW, Cirino PC (2011) Improved NADPH supply for xylitol production by engineered *Escherichia coli* with glycolytic mutations. Biotechnol Prog 27 (2):333-341.

Chin JW, Khankal R, Monroe CA, Maranas CD, Cirino PC (2009) Analysis of NADPH supply during xylitol production by engineered *Escherichia coli*. Biotechnol Bioeng 102 (1):209-220.

Egorov AM, Avilova TV, Dikov MM, Popov VO, Rodionov YV, Berezin IV (1979) NAD-dependent formate dehydrogenase from methylotrophic bacterium, strain 1. Purification and characterization. Eur J Biochem 99 (3):569-576.

Eguchi T, Kuge Y, Inoue K, Yoshikawa N, Mochida K, Uwajima T (1992) NADPH regeneration by glucose dehydrogenase from *Gluconobacter scleroides* for l-leucovorin synthesis. Biosci Biotechnol Biochem 56 (5):701-703.

Ernst M, Kaup B, Müller M, Bringer-Meyer S, Sahm H (2005) Enantioselective reduction of carbonyl compounds by whole-cell biotransformation, combining a formate dehydrogenase and a (*R*)-specific alcohol dehydrogenase. Appl Microbiol Biotechnol 66 (6):629-634.

Faber K (2000) Biotransformations in organic chemistry. 4th edn. Springer, Berlin Heidelberg New York

Fraenkel DG, Kotlarz D, Buc H (1973) Two fructose 6-phosphate kinase activities in *Escherichia coli*. J Biol Chem 248 (13):4865-4866.

Gabor E, Göhler AK, Kosfeld A, Staab A, Kremling A, Jahreis K (2011) The phosphoenolpyruvate-dependent glucose-phosphotransferase system from *Escherichia coli* K-12 as the center of a network regulating carbohydrate flux in the cell. Eur J Cell Biol 90 (9):711-720.

Galkin A, Kulakova L, Yoshimura T, Soda K, Esaki N (1997) Synthesis of optically active amino acids from alpha-keto acids with *Escherichia coli* cells expressing heterologous genes. Appl Environ Microbiol 63 (12):4651-4656.

Gaudu P, Weiss B (1996) SoxR, a [2Fe-2S] transcription factor, is active only in its oxidized form. Proc Natl Acad Sci U S A 93 (19):10094-10098.

Georgellis D, Kwon O, Lin EC (2001) Quinones as the redox signal for the *arc* two-component system of bacteria. Science 292 (5525):2314-2316.

Goldberg K, Schroer K, Lütz S, Liese A (2007) Biocatalytic ketone reduction--a powerful tool for the production of chiral alcohols-part II: whole-cell reductions. Appl Microbiol Biotechnol 76 (2):249-255.

Gredell JA, Frei CS, Cirino PC (2012) Protein and RNA engineering to customize microbial molecular reporting. Biotechnol J 7 (4):477-499.

Green J, Paget MS (2004) Bacterial redox sensors. Nat Rev Microbiol 2 (12):954-966.

Gu M, Imlay JA (2011) The SoxRS response of *Escherichia coli* is directly activated by redox-cycling drugs rather than by superoxide. Mol Microbiol 79 (5):1136-1150.

Heuser F, Schroer K, Lütz S, Bringer-Meyer S, Sahm H (2007) Enhancement of the NAD(P)(H) Pool in *Escherichia coli* for Biotransformation. Eng Life Sci 7 (4):343-353.

Hidalgo E, Demple B (1994) An iron-sulfur center essential for transcriptional activation by the redox-sensing SoxR protein. Embo J 13 (1):138-146.

Hummel W (1997) New alcohol dehydrogenases for the synthesis of chiral compounds. Adv Biochem Eng Biotechnol 58:145-184.

Hummel W (1999) Large-scale applications of NAD(P)-dependent oxidoreductases: recent developments. Trends Biotechnol 17 (12):487-492.

Hummel W, Kula MR (1989) Dehydrogenases for the synthesis of chiral compounds. Eur J Biochem 184 (1):1-13.

Ishige T, Honda K, Shimizu S (2005) Whole organism biocatalysis. Curr Opin Chem Biol 9 (2):174-180.

Jair KW, Fawcett WP, Fujita N, Ishihama A, Wolf RE, Jr. (1996) Ambidextrous transcriptional activation by SoxS: requirement for the C-terminal domain of the RNA polymerase alpha subunit in a subset of *Escherichia coli* superoxide-inducible genes. Mol Microbiol 19 (2):307-317.

Kaup B, Bringer-Meyer S, Sahm H (2004) Metabolic engineering of *Escherichia coli*: construction of an efficient biocatalyst for D-mannitol formation in a whole-cell biotransformation. Appl Microbiol Biotechnol 64 (3):333-339.

Kaup B, Bringer-Meyer S, Sahm H (2005) D: -Mannitol formation from D: -glucose in a whole-cell biotransformation with recombinant *Escherichia coli*. Appl Microbiol Biotechnol 69 (4):397-403.

Kimata K, Tanaka Y, Inada T, Aiba H (2001) Expression of the glucose transporter gene, *ptsG*, is regulated at the mRNA degradation step in response to glycolytic flux in *Escherichia coli*. Embo J 20 (13):3587-3595.

Koo MS, Lee JH, Rah SY, Yeo WS, Lee JW, Lee KL, Koh YS, Kang SO, Roe JH (2003) A reducing system of the superoxide sensor SoxR in *Escherichia coli*. Embo J 22 (11):2614-2622.

Krapp AR, Humbert MV, Carrillo N (2011) The *soxRS* response of *Escherichia coli* can be induced in the absence of oxidative stress and oxygen by modulation of NADPH content. Microbiology 157 (Pt 4):957-965.

Kruger NJ, von Schaewen A (2003) The oxidative pentose phosphate pathway: structure and organisation. Curr Opin Plant Biol 6 (3):236-246.

Kula MR, Wandrey C (1987) Continuous enzymatic transformation in an enzyme-membrane reactor with simultaneous NADH regeneration. Methods Enzymol 136:9-21.

Kundig W, Ghosh S, Roseman S (1964) Phosphate Bound to Histidine in a Protein as an Intermediate in a Novel Phospho-Transferase System. Proc Natl Acad Sci U S A 52:1067-1074.

Lamzin VS, Aleshin AE, Strokopytov BV, Yukhnevich MG, Popov VO, Harutyunyan EH, Wilson KS (1992) Crystal structure of NAD-dependent formate dehydrogenase. Eur J Biochem 206 (2):441-452.

Lee HC, Kim JS, Jang W, Kim SY (2010) High NADPH/NADP+ ratio improves thymidine production by a metabolically engineered *Escherichia coli* strain. J Biotechnol 149 (1-2):24-32.

Lee JN, Shin HD, Lee YH (2003) Metabolic engineering of pentose phosphate pathway in *Ralstonia eutropha* for enhanced biosynthesis of poly-beta-hydroxybutyrate. Biotechnol Prog 19 (5):1444-1449.

Lee WH, Chin YW, Han NS, Kim MD, Seo JH (2011) Enhanced production of GDP-L-fucose by overexpression of NADPH regenerator in recombinant *Escherichia coli*. Appl Microbiol Biotechnol 91 (4):967-976.

Li Z, Demple B (1994) SoxS, an activator of superoxide stress genes in *Escherichia coli*. Purification and interaction with DNA. J Biol Chem 269 (28):18371-18377.

Li Z, Demple B (1996) Sequence specificity for DNA binding by *Escherichia coli* SoxS and Rob proteins. Mol Microbiol 20 (5):937-945.

Lim SJ, Jung YM, Shin HD, Lee YH (2002) Amplification of the NADPH-related genes *zwf* and *gnd* for the oddball biosynthesis of PHB in an *E. coli* transformant harboring a cloned *phbCAB* operon. J Biosci Bioeng 93 (6):543-549.

Lindner SN, Knebel S, Pallerla SR, Schoberth SM, Wendisch VF (2010) Cg2091 encodes a polyphosphate/ATP-dependent glucokinase of *Corynebacterium glutamicum*. Appl Microbiol Biotechnol 87 (2):703-713.

Lindner SN, Seibold GM, Henrich A, Krämer R, Wendisch VF (2011) Phosphotransferase system-independent glucose utilization in *corynebacterium glutamicum* by inositol permeases and glucokinases. Appl Environ Microbiol 77 (11):3571-3581.

Liochev SI, Fridovich I (1992) Fumarase C, the stable fumarase of *Escherichia coli*, is controlled by the *soxRS* regulon. Proc Natl Acad Sci U S A 89 (13):5892-5896.

Litsanov B, Brocker M, Bott M (2012a) Toward homosuccinate fermentation: metabolic engineering of *Corynebacterium glutamicum* for anaerobic production of succinate from glucose and formate. Appl Environ Microbiol 78 (9):3325-3337.

Liu X, De Wulf P (2004) Probing the ArcA-P modulon of *Escherichia coli* by whole genome transcriptional analysis and sequence recognition profiling. J Biol Chem 279 (13):12588-12597.

Malpica R, Franco B, Rodriguez C, Kwon O, Georgellis D (2004) Identification of a quinone-sensitive redox switch in the ArcB sensor kinase. Proc Natl Acad Sci U S A 101 (36):13318-13323.

Malpica R, Sandoval GR, Rodriguez C, Franco B, Georgellis D (2006) Signaling by the *arc* two-component system provides a link between the redox state of the quinone pool and gene expression. Antioxid Redox Signal 8 (5-6):781-795.

Martin RG, Gillette WK, Martin NI, Rosner JL (2002) Complex formation between activator and RNA polymerase as the basis for transcriptional activation by MarA and SoxS in *Escherichia coli*. Mol Microbiol 43 (2):355-370.

Morita T, El-Kazzaz W, Tanaka Y, Inada T, Aiba H (2003) Accumulation of glucose 6-phosphate or fructose 6-phosphate is responsible for destabilization of glucose transporter mRNA in *Escherichia coli*. J Biol Chem 278 (18):15608-15614.

Mustafi N, Grünberger A, Kohlheyer D, Bott M, Frunzke J (2012) The development and application of a single-cell biosensor for the detection of l-methionine and branched-chain amino acids. Metab Eng 14 (4):449-457.

Nanchen A, Fuhrer T, Sauer U (2007) Determination of metabolic flux ratios from 13C-experiments and gas chromatography-mass spectrometry data: protocol and principles. Methods Mol Biol 358:177-197.

Nunoshiba T, Hidalgo E, Amabile Cuevas CF, Demple B (1992) Two-stage control of an oxidative stress regulon: the *Escherichia coli* SoxR protein triggers redox-inducible expression of the *soxS* regulatory gene. J Bacteriol 174 (19):6054-6060.

Panke S, Wubbolts M (2005) Advances in biocatalytic synthesis of pharmaceutical intermediates. Curr Opin Chem Biol 9 (2):188-194.

Park SY, Kim HK, Yoo SK, Oh TK, Lee JK (2000) Characterization of *glk*, a gene coding for glucose kinase of *Corynebacterium glutamicum*. FEMS Microbiol Lett 188 (2):209-215.

Parker C, Barnell WO, Snoep JL, Ingram LO, Conway T (1995) Characterization of the *Zymomonas mobilis* glucose facilitator gene product (*glf*) in recombinant *Escherichia coli*: examination of transport mechanism, kinetics and the role of glucokinase in glucose transport. Mol Microbiol 15 (5):795-802.

Poulsen BR, Nohr J, Douthwaite S, Hansen LV, Iversen JJL, Visser J, Ruijter GJG (2005) Increased NADPH concentration obtained by metabolic engineering of the pentose phosphate pathway in *Aspergillus niger*. Febs J 272 (6):1313-1325.

Reetz MT (2003) An overview of high-throughput screening systems for enantioselective enzymatic transformations. Methods Mol Biol 230:259-282.

Riebel B (1996) Biochemische und molekularbiologische Charakterisierung neuer mikrobieller NAD(P)-abhängiger Alkoholdehydrogenasen. Inaugural-Dissertation Universität Düsseldorf.

Robinson JP, Fraenkel DG (1978) Allosteric and non-allosteric *E. coli* phosphofructokinases: effects on growth. Biochem Biophys Res Commun 81 (3):858-863.

Roehl RA, Vinopal RT (1976) Lack of glucose phosphotransferase function in phosphofructokinase mutants of *Escherichia coli*. J Bacteriol 126 (2):852-860.

Rui B, Shen T, Zhou H, Liu J, Chen J, Pan X, Liu H, Wu J, Zheng H, Shi Y (2010) A systematic investigation of *Escherichia coli* central carbon metabolism in response to superoxide stress. BMC Syst Biol 4:122.

Sauer U, Canonaco F, Heri S, Perrenoud A, Fischer E (2004) The soluble and membrane-bound transhydrogenases UdhA and PntAB have divergent functions in NADPH metabolism of *Escherichia coli*. J Biol Chem 279 (8):6613-6619.

Schewe H, Kaup BA, Schrader J (2008) Improvement of P450$_{BM-3}$ whole-cell biocatalysis by integrating heterologous cofactor regeneration combining glucose facilitator and dehydrogenase in *E. coli*. Appl Microbiol Biotechnol 78 (1):55-65.

Schlieben NH, Niefind K, Müller J, Riebel B, Hummel W, Schomburg D (2005) Atomic resolution structures of *R*-specific alcohol dehydrogenase from *Lactobacillus brevis* provide the structural bases of its substrate and cosubstrate specificity. J Mol Biol 349 (4):801-813.

Schroer K, Zelic B, Oldiges M, Lütz S (2009) Metabolomics for biotransformations: Intracellular redox cofactor analysis and enzyme kinetics offer insight into whole cell processes. Biotechnol Bioeng 104 (2):251-260.

Schwaneberg U, Otey C, Cirino PC, Farinas E, Arnold FH (2001) Cost-effective whole-cell assay for laboratory evolution of hydroxylases in *Escherichia coli*. J Biomol Screen 6 (2):111-117.

Shaked Z, Whitesides GM (1980) Enzyme-Catalyzed Organic Synthesis: NADH Regeneration Using Formate Dehydrogenase. J Am Chem Soc 102:7104-7105.

Siedler S, Bringer S, Blank LM, Bott M (2012) Engineering yield and rate of reductive biotransformation in *Escherichia coli* by partial cyclization of the pentose phosphate pathway and PTS-independent glucose transport. Appl Microbiol Biotechnol 93 (4):1459-1467.

Sprenger GA (1995) Genetics of pentose-phosphate pathway enzymes of *Escherichia coli* K-12. Arch Microbiol 164 (5):324-330.

Stephanopoulos GN, Aristidou AA, Nielsen J (1998) Review of cellular metabolism. In: Stephanopoulos GN, Aristidou AA, Nielsen J (eds) Metabolic engineering: principles and methodologies. Academic press, San Diego, pp 21-79

Straathof AJ, Panke S, Schmid A (2002) The production of fine chemicals by biotransformations. Curr Opin Biotechnol 13 (6):548-556.

Tan I (2006) Applications of whole cell biotransformations for the production of chiral alcohols. Rheinische Friedrich-Wilhelms University of Bonn, Bonn, Dissertation

Tang SY, Cirino PC (2011) Design and application of a mevalonate-responsive regulatory protein. Angew Chem Int Ed Engl 50 (5):1084-1086.

Toya Y, Ishii N, Nakahigashi K, Hirasawa T, Soga T, Tomita M, Shimizu K (2010) 13C-metabolic flux analysis for batch culture of *Escherichia coli* and its Pyk and Pgi gene knockout mutants based on mass isotopomer distribution of intracellular metabolites. Biotechnol Prog 26 (4):975-992.

Tsien RY (1998) The green fluorescent protein. Annu Rev Biochem 67:509-544.

Tsotsou GE, Cass AE, Gilardi G (2002) High throughput assay for cytochrome P450 BM3 for screening libraries of substrates and combinatorial mutants. Biosens Bioelectron 17 (1-2):119-131.

Vinopal RT, Clifton D, Fraenkel DG (1975) *PfkA* locus of *Escherichia coli*. J Bacteriol 122 (3):1162-1171.

Vinopal RT, Fraenkel DG (1975) *PfkB* and *pfkC* loci of *Escherichia coli*. J Bacteriol 122 (3):1153-1161.

Weckbecker A, Gröger H, Hummel W (2010) Regeneration of nicotinamide coenzymes: principles and applications for the synthesis of chiral compounds. Adv Biochem Eng Biotechnol 120:195-242.

Weisser P, Kramer R, Sahm H, Sprenger GA (1995) Functional expression of the glucose transporter of *Zymomonas mobilis* leads to restoration of glucose and fructose uptake in *Escherichia coli* mutants and provides evidence for its facilitator action. J Bacteriol 177 (11):3351-3354.

Wu J, Weiss B (1991) Two divergently transcribed genes, *soxR* and *soxS*, control a superoxide response regulon of *Escherichia coli*. J Bacteriol 173 (9):2864-2871.

Zhao J, Shimizu K (2003) Metabolic flux analysis of *Escherichia coli* K12 grown on 13C-labeled acetate and glucose using GC-MS and powerful flux calculation method. J Biotechnol 101 (2):101-117.

Appendix

Supplemental material Increased NADPH availability in *Escherichia coli*

Table S1A Intracellular concentrations of NADPH and NADP$^+$ and ratios of [NADPH]/[NADP$^+$] and [NADH]/[NAD$^+$] in *E. coli* reference strain and deletion mutants at three time points during biotransformation. All strains expressed the plasmid-encoded alcohol dehydrogenase gene from *L. brevis*. Samples taken at the time point zero did not yet contain the biotransformation substrate MAA. Results were derived from at least two independent experiments.

Strain	[NADPH] μmol (g cdw)$^{-1}$			[NADP$^+$] μmol (g cdw)$^{-1}$			[NADPH]/[NADP$^+$]		
	Time (min)			Time (min)			Time (min)		
	0	30	120	0	30	120	0	30	120
Reference strain	0.22 ± 0.06	0.28 ± 0.05	0.30 ± 0.01	1.05 ± 0.11	1.82 ± 0.31	2.12 ± 0.51	0.21 ± 0.03	0.17 ± 0.04	0.17 ± 0.05
Δ*pfkB*	0.26 ± 0.07	0.20 ± 0.07	0.20 ± 0.05	1.12 ± 0.24	2.13 ± 0.83	1.57 ± 0.43	0.22 ± 0.01	0.10 ± 0.02	0.15 ± 0.07
Δ*pfkA*	0.44 ± 0.09	0.46 ± 0.07	0.42 ± 0.07	0.88 ± 0.12	1.79 ± 0.15	2.25 ± 0.28	0.50 ± 0.04	0.28 ± 0.02	0.21 ± 0.05
Δ*pfkA*Δ*pfkB*	0.36 ± 0.01	0.13 ± 0.01	0.13 ± 0.08	0.67 ± 0.24	1.29 ± 0.20	1.22 ± 0.09	0.61 ± 0.09	0.10 ± 0.01	0.11 ± 0.07
Δ*pgi*	0.60 ± 0.01	0.27 ± 0.09	0.20 ± 0.06	1.31 ± 0.18	1.71 ± 0.86	1.51 ± 0.48	0.46 ± 0.05	0.26 ± 0.09	0.16 ± 0.09

Table S1B Intracellular concentrations of NADH and NAD$^+$ (µmol (g cdw)$^{-1}$) and ratios of [NADH]/[NAD$^+$] in *E. coli* reference strain and deletion mutants at three time points during biotransformation. All strains expressed the plasmid-encoded alcohol dehydrogenase gene from *L. brevis*. Samples taken at the time point zero did not yet contain the biotransformation substrate MAA. Results were derived from at least two independent experiments.

Strain	[NADH] µmol (g cdw)$^{-1}$			[NAD$^+$] µmol (g cdw)$^{-1}$			[NADH]/[NAD$^+$]		
	Time (min)			Time (min)			Time (min)		
	0	30	120	0	30	120	0	30	120
Reference strain	3.21 ± 1.53	3.40 ± 0.89	2.71 ± 0.13	7.65 ± 1.84	6.97 ± 0.64	4.16 ± 0.40	0.39 ± 0.10	0.48 ± 0.08	0.65 ± 0.03
Δ*pfkB*	3.18 ± 1.65	3.67 ± 2.79	2.96 ± 1.21	7.62 ± 2.73	7.93 ± 0.94	4.22 ± 0.38	0.39 ± 0.07	0.42 ± 0.30	0.73 ± 0.35
Δ*pfkA*	2.40 ± 0.96	2.97 ± 0.58	1.86 ± 0.24	7.52 ± 1.31	6.87 ± 0.22	4.06 ± 0.09	0.35 ± 0.19	0.44 ± 0.10	0.46 ± 0.05
Δ*pfkA*Δ*pfkB*	1.81 ± 0.53	3.34 ± 0.79	1.40 ± 0.85	6.04 ± 0.98	6.04 ± 0.58	3.48 ± 0.52	0.30 ± 0.08	0.45 ± 0.24	0.40 ± 0.11
Δ*pgi*	2.39 ± 1.67	2.65 ± 1.13	2.27 ± 1.40	7.39 ± 0.89	5.33 ± 1.42	3.37 ± 0.66	0.30 ± 0.18	0.42 ± 0.29	0.61 ± 0.30
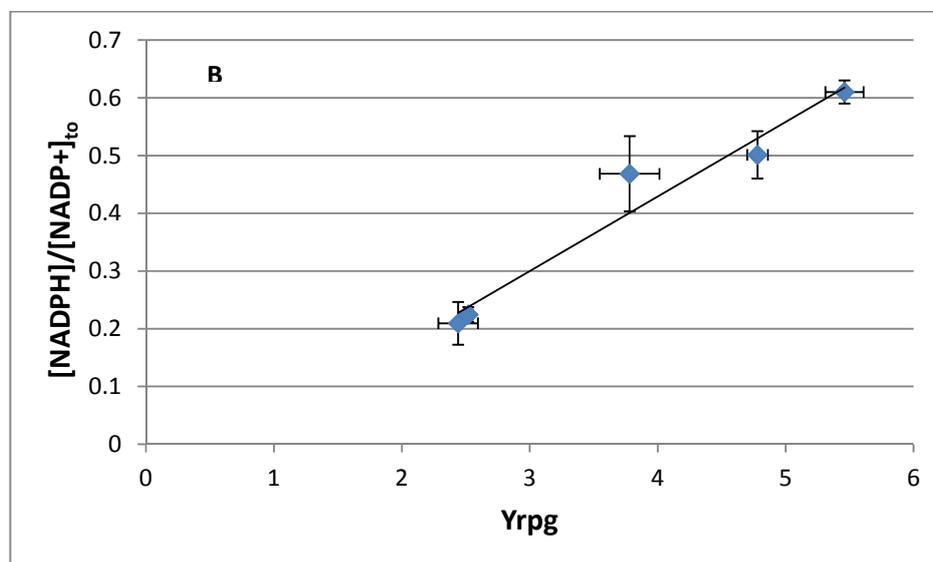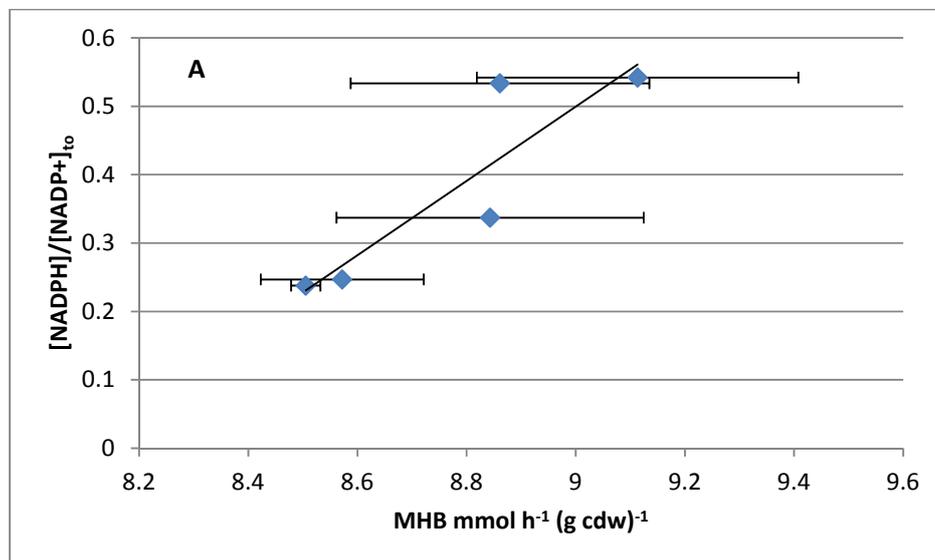
Supplement Figure S2A,B Correlation of the NADPH/NADP$^+$ ratios before MAA addition to the biotransformation test mixtures (t_0) and the MHB production rates, **A**; Correlation of the difference of NADPH/NADP$^+$ ratios before MAA addition to the biotransformation test mixtures (t_0) and the NADPH/NADP$^+$ ratios during biotransformation and the biotransformation yield (Y_{RPG}), **B**.

Supplemental material Characterization of *E. coli* BL21(DE3) and its *pfkA* deletion mutant
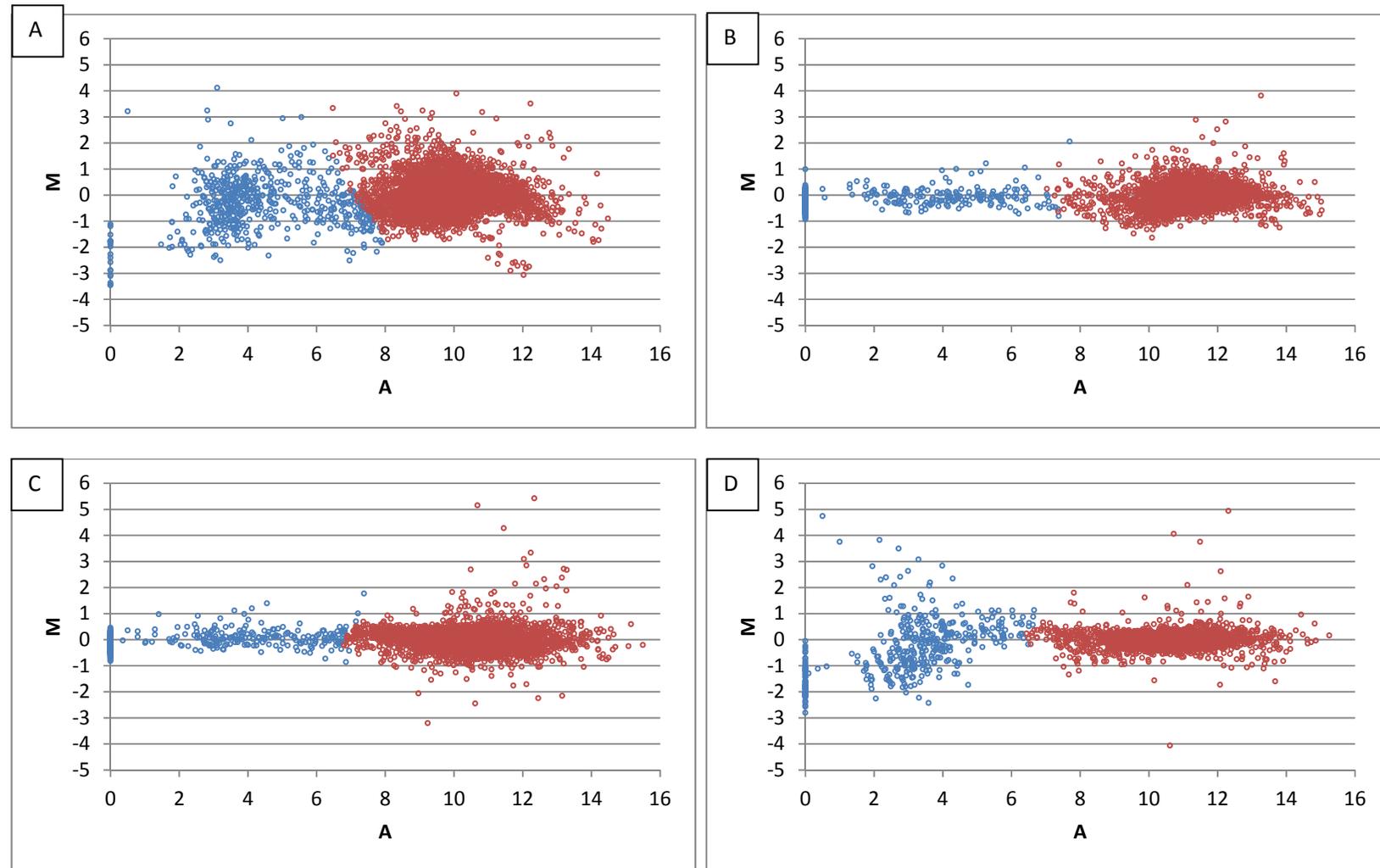
Fig. S1: MA plots of DNA microarray analyses of the response to MAA. Values with a signal to noise ratio <3 are shown in blue and those >3 are shown in red. A+B shows the results of the wild type and C+D the results of the Δ*pfkA* mutant of independent analyses.

Table SII: Regulated genes of a genome-wide comparison of mRNA levels of *E. coli* Δ*pfkA* versus the reference strain under biotransformation conditions in the presence of the substrate MAA. Cells were suspended at a cell density of 3 g_{cdw} L^{-1} for 10 min in biotransformation medium and samples were taken for RNA isolation. Genes with an mRNA ratio ≥2.0 or ≤0.5 and a p-value of ≤0.05 are listed. The data shown represent mean values from three biological replicates. The genes were grouped into different functional categories within which they were grouped into up- and downregulated genes, ordered according to their locus tag.

Locus tag	Gene name	Annotation	mRNA ratio	p-value
Respiration				
ECD_00692	cydA	cytochrome d terminal oxidase, subunit I	0.27	1.41E-02
ECD_00382	cyoB	cytochrome o ubiquinol oxidase subunit I	2.80	2.81E-03
ECD_00383	cyoA	cytochrome o ubiquinol oxidase subunit II	5.26	2.99E-03
Metabolism				
ECD_01234	trpA	tryptophan synthase subunit alpha	0.17	2.28E-03
ECD_01235	trpB	tryptophan synthase subunit beta	0.14	8.69E-04
ECD_01236	trpC	bifunctional indole-3-glycerol phosphate	0.10	5.50E-06
ECD_01237	trpD	bifunctional indole-3-glycerol-phosphate	0.06	1.09E-09
ECD_01238	trpE	anthranilate synthase component I	0.07	1.21E-02
ECD_01239	trpL	trp operon leader peptide	0.05	2.41E-03
ECD_01673	aroH	3-deoxy-D-arabino-heptulosonate-7-phosphate synthase, tryptophan repressible	0.30	5.83E-03
ECD_02704	ygeX	diaminopropionate ammonia-lyase	0.26	1.57E-02
ECD_02712	ssnA	putative chlorohydrolase/aminohydrolase	0.15	3.31E-24
ECD_02714	xdhD	fused predicted xanthine/hypoxanthine oxidase:	0.13	3.98E-04
ECD_02981	tdcE	pyruvate formate-lyase 4/2-ketobutyrate formate-lyase	0.31	2.09E-03
ECD_03280	glgP	glycogen phosphorylase	0.49	6.59E-17
ECD_03592	tnaA	tryptophanase/L-cysteine desulfhydrase, PLP-dependent	0.02	2.48E-03
ECD_03801	pfkA	6-phosphofructokinase	0.06	2.24E-02
ECD_03990	melA	alpha-galactosidase, NAD(P)-binding	0.16	1.93E-03
ECD_04113	pyrB	aspartate carbamoyltransferase catalytic subunit	0.41	6.57E-03
ECD_00115	lpdA	dihydrolipoamide dehydrogenase	2.34	3.47E-04
ECD_00681	sdhC	succinate dehydrogenase cytochrome b556 large membrane subunit	15.46	4.23E-03
ECD_00682	sdhD	succinate dehydrogenase cytochrome b556 small membrane subunit	12.58	1.93E-04
ECD_00683	sdhA	succinate dehydrogenase flavoprotein subunit	6.71	7.39E-03
ECD_00684	sdhB	succinate dehydrogenase, FeS subunit	3.04	1.81E-02
ECD_01164	dadA	D-amino acid dehydrogenase small subunit	5.44	3.72E-03
ECD_01273	puuA	gamma-Glu-putrescine synthase	3.22	2.42E-02
ECD_01747	yeaA	methionine sulfoxide reductase B	3.44	5.90E-04
ECD_02266	yfcY	acetyl-CoA acetyltransferase	3.36	7.35E-03

ECD_02950	fadH	2,4-dienoyl-CoA reductase, NADH and FMN-linked	3.71	6.34E-34
ECD_03455	mtlD	mannitol-1-phosphate 5-dehydrogenase	2.42	3.71E-03
ECD_03737	fadB	fused 3-hydroxybutyryl-CoA	13.37	3.60E-03
ECD_03909	malM	maltose regulon periplasmic protein	5.94	2.47E-03
ECD_03941	acs	acetyl-coenzyme A synthetase	6.81	1.39E-03

Regulation; Signaltransduction

ECD_00112	pdhR	transcriptional regulator of pyruvate dehydrogenase complex	0.39	5.54E-03
ECD_02214	lrhA	DNA-binding transcriptional repressor of flagellar, motility and chemotaxis genes	0.36	8.61E-03
ECD_02539	mprA	DNA-binding transcriptional repressor of microcin B17 synthesis and multidrug efflux	0.45	6.14E-20
ECD_00300	mhpR	DNA-binding transcriptional activator, 3HPP-binding	2.60	1.66E-02
ECD_02423	iscR	DNA-binding transcriptional repressor	2.49	1.01E-03
ECD_02429	hcaR	DNA-binding transcriptional activator of 3-phenylpropionic acid catabolism	2.73	8.01E-04

Transport

ECD_00908	focA	formate transporter	0.25	6.04E-04
ECD_02079	mglB	methyl-galactoside transporter subunit	0.17	2.25E-02
ECD_03028	mtr	tryptophan transporter of high affinity	0.14	5.95E-06
ECD_03593	tnaB	tryptophan transporter of low affinity	0.23	1.16E-03
ECD_03637	rbsB	D-ribose transporter subunit	0.35	5.30E-03
ECD_03991	melB	melibiose:sodium symporter	0.31	3.70E-03
ECD_02078	mglA	fused methyl-galactoside transporter subunits of ABC superfamily: ATP-binding components	0.38	7.78E-03
ECD_02019	gatB	galactitol-specific enzyme IIB component of PTS	0.33	7.85E-03
ECD_02020	gatA	galactitol-specific enzyme IIA component of PTS	0.34	9.75E-03
ECD_00961	ompA	outer membrane protein A (3a;II*;G;d)	2.99	1.95E-02
ECD_02235	argT	lysine/arginine/ornithine transporter subunit	3.07	4.90E-03
ECD_03151	prlA	protein translocase subunit SecY	4.52	3.13E-02
ECD_03287	gntU	gluconate transporter, low affinity GNT 1 system	2.59	3.56E-03
ECD_03302	ugpB	glycerol-3-phosphate transporter subunit	2.65	9.37E-04
ECD_03905	malF	maltose transporter subunit	3.31	1.12E-02
ECD_03906	malE	maltose ABC transporter periplasmic protein	3.22	6.82E-03
ECD_03907	malK	fused maltose transport subunit, ATP-binding	3.74	8.83E-03
ECD_03908	lamB	maltoporin precursor	6.78	5.70E-03

Motility

ECD_01067	flgM	anti-sigma factor for FliA (sigma 28)	2.50	1.58E-03
ECD_01068	flgA	flagellar basal body P-ring biosynthesis protein A	2.99	7.25E-03
ECD_01069	flgB	flagellar basal-body rod protein B	3.21	8.97E-04
ECD_01070	flgC	flagellar basal-body rod protein C	2.86	4.37E-03
ECD_01071	flgD	flagellar basal body rod modification protein D	3.07	2.93E-03
ECD_01072	flgE	flagellar hook protein E	2.76	9.77E-07
ECD_01073	flgF	flagellar component of cell-proximal portion of basal-body rod	2.44	3.19E-05
ECD_01074	flgG	flagellar component of cell-distal portion of basal-body rod	2.69	5.30E-05

Stress response

ECD_00885	cspD	cold shock protein homolog	0.26	3.49E-03
ECD_02464	rseC	RseC protein involved in reduction of the SoxR iron-sulfur cluster	0.45	6.71E-04
ECD_10012	ybcC	DLP12 prophage; predicted exonuclease	0.44	1.43E-03
ECD_00014	dnaK	molecular chaperone DnaK	3.88	2.45E-02
ECD_00268	betB	betaine aldehyde dehydrogenase, NAD-dependent	7.45	2.50E-03
ECD_00269	betI	transcriptional regulator BetI	6.44	4.47E-03
ECD_00270	betT	choline transporter of high affinity	3.79	1.37E-03
ECD_00503	nmpC	DLP12 prophage; truncated outer membrane porin pseudogene)	3.20	3.77E-03
ECD_03847	udhA	soluble pyridine nucleotide transhydrogenase	3.06	1.48E-04
ECD_03934	soxS	DNA-binding transcriptional dual regulator	6.25	5.03E-03
ECD_04012	groES	co-chaperonin GroES	3.81	3.79E-02

Transcription & translation

ECD_00957	rmf	ribosome modulation factor	0.41	1.44E-02
ECD_01438	sra	30S ribosomal subunit protein S22	0.36	3.66E-03
ECD_02465	rseB	periplasmic negative regulator of sigmaE	0.45	1.99E-03
ECD_02495	rplS	50S ribosomal protein L19	3.20	1.60E-02
ECD_02496	trmD	tRNA (guanine-N(1)-)-methyltransferase	3.49	1.10E-02
ECD_02497	rimM	16S rRNA-processing protein	3.98	5.56E-03
ECD_02498	rpsP	30S ribosomal protein S16	3.96	7.43E-03
ECD_03145	rplQ	50S ribosomal protein L17	2.93	5.16E-02
ECD_03146	rpoA	DNA-directed RNA polymerase subunit alpha	4.40	2.39E-02
ECD_03147	rpsD	30S ribosomal protein S4	5.11	1.17E-02
ECD_03148	rpsK	30S ribosomal protein S11	4.52	2.25E-02
ECD_03149	rpsM	30S ribosomal protein S13	4.30	2.59E-02
ECD_03150	rpmJ	50S ribosomal protein L36	3.69	5.64E-02
ECD_03152	rplO	50S ribosomal protein L15	4.64	3.02E-02
ECD_03153	rpmD	50S ribosomal protein L30	5.14	2.94E-02
ECD_03154	rpsE	30S ribosomal protein S5	4.43	4.24E-02
ECD_03155	rplR	50S ribosomal protein L18	5.14	2.80E-02
ECD_03156	rplF	50S ribosomal protein L6	4.00	5.48E-02
ECD_03157	rpsH	30S ribosomal protein S8	4.19	4.96E-02
ECD_03158	rpsN	30S ribosomal protein S14	4.17	4.74E-02
ECD_03159	rplE	50S ribosomal protein L5	4.39	4.21E-02
ECD_03161	rplN	50S ribosomal protein L14	4.39	4.05E-02
ECD_03163	rpmC	50S ribosomal protein L29	5.85	4.90E-02
ECD_03164	rplP	50S ribosomal protein L16	9.52	1.32E-02
ECD_03165	rpsC	30S ribosomal protein S3	6.44	4.98E-02
ECD_03166	rplV	50S ribosomal protein L22	10.20	2.38E-02
ECD_03167	rpsS	30S ribosomal protein S19	8.31	4.37E-02
ECD_03168	rplB	50S ribosomal protein L2	14.76	7.37E-03
ECD_03169	rplW	50S ribosomal protein L23	10.56	2.85E-02
ECD_03170	rplD	50S ribosomal protein L4	12.06	1.32E-02
ECD_03171	rplC	50S ribosomal protein L3	15.97	3.89E-03

ECD_03172	rpsJ	30S ribosomal protein S10	15.01	6.14E-03
ECD_03190	tufA	protein chain elongation factor EF-Tu (duplicate of tufB)	3.91	1.14E-02
ECD_03191	fusA	elongation factor EF-2	5.77	1.15E-02
ECD_03192	rpsG	30S ribosomal protein S7	6.52	1.18E-02
ECD_03193	rpsL	30S ribosomal protein S12	8.48	1.06E-02
ECD_03856	tufB	protein chain elongation factor EF-Tu (duplicate of tufA)	3.44	1.24E-02
ECD_04067	rpsF	30S ribosomal protein S6	5.09	3.87E-02
ECD_04068	priB	primosomal replication protein N	5.10	3.37E-02
ECD_04069	rpsR	30S ribosomal protein S18	7.25	2.59E-02
ECD_04070	rplI	50S ribosomal protein L9	3.78	5.50E-02

Predicted function

ECD_00931	ycbL	predicted metal-binding enzyme	0.41	5.30E-05
ECD_01888	yodA	conserved metal-binding protein	0.33	1.59E-02
ECD_02240	yphF	predicted sugar transporter subunit: periplasmic-binding component of ABC superfamily	0.30	6.74E-05
ECD_02702	ygeV	predicted DNA-binding transcriptional regulator	0.26	1.05E-02
ECD_02711	ygfK	predicted oxidoreductase, Fe-S subunit	0.18	4.01E-04
ECD_02713	ygfM	predicted oxidoreductase	0.17	3.02E-03
ECD_02940	yqjI	predicted transcriptional regulator	0.41	8.07E-05
ECD_01022	phoH	conserved protein with nucleoside triphosphate hydrolase domain	2.30	1.38E-03

Hypothetical protein

ECD_00284	yahO	hypothetical protein	0.32	5.10E-02
ECD_00930	ycbK	hypothetical protein	0.43	7.62E-04
ECD_01108	ycfR	hypothetical protein	0.24	6.96E-03
ECD_02703	ygeW	hypothetical protein	0.21	4.84E-04
ECD_02705	ygeY	hypothetical protein	0.31	1.49E-02
ECD_02709	yqeC	hypothetical protein	0.43	2.33E-04
ECD_00694	ybgT	hypothetical protein	0.26	1.83E-02
ECD_02111	yejG	hypothetical protein	3.18	3.55E-03
ECD_03699	yigI	hypothetical protein	2.57	3.64E-03

Danksagung

An erster Stelle möchte ich mich bei Prof. Dr. Michael Bott bedanken, für die großartigen Forschungsbedingungen am IBG-1, die Möglichkeit auf viele für mich richtungsweisende Konferenzen zu fahren und dafür, dass er mich an seinem wissenschaftlichen Knowhow teilhaben ließ.

Bei Prof. Dr. Georg Groth bedanke ich mich für die freundliche Übernahme des Zweitgutachtens.

Ein ganz besonderer Dank gilt Dr. Stephanie Bringer, für die Überlassung eines sehr spannenden und abwechslungsreichen Themas und dafür, dass sie mir immer mit Rat und Tat zur Seite stand und mich, wenn es nötig war, wieder aufgebaut hat.

Bei Prof. Dr. Lars Blank möchte ich mich für die tolle und effektive Zusammenarbeit bedanken- ich denke schneller kann man ein Manuskript nicht fertig bekommen ☺

Für die guten Diskussionen auf Konferenzen und die daraus entstandene Kooperation bedanke ich mich sehr herzlich bei Steffen. Auch Prof. Dr. Volker Wendisch möchte ich für die Ratschläge danken, die zu dem Erfolg der Publikation beigetragen haben.

Bei Georg, Stephan und Lothar möchte ich mich für so vieles bedanken- für die gute Laune, die tolle Zusammenarbeit und die vielen hilfreichen Ratschläge.

Tino danke ich für die Tipps und Kniffe bei der Durchführung und Auswertung der Microarrays und den Korrekturen an meinem Manuskript.

Außerdem gilt mein Dank noch Janine, Steffi, Helga und Ines für die lehrreiche Zeit und Ratschläge auch beim z.B. 20. Entwurf meines Posters- der Kuchen kommt bestimmt!

Allen Mitarbeitern des IBG-1 danke ich für die schöne Zeit und die stete Hilfsbereitschaft. Besonders danke ich Antonia und Kristina für die vielen Gespräche und die Einweisung in Microarrays und/bzw. Bandshifts.

Mein größter Dank gilt meiner Familie: meiner Mutter Sybille und meiner Oma Lotte, dafür dass sie mich in allen Lebenslagen unterstützen und immer für mich da sind; Bernd dafür dass er mich versteht und mich so nimmt wie ich bin; und meinem Vater Jost dafür, dass er so ist wie er ist. DANKE!

Erklärung

Die hier vorgelegte Dissertation habe ich eigenständig und ohne unerlaubte Hilfe angefertigt. Die Dissertation wurde in der vorgelegten oder in ähnlicher Form noch bei keiner anderen Institution eingereicht. Ich habe bisher keine erfolglosen Promotionsversuche unternommen.

_____

Solvej Siedler

Aachen, den 07.09.2012